Novel Molecular Targets of Boswellic Acids and Characterization of Bioactive Ingredients of Frankincense

Neue molekulare Targets von Boswelliasäuren und Charakterisierung bioaktiver Inhaltsstoffe aus Weihrauch

Dissertation

der Mathematisch-Naturwissenschaftlichen Fakultät

der Eberhard Karls Universität Tübingen

zur Erlangung des Grades eines

Doktors der Naturwissenschaften

(Dr. rer. nat.)

vorgelegt von

Arne Henkel

aus Münster

Tübingen

2011

Tag der mündlichen Qualifikation: 28.04.2011

Dekan: Prof. Dr. Wolfgang Rosenstiel

1. Berichterstatter: Prof. Dr. Oliver Werz

2. Berichterstatter: PD Dr. Martina Düfer

Table of Contents

1.   Abbreviations

5-HETE	5-hydroxyeicosatetraenoic acid
5-LO	5-lipoxygenase
ABA	3-*O*-acetyl-β-boswellic acid
ac-lup	3-α-acetyl-lupanic acid
ac-OH-lup	3-α-acetyl-28-hydroxy-lupanic acid
3-α-ac-TA	3-α-acetyl-8,24-TA
AKBA	3-*O*-acetyl-11-keto-β-boswellic acid
ADP	adenosine diphosphate
AM	acetoxymethylester
Amp	ampicillin
AMPs	antimicrobial peptides
Apaf1	apoptotic protease-activation factor 1
ATP	adenosine triphosphate
BCIP	5-bromo-4-chloro-3-indolylphosphate toluidine salt
BA	β-boswellic acid
BE	*Boswellia* extract
BSA	bovine serum albumin
casp	caspase
catG	cathepsin G
CD	cluster of differentiation
CGI	cathepsin G inhibitor I
CHX	cycloheximide
COX	cyclooxygenase
CRAMP	cathelin-related antimicrobial peptide
cytB	cytochalasin B
DH-rob	4(23)-dihydro-roburic acid
DHK-rob	4(23)-dihydro-11-keto-roburic acid
DMEM	Dulbecco's modified Eagle medium
DMSO	dimethyl sulfoxide
e(K)BA	3-*O*-ether-(11-keto)-BA
EDTA	ethylenediaminetetraacetate
EGFR	epidermal growth factor receptor

ERK	extracellular signal-regulated kinase
FCS	fetal calf serum
fMLP	N-formylmethionyl-leucyl-phenylalanine
FPRL-1	formyl peptide receptor-like 1
Fura-2	1-[2-(5-carboxyoxazol-2-yl)-6-aminobenzofuran-5-oxyl]-2-(2`-amino-5`-methyl-phenoxy)ethane-N,N,N`,N`-tetraacetic acid
GAP	GTPase activating protein
GDP	guanine diphosphate
GEF	Guanine-nucleotide exchange factor
glu(K)BA	3-O-glutaroyl-(11-keto)-β-boswellic acid
GSH	glutathione
GTP	guanine triphosphate
GST	glutathione-S transferase
hCAP18	human cathelicidin antimicrobial protein
HEPES	4-(2-hydroxyethyl)-1-piperazineethanesulfonic acid
HLE	human leukocyte elastase
HPLC	high performance liquid chromatography
HRP	horseradish peroxidase
ICU	intensive care unit
IFN-γ	Interferon-γ
IKK	IκB kinase
iNOS	inducible nitric oxide synthase
IPTG	isopropyl-β-D-thiogalactopyranoside
IRAK	interleukin-1 receptor-associated kinase
JNK	c-Jun N-terminal kinase
KBA	11-keto-β-boswellic acid
6-keto-$PGF_{1\alpha}$	6-keto-prostaglandin 1α
LAs	lupanic acids
lup	lupanic acid
LB	Luria broth
LBP	lipopolysaccharide binding protein
LPS	lipopolysaccharide
LTB_4	leukotriene B_4
LTC_4	leukotriene C_4

MALDI-TOF-MS	matrix-assisted laser desorption ionization-time of flight-mass spectrometry
MAP3K	MAPK kinase kinase
MAPK	mitogen-activated protein kinase
MEKK	MAPK/ERK kinase kinase
mRap1B	mant-GppNHp-loaded Rap1B
MTT	3-(4,5-dimethylthiazol-2-yl)-2,5-diphenyltetrazolium bromide
NBT	nitro-blue tetrazolium chloride
NF	nuclear factor
NO	nitric oxide
NP-40	Nonidet$^{®}$ P40
OD	optical density
3-α-OH-TA	3-α-hydroxy-8,24-dien-TA
3-β-OH-TA	3-β-hydroxy-8,24-dien-TA
OH-lup	28-hydroxy-lupanic acid
ox(K)BA	3-*O*-oxaloyl-(11-keto)-β-boswellic acid
3-oxo-TA	3-oxo-8,24-dien-TA
p12-LO	platelet-type 12-lipoxygenase
PAR4	protease-activated receptor 4
PARP	poly ADP-ribose polymerase
PBMC	peripheral blood mononuclear cells
PBS	phosphate buffered saline
PGE$_2$	prostaglandin E$_2$
PI	propidium iodide
PI 3 kinase	phosphatidylinositol 3 kinase
PMNL	polymorphonuclear leukocytes
PMSF	phenylmethanesulfonylfluoride
PxB	polymyxin B
RAs	roburic acids
RBD	Ras-binding domain
rob	roburic acid
RPMI	Roswell Park Memorial Institute medium
RT	room temperature
SDS	sodium dodecyl sulfate

SDS-PAGE	SDS-polyacrylamide gelelectrophoresis
seph	sepharose
stauro	staurosporine
suc(K)BA	3-O-succinoyl-(11-keto)-β-boswellic acid
s.e.	standard error
TAs	tirucallic acids
TEMED	tetramethylethylenediamine
TNF	tumor necrosis factor
TRAF	TNF Receptor Associated Factor
w/o	without

2.   Introduction

2.1   *Boswellia serrata* and Boswellic acids

2.1.1   Origin and historical background

Boswellic acids (BAs), belonging to the group of pentacyclic triterpenes, originate from gum resin of trees of the genus *Boswellia spec.* of the burseracea family of plants. The genus *Boswellia* comprises 25 species, among them *B. serrata* Roxb. Ex. Colebr.*, B. carterii* Birdw., *B. frereana* Birdw., *B. papyrifera* Hochst. and *B. socotrana* Balf.. The trees are widely distributed in India, on the Arabian Peninsula and in North Africa (Somalia, Ethiopia, Eritrea and Sudan).

The gum resin from the trees, termed frankincense or olibanum, is used since millennia in traditional and Indian ayurvedic medicine. The use of frankincense as a drug was firstly described in the papyrus Ebers, which is thought to be written around 1,500 BC [1]. This document was written on a papyrus scroll and contains medical information for the treatment and diagnosis of various diseases. Major diseases treated with frankincense extracts were tumor and tumor-related disorders (carcinomas, edema), inflammatory diseases and diseases of the respiratory tract [2].

The usage of frankincense as a drug is not restricted to ancient times. Olibanum was mentioned in the first edition of the German Pharmacopoeia until the sixth edition in 1926. It was mainly used as a drug in folk medicine, but due to a lack of modern scientific knowledge about its efficacy and modes of action, olibanum disappeared from medical treatments in modern medicine. Initial animal and clinical studies were performed in the 1980s [3-7] and the discovery of the 5-lipoxygenase as a molecular target of Boswellia extracts (BEs) [8] resulted in a large interest in using frankincense as a drug to treat several diseases in modern medicine.
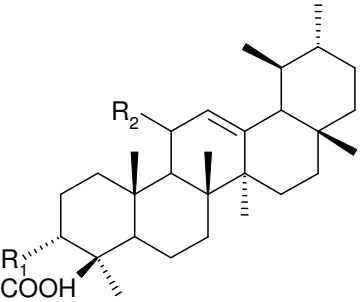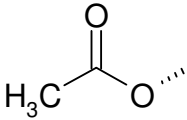
Today, many ingredients of the gum resins are identified (see **2.1.2**) and a number of molecular targets for some of these compounds were found (see **2.1.3.1**). Several animal and clinical studies indicate effectiveness in the treatment of diverse diseases (see **2.1.3.3**). Due to these studies, a medicinal product based on the gum resin of *B. serrata*

(H15^{TM}) was approved in a part of Switzerland and additionally, H15^{TM} was designated as an orphan drug for the treatment of peritumoral brain edema by the European Medicines Agency (EMA).

2.1.2   Composition of *Boswellia* gum resin

Modern analytical techniques allowed the identification of more than 200 compounds in *Boswellia* gum resin. The major components are volatile oil (5-15%), mucus (12-23%) and a lipophilic fraction (55-66%) [9]. The exact composition varies between different *Boswellia* species and resin harvesting time and methods. The lipophilic fraction contains several terpenes as di-, tetra- and pentacyclic triterpenes. Among the pentacyclic triterpenes, BAs were identified as major constituents [10,11]. BAs exist in α- and β-configurations, depending on the position of two methyl groups on C-19/C-20 (α-BAs: geminal groups on C-20, β-BAs: vicinal groups on C-19/C-20). Further structural variety can be given by the presence or absence of a keto group on C-11 and an acetoxy group at C-3. The most abundant BAs present in *Boswellia* extracts (BEs) are mostly β-configured BAs: β-boswellic acid (β-BA), 11-keto-β-boswellic acid (KBA), 3-*O*-acetyl-β-boswellic acid (ABA) and 3-*O*-acetyl-11-keto-β-boswellic acid (AKBA) (**tab. 2.1**).

Tab. 2.1: Structures of common BAs.

Structure	R$_1$	R$_2$	name
	HO '''''	H	β-BA
		O	KBA
	H$_3$C—C(=O)—O ''''	H	ABA
		O	AKBA
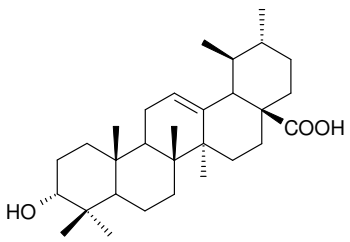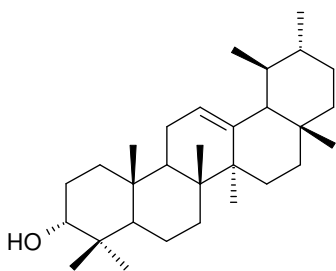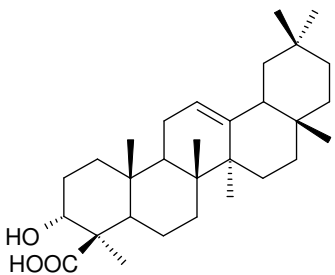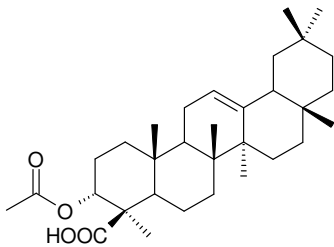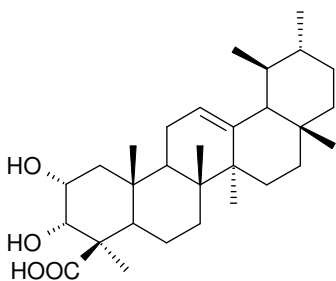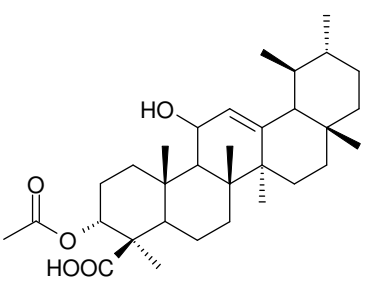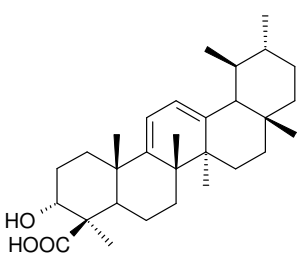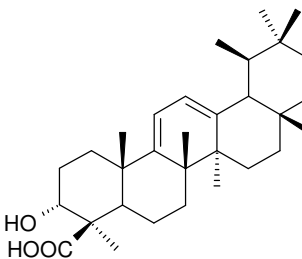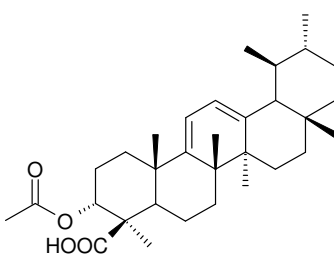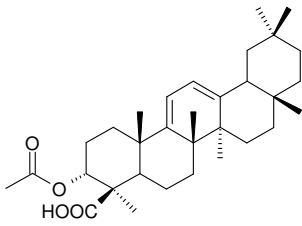
The amount of different BAs in a dry extract of the gum resin from *B. serrata* (BSE-018) is listed in **tab. 2.2**. While the non-11-keto BAs ABA and β-BA occur in relative high concentrations, the amount of the 11-keto-BAs AKBA and KBA is much lower.

Tab. 2.2: Composition of a dry extract of the gum resin from **B. serrata** *(BSE-018). Enlisted are the most abundant boswellic acids (according to [11]).*

ingredient	content [%]
BA	18.2
ABA	10.5
KBA	6.1
AKBA	3.7
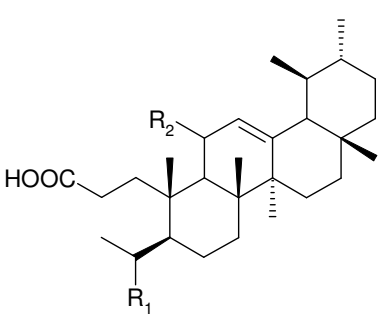
Besides the β-configured triterpenes β-BA, ABA, KBA and AKBA, a variety of additional pentacyclic triterpenes have been identified, among them α-BA, acetyl-α-BA, 2-hydroxy-β-BA [12], 3-*O*-acetyl-11-hydroxy-β-BA [13], α-amyrin [14], ursolic acid, 9,11-dehydro-ß-BA [14], 9,11-dehydro-α-BA, 3-*O*-acetyl-9,11-dehydro-β-BA and 3-*O*-acetyl-9,11-dehydro-β-BA [10] (**tab. 2.3**).

Tab. 2.3: Structures of pentacyclic triterpenes isolated from BEs.

Structure	Structure	Structure
ursolic acid	α-amyrin	α-BA
acetyl-α-BA	2-hydroxy-β-BA	3-*O*-acetyl-11-hydroxy-β-BA
9,11-dehydro-β-BA	9,11-dehydro-α-BA	3-*O*-acetyl-9,11-dehydro-β-BA
3-*O*-acetyl-9,11-dehydro-α-BA		
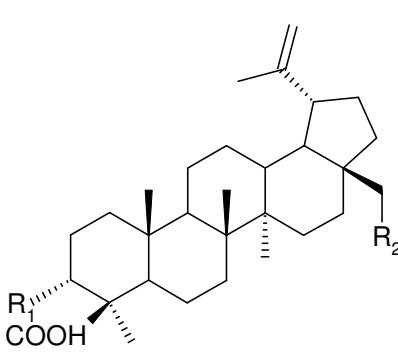
In addition, several pentacyclic triterpenes with an open A-ring (3,4-seco-triterpenic acids, RAs) were identified in *B. socotrana* Balf. (**tab. 2.4**): 4(23)-dihydro-roburic acid (DH-RA) [15], roburic acid (RA), 11-keto-roburic acid and 4(23)-dihydro-11-keto-roburic acid (DHK-RA) [16].

Tab. 2.4: Structures of RAs identified in frankincense extracts.

Structure	R_1	R_2	name
	H$_2$C=	H	RA
	H$_3$C—	H	DH-RA
	H$_3$C—	O=	DHK-RA
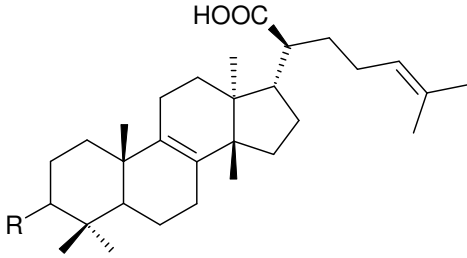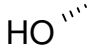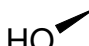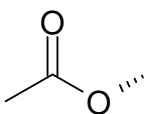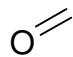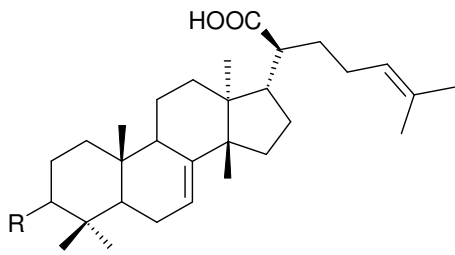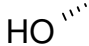
Lupanic acids (LAs) were also found as ingredients from *B. papyrifera* and *B. socotrana* extracts (**tab. 2.5**): lupanic acid (LA) [17], 3-α-acetyl-lupanic acid (Ac-LA) [18], 3-α-acetyl-28-hydroxy-lupanic acid (Ac-OH-LA) [19] and 28-hydroxy-lupanic acid (OH-LA, Jauch, personal communication).

Tab. 2.5: Structures of LAs identified in frankincense extracts.

Structure	R_1	R_2	name
	HO—	HO—	OH-LA
	AcO—	HO—	Ac-OH-LA
	AcO—	H	Ac-LA

Several tetracyclic triterpene acids were identified as ingredients of *B. papyrifera* extracts, among them following tirucallic acids (TAs): 3-oxo-8,24-dien-TA (3-oxo-TA), 3-α-hydroxy-8,24-dien-TA (3-α-OH-TA), 3-β-hydroxy-8,24-dien-TA (3-β-OH-TA), 3-α-acetyl-8,24-TA (3-α-Ac-TA) and 3-α-hydroxy-7,24-dien-TA [20,21] (**tab. 2.6**).

Tab. 2.6: Structures of TAs found in frankincense extracts.

Structure	R	name
	HO'''	3-α-OH-TA
	HO (wedge)	3-β-OH-TA
	acetyl O'''	3-α-Ac-TA
	O=	3-oxo-TA
	HO''''	3-α-OH-7,24-dien-TA

2.1.3 Scientific studies

Since the 1980s, a multitude of modern scientific studies were performed in order to investigate the effectiveness of BEs and its single constituents, including *in vitro* (see **2.1.3.1**), animal and human (see **2.1.3.3**) studies. Also, some investigations were performed analyzing the pharmacokinetic profile of BAs and BEs (see **2.1.3.2**).

2.1.3.1 Identified molecular targets of BAs

Several molecular targets for BAs were identified up to now. One of the first identified target of AKBA was 5-lipoxygenase (5-LO). Ammon *et al.* investigated an inhibitory effect of a *B. serrata* extract on 5-LO of rat peritoneal polymorphonuclear leukocytes (PMNL) [8]. 5-LO is an enzyme which catalyzes the transformation of arachidonic acid to LTA_4, which is in turn converted into leukotriene B_4 (LTB_4) or leukotriene C_4 (LTC_4) [22]. More detailed investigations revealed BAs as novel non-redox inhibitors, which bind to a selective site for pentacyclic triterpenes on 5-LO [23-25]. AKBA was the most efficient BA tested with IC_{50} values of 1.5-50 µM, depending on the experimental settings (cell type, stimulus, animal or human cells) [23-30]. Higher concentrations of AKBA were needed to inhibit isolated 5-LO than 5-LO in intact cells. This indicates that the efficient inhibition in intact cells may be dependent on additional cellular mechanisms. In contrast to the inhibitory effects, principles from BEs may also stimulate 5-LO activity. When used in lower concentrations, a *B. serrata* extract elevated 5-LO activity [28], and when AKBA or KBA (<30 µM) are incubated with arachidonic acid in polymorphonuclear leukocytes (PMNL), an enhanced 5-LO activity was observed [27].

Besides 5-LO, other targets of the arachidonic acid metabolism have been identified. AKBA was identified as a direct inhibitor of cyclooxygenase-1 (COX-1), while COX-2 was only slightly inhibited by BAs [31]. In addition, BAs were found to modulate platelet-type 12-lipoxygenase (p12-LO) activity [32], implicating that BAs may not be regarded as specific modulators of the 5-LO pathway.

Human leukocyte elastase (HLE) was identified as a target of BAs [33]. AKBA was the most potent BA tested with an IC_{50} value of 13.8 µM. β-BA did also inhibit HLE, but less efficient. Other triterpenes derived from frankincense were effective as well (ursolic acid and α-amyrin) [33,34], indicating a more general mode of action not only specific

for BAs. HLE is a serine protease released by PMNL at sites of inflammation, and a role in several diseases like cystic fibrosis, chronic bronchitis, rheumatoid arthritis, pulmonary emphysema and acute respiratory distress syndrome have been proposed [35].

Several protein kinases are modulated by BAs. In PMNL and in granulocytic HL-60 cells, AKBA activated extracellular signal-regulated kinase (ERK) 1/2 and p38 mitogen-activated protein kinase (MAPK) and increased the intracellular Ca^{2+} concentration [27,36]. Additionally, AKBA induced the release of arachidonic acid from PMNL [27], this may be a consequence of the modulation of Ca^{2+} levels and MAPK activation [37]. AKBA-dependent MAPK activation and Ca^{2+} mobilization were sensitive to pertussis toxin [27], and inhibition of phosphatidylinositol 3 (PI 3)-kinase as well as chelation of Ca^{2+} reduced the AKBA-induced ERK activation [36]. This implicates an involvement of a G-protein coupled receptor, PI 3-kinase and Ca^{2+} signaling upstream of ERK activation in PMNL.

In human platelets, ABA, β-BA, KBA and AKBA induced p38 MAPK activation [38]. ERK1/2 phosphorylation was only activated by non-11-keto BAs, as well as Ca^{2+} influx, arachidonic acid release, p12-LO product formation and thrombin generation. In addition, platelet aggregation was induced by β-BA. The molecular signaling induced by β-BA in platelets might involve Akt as well, which becomes phosphorylated after stimulation. On the other hand, AKBA suppressed Akt phosphorylation and inhibited tumor necrosis factor α (TNF-α)-induced Akt phosphorylation in human myeloid KBM-7 cells [39]. A direct interaction of AKBA and Akt might explain these effects [40].

Some studies identified general effects of *B. serrata* extracts on the immune system. Therefore, an inhibition of C3-convertase of the classical component pathway was described [41]. Leukocyte infiltration was found to be suppressed by a *B. serrata* extract [5], and humoral antibody synthesis was modulated by BAs [42]. A *B. serrata* extract delayed a heart transplant rejection in mice [43]. All these effects are general observations and led to the question of the involved molecular pathways, which still have to be identified.

In experiments analyzing the cytotoxicity of BAs, an apoptotic mode of action was identified. Initial studies describing the growth inhibition of promyocytic HL-60 cells

by a BA mixture isolated from *B. carterii* revealed inhibitory effects on proliferation while cell differentiation was induced [44]. A general inhibitory effect of BAs on DNA, RNA and protein synthesis was identified [45]. Up to now, cell growth inhibition by BEs and BAs were found in several cell lines, including glioblastoma cells, leukemia cells (K562, U937, MOLT-4, THP-1 [46], CCRF-CRM [47], NB4, SKNO-1, ML-1 [48]), liver cancer Hep G2 cells [49], brain tumor cells (LN-18, LN-229) [46], colon cancer HT-29 cells [50,51], prostate cancer PC3 cells [52] and fibrosarcoma HT-1080 cells [53]. An induction of apoptotic mechanisms of a BA mixture in HL-60 cells was shown by morphological cell changes and DNA fragmentation [54]. AKBA as a pure compound induced DNA fragmentation in HL-60 cells, leading to apoptotic cell death [47]. Since HL-60 cells do not express 5-LO constitutively [55], a 5-LO inhibition as molecular basis for the apoptotic induction seems unlikely. The apoptosis-inducing effects may be partly explained by the identification of topoisomerase I and IIa as a target of BAs [47,56,57]. In addition, AKBA and KBA can activate caspase 8, caspase 9 and caspase 3 in liver cancer Hep G2 cells [49].

Generally, there are two pathways of apoptosis induction known. The extrinsic pathway involves the activation of a death receptor like Fas [58]. The activated Fas receptor associates with the Fas associated death domain [59] and procaspase 8 or procaspase 10, which in turn become activated by proteolytic cleavage [60]. Then, the initiator caspase 8 activates the effector caspase 3 in a proteolytic cascade [61]. On the other hand, the intrinsic pathway of apoptosis induction is triggered by a variety of extra- and intracellular stress factors [58]. A release of cytochrome c from the mitochondria can be observed as an early event and a loss of mitochondrial membrane potential might be involved, as well as the permeabilization of mitochondria and activation of Bcl-2 proteins [62]. When cytochrome c is released, it binds to apoptotic protease-activation factor 1 (Apaf1) [63]. This leads to the formation of the apoptosome, which consists of cytochrome c, ATP and procaspase 9. Procaspase 9 becomes activated and activates caspase 3.

In order to analyze whether the intrinsic or the extrinsic pathway is activated by BAs, caspase-inhibitor studies were performed [50]. While caspase 3 and caspase 8 inhibitors blocked the AKBA-induced apoptosis completely, a caspase 9 inhibitor was only partially effective. This implicates an involvement of the extrinsic pathway, which may in turn activate caspase 9 as a late event [49]. The apoptosis induction seemed to be

independent of Fas, however [50]. In prostate cancer cells, a death-receptor 5-mediated pathway seemed to be involved in the induction of apoptosis by AKBA [64]. An expressional downregulation of TNF-α-induced antiapoptotic proteins as IAP1/2, XIAP, Bcl-2, Bcl-X_L, Bfl-1/A1 and FLIP by AKBA may contribute to the proapoptotic effects [39]. This effect might be explained by inhibition of the nuclear factor κB (NF-κB) pathway, either by inhibition of Akt [39], or by direct inhibition of IκB kinases (IKK) [65]. In conclusion, several reports exist about the apoptosis inducing properties of BEs and BAs and some parts of the responsible pathways were identified.

2.1.3.2 Pharmacokinetic properties of BAs

The understanding of the pharmacokinetic properties of a drug is very important in order to investigate the molecular mode of action. A single dose of a BE (1,600 mg, orally administered) resulted in plasma concentrations of KBA up to about 1.7 µM, while AKBA was not detected [66]. Another study determined maximum plasma levels of KBA (2.7 µM) [67]. This maximal concentration was reached after 4.5 h, and the mean elimination half life was about 6 h. In the plasma of a patient with a brain tumor treated for 10 days with a BE (4 × 786 mg/day), 0.34 µM KBA, 0.1 µM AKBA, 2.4 µM ABA and 10.1 µM β-BA were found [10]. In Crohn's disease patients treated with BE (3 × 800 mg, 4 weeks), plasma concentrations of 0.04 µM AKBA, 0.33 µM KBA, 4.9 µM ABA and 6.35 µM β-BA were determined [68]. This indicates a higher bioavailability of non-11-keto BAs (ABA and β-BA), while AKBA and KBA were only present in lower concentrations. The effect of food intake on bioavailability was analyzed as well. When applied with a high-fat meal, plasma concentrations of BAs were strongly increased when compared to the fasted state [11]. The permeability of AKBA was very poor while the absorption of KBA was moderate in the Caco-2 model [69]. In addition, KBA was found to be subjected to an extensive phase I metabolism [70]. Neither KBA nor AKBA are substrates for P-glycoprotein, indicating that the low plasma levels are a result of poor absorption [69]. Finally, BAs were found to be inhibitors of cytochrome P450 enzymes, and so a possible interaction with other drugs should be considered while administering BE to humans [71].

2.1.3.3 *In vivo* studies

Several *in vivo* studies have been performed in animals and humans in order to investigate the effects of BEs and BAs. One of the first studies performed in 1969 described analgesic and sedative effects in rats [72], as determined by the hot wire and mechanical compression methods. In a later study, however, the analgesic actions in rats could not be confirmed [73]. It may be possible that the analgesic actions are based on a general reduction of inflammation rather than being a direct effect [2]. BEs and isolated BAs have been tested in several inflammatory animal models since then.

In the rat adjuvant arthritis model, extracts from *B. serrata* and *B. carterii* displayed prominent anti-arthritic activity [73,74]. In a similar model of adjuvant-induced arthritis, application of a BE decreased the urinary excretion of connective tissue metabolites as hydroxyproline, hexosamine and uronic acid [4]. The inhibition of excretion was very prominent in the chronic phase of inflammation. In the bovine serum albumin (BSA)-induced rat arthritis model, oral application of a BA-mixture resulted in lower leukocyte counts in the knee joint [6]. Treatment with a *B. serrata* extract resulted in a reduction of severity and resolution of typical clinical signs in osteoarthritic dogs with manifestations of chronic joint and spinal disease [75]. In a randomized, double-blind, placebo-controlled cross-over study, patients suffering from osteoarthritis were treated with a *B. serrata* extract [76]. All of the 15 extract-treated patients reported an amendment after 8 weeks. In another placebo-controlled study, beneficial effects of a herbomineral formulation containing *B. serrata* extract on osteoarthritis in patients were found [77]. The beneficial effects of a *B. serrata* extract on osteoarthritis were confirmed in a double-blind, randomized and placebo-controlled study [78] and in a randomized, prospective, open-label, comparative study [79]. However, in a study of rheumatoid arthritis, frankincense displayed no beneficial effects [80].

There are indications that frankincense might be effective in treating inflammatory bowel diseases. AKBA attenuated tissue injury scores and decreased the number of rolling and adherent leukocytes in indomethacin-induced ileitis in rats [81]. In dextran sodium sulfate-induced murine colitis, AKBA blunted disease activity and reduced the number of adherent leukocytes and platelets in inflamed colonic venules [82]. However, another study could not confirm the beneficial effects of a *B. serrata* extract in dextran sodium sulfate-induced colitis [83]. In a clinical study, 34 patients with ulcerative colitis

grades II and III were treated with an alcoholic *B. serrata* extract. Several clinical parameters improved, and the treatment with frankincense was not inferior compared to the standard treatment with sulfasalazine [84]. Frankincense seems to be beneficial in the treatment of Crohn's disease as well. In a randomized, double-blind, verum-controlled study the *B. serrata* extract H15^{TM} reduced the Crohn Disease Activity Index in a similar matter as the standard treatment mesalazin [85]. In a study on chronic colitis, 18 of 20 frankincense-extract treated patients showed an improvement in at least one disease parameter, compared to 6 of 10 in the control group receiving sulfasalazine [86].

In order to investigate whether the observed proapoptotic properties of frankincense (see **2.1.3.1**) could lead to a tumor inhibition *in vivo*, several studies were performed. Phorbol-ester-induced increases in skin inflammation, epidermal cell layers, proliferation and tumor promotion were reduced by topical application of a methanolic *B. serrata* extract in mice [87]. Survival time of rats with implanted C6 tumor cells were increased by application of a *B. serrata* extract [88]. In a preclinical study, 19 patients with intracranial tumors received a palliative therapy with the *B. serrata* extract H15^{TM} [89]. No obvious anti-proliferative effect on tumor progression was observed, but there were indications for beneficial effects due to edema reduction. In another trial with patients with brain tumor and progressive edema, no influence of H15^{TM} on tumor growth was observed [90], while the accompanying edema was reduced by treatment with frankincense in some patients.

A *B. serrata* extract was found to be beneficial in the treatment of asthma. In a double-blind, placebo-controlled study, 40 patients were treated with 3×300 mg/day BE for 6 weeks [91]. 70% of BE-treated patients showed an improvement, compared to 27% placebo-treated patients.

2.2   hCAP18 and LL-37

In this study, human cathelicidin antimicrobial protein (hCAP18) and LL-37 were identified as molecular targets of BAs. hCAP18 belongs to the protein family of cathelicidins, and it is the only member of this family expressed in humans [92]. hCAP18 is synthesized as a preproprotein, consisting of a signal sequence, a cathelin domain and an LL-37 domain (see **fig. 2.1**) [93].

signal peptide	cathelin	LL-37
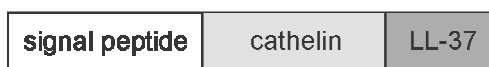
Fig. 2.1: Structure of hCAP18.

Cathelin was first identified as an inhibitor of the cysteine proteinase cathepsin L [94]. This domain is highly conserved in cathelicidins throughout species [95,96]. The cathelin domain can be separated from the LL-37 domain by proteolytic cleavage, resulting in the liberation of LL-37 peptides. Some proteases able to process hCAP18 were identified, among them proteinase-3 [97] from neutrophils and gastricsin from seminal plasma [98]. LL-37 is a small peptide consisting of 37 amino acids. It is thought to be the active component of hCAP18, which itself is generally regarded as an inactive precursor protein. LL-37 belongs to the group of antimicrobial peptides (AMPs), which are characterized by their bactericidal potential [99]. Besides its antimicrobial effects, it was found to modulate the immune response (see **2.2.2**). In sweat, LL-37 was found to be further degraded by serine proteases after liberation from hCAP18, leading to shorter peptides with enhanced antimicrobial properties but weakened immunomodulating effects [100].

2.2.1   Expression pattern and occurrence of hCAP18

hCAP18 is expressed in a large variety of cells, tissues and body fluids, among them leukocytes [101,102], skin [103,104], sweat [105], wound fluid [106], diverse epithelia [107-109], testis [110] and colon mucosa [111]. In addition, hCAP18 was identified in the plasma, where it occurs bound to lipoproteins [112]. hCAP18 expression rates are influenced in several diseases. Expressional upregulation was found in the course of

inflammatory disorders (psoriasis, contact dermatitis) [113-115], bacterial infection [116] and breast cancer [117]. A downregulation was found in atopic dermatitis [118], chronic ulcer epithelium [119], acute myeloid leukemia [120] and during enteric infection [121].

2.2.2   Molecular mode of actions of LL-37

Once liberated from hCAP18 by proteolytic cleavage, LL-37 can exert its biological effects. Initially, antibacterial effects were reported [122], followed by the identification of antifungal [123] and antiviral activities [124]. LL-37 is able to kill bacteria, most likely via an interaction with the membrane [125]. The bacterial cell surface is negatively charged, while the membrane of many mammalian cells has a neutral surface [126]. This allows the cationic LL-37 to target bacterial membranes with a higher binding rate. Nonetheless, some cytotoxic actions of LL-37 on mammalian cells have been described as well. Incubation of LL-37 with leukocytes and T-cells resulted in cytotoxicity [127] and red blood cells were lysed in a similar manner [128]. Since LL-37 is cytotoxic for both bacterial and mammalian cells, it may be considered as a toxin as well [129]. Besides its cytotoxic properties, diverse immunomodulatory effects were found. LL-37 stimulates wound healing [119] and angiogenesis [130] and induces chemotaxis in different cell types such as neutrophils, eosinophils and mast cells [131,132]. In addition, mast cells were shown to degranulate after LL-37-stimulation, leading to a release of pro-inflammatory mediators as histamine and prostaglandins [133]. Three different receptors were found to be activated by LL-37, namely formyl peptide receptor-like 1 (FPRL-1) [134], P2X7 [135] and epidermal growth factor receptor (EGFR) [136]. Receptor activation by LL-37 leads to an intracellular activation of ERK and p38 MAPK in monocytes [137] and keratinocytes [138].

In addition to its antimicrobial and immunomodulatory effects, LL-37 has strong lipopolysaccharide (LPS) binding properties [139]. LPS occurs in the outer membrane leaflet of Gram-negative bacteria and is a strong pro-inflammatory stimulus (see **2.3.1** and **2.3.2**). LL-37 can neutralize the biological activities of LPS by direct binding with a high affinity. LL-37 inhibits the LPS-induced cytokine secretion [140], as well as the LPS-induced nitric oxide and TNF-α release in macrophages [141].

2.3 Lipopolysaccharides

Lipopolysaccharides (LPS) were identified as molecular targets of BAs in this study. They are known to be very powerful immunostimulators (see **2.3.2**) which can cause several critical disease states (see **2.3.3**). An introduction about its origin and its molecular modes of actions is given in the following paragraphs.

2.3.1 Structure and origin of LPS

LPS is an essential component of the outer membrane of various Gram-negative bacteria [142] and is composed of a lipophilic region (lipid A) and a hydrophilic oligo- or polysaccharide portion [143]. The lipid part is anchored in the membrane and the saccharide portion can be divided in two parts, the core region and the O-specific chain (**fig. 2.2**). The core region consists of an oligosaccharide with up to fifteen monosaccharides and is linked to the O-specific chain, which is comprised of repeating saccharide units. Some LPS classes lacking this O-specific chain have been identified, and so two main classes of LPS can be divided [142], the smooth form (S form, with O-specific chain) and the rough form (R form, without O-specific chain). The O-specific chain is highly variable in different bacteria. In most cases, it is a heteropolysaccharide consisting of repeating units of two to eight sugar monomers [143-145]. The core region is a bit more conserved. Two components are characteristic, 3-deoxy-D-manno-2-octulosonic acid (Kdo) and heptopyranose (Hep) [143]. Additional sugars may be present, but the lipid A region is linked to a Kdo molecule in the vast majority of LPS molecules [143,146,147]. The lipid A region is thought to be responsible for biological effects of LPS [148-150]. Most lipid A molecules consist of a phosphorylated disaccharide which is acylated at several sites [143]. Characteristic acyl components are (R)-3-hydroxy fatty acids, which are partly esterified by other fatty acids.
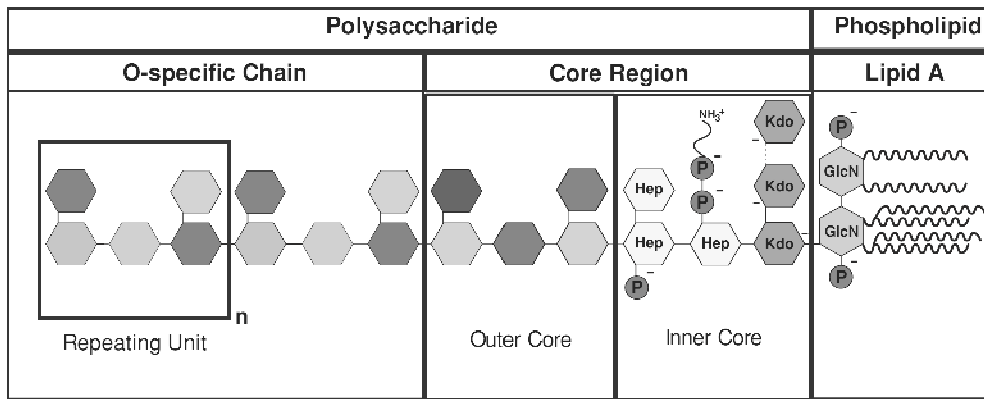
Fig. 2.2: General structure of LPS (S form) from Gram-negative bacteria (modified according to [142]). LPS is composed of an O-specific chain, a core region and lipid A. GlcN, glucosamine, Kdo, 3-deoxy-D-manno-2-octulosonic acid, Hep, heptopyranose.

2.3.2 Signal transduction pathways involved in LPS-signaling

Several cell types respond to exposure to LPS. Primary target cells are monocytes, macrophages, neutrophils and dendritic cells, all expressing membrane-bound CD14 as well as toll-like receptor 4 (TLR4) [151-155]. In a physiological context, a bacterial infection is recognized by the immune system, and phagocytes become activated, as well as humoral serine protease cascades. The adaptive immune response is activated as well, leading to a generation of antibodies, mostly against the O-specific side chain of LPS [143,146]. Elementary parts of the LPS signaling in phagocytes are shown in **fig. 2.3**.
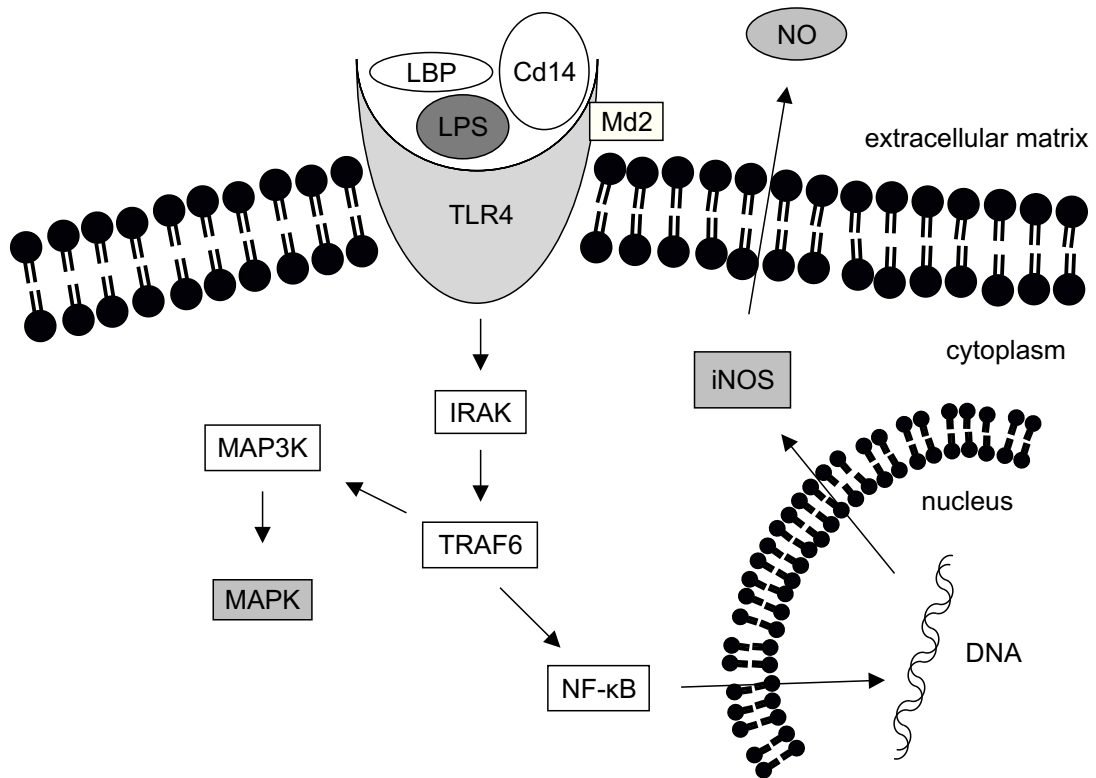
Fig. 2.3: LPS signaling in phagocytes *[142,156]. LPS binds to LBP and CD14 and activate the TLR4/MD2 receptor complex. Interleukin-1 receptor-associated kinase (IRAK) becomes activated and transfers the signal to TNF Receptor Associated Factor 6 (TRAF6). TRAF6 activation results in phosphorylation of MAPK kinase kinases (MAP3Ks), which eventually activate MAPKs. In addition, TRAF6 activate NF-κB, which induces the gene expression of inducible nitric oxide synthase (iNOS). Enhanced iNOS levels lead to an enhanced NO generation.*

LPS binds to membrane-bound CD14 molecules [157]. The binding affinity is greatly enhanced by the presence of lipopolysaccharide binding protein (LBP), a protein common in blood serum [158,159]. The LPS/LBP/CD14-complex activates the TLR4/MD2 receptor complex, which transfers the signal to the cytosolic region [160]. The signal transduction cascade includes the activation of interleukin-1-receptor associated kinases (IRAKs), among them IRAK1 and IRAK4 [161], TRAF6 and a subsequent activation of the NF-κB signaling [153]. Additionally, activation of TRAF6 leads to an activation of several mitogen-activated kinase kinase kinases (MAP3K), which eventually results in the activation of MAPKs [162,163]. Activation of NF-κB leads to a modulation of gene expression. Several pro-inflammatory genes are activated, among them the gene coding for the inducible nitric oxide synthase (iNOS) [164]. iNOS

catalyzes the generation of nitric oxide (NO) from L-arginine [165]. NO is an important messenger molecule involved in many physiological and pathological processes.

2.3.3 LPS-mediated diseases

LPS plays a major role in sepsis and septic shock. Septic diseases are the most common complications in intensive care units (ICU). More than 50% of all ICU patients are affected from these diseases [166]. Sepsis and septic shock are often preceded by a phase of immunosuppression or predominant anti-inflammatory activation [142,167]. This phase might promote bacterial infections [168-170]. The severity of septic syndromes was found to be correlated to the amount of bacteria present in the blood [171-173], while elevated LPS levels were identified in 70-90% of all patients with severe sepsis and septic shock [173-175]. The amount of LPS in the blood correlates with the lethal outcome. LPS triggers the generation of pro- and anti-inflammatory mediators, leading to a state of high fever, hypotension, disseminated intravascular coagulation, multi-organ dysfunction and failure and finally a lethal shock [142].

2.4   Cathepsin G

Cathepsin G (catG) is a serine protease expressed in leukocytes, mainly in neutrophils, but to a lesser extent also in monocytes, myeloid and plasmacytoid dendritic cells [176]. In neutrophils, catG is synthesized during their differentiation process in the bone marrow and is stored in azurophilic granules [177]. It is synthesized as a preproprotein. After cleavage of the signal peptide, a pro-dipeptide is removed by enzymatic cleavage before or during the transport to the granules, resulting in the storage of active catG in the granules.

2.4.1   Functions of cathepsin G

A major function of neutrophils is the killing of invading bacteria. Many bacteria are destroyed by phagocytosis carried out by neutrophils. Internalized bacteria are killed in the phagolysosome, in which the content of azurophilic granules is released (**fig. 2.4**). However, the exact mode of action how catG and other serine proteases kill bacteria is still unknown [177]. A proteolytic activity seems unlikely, since the pH of the acidic

lysosomes is in a different range than the neutral pH optimum of catG [178]. Additionally, synthetic smaller peptides based on catG were found to have microbicidal properties *in vivo* [179,180], indicating that catG might have other functions besides its role as a serine protease.
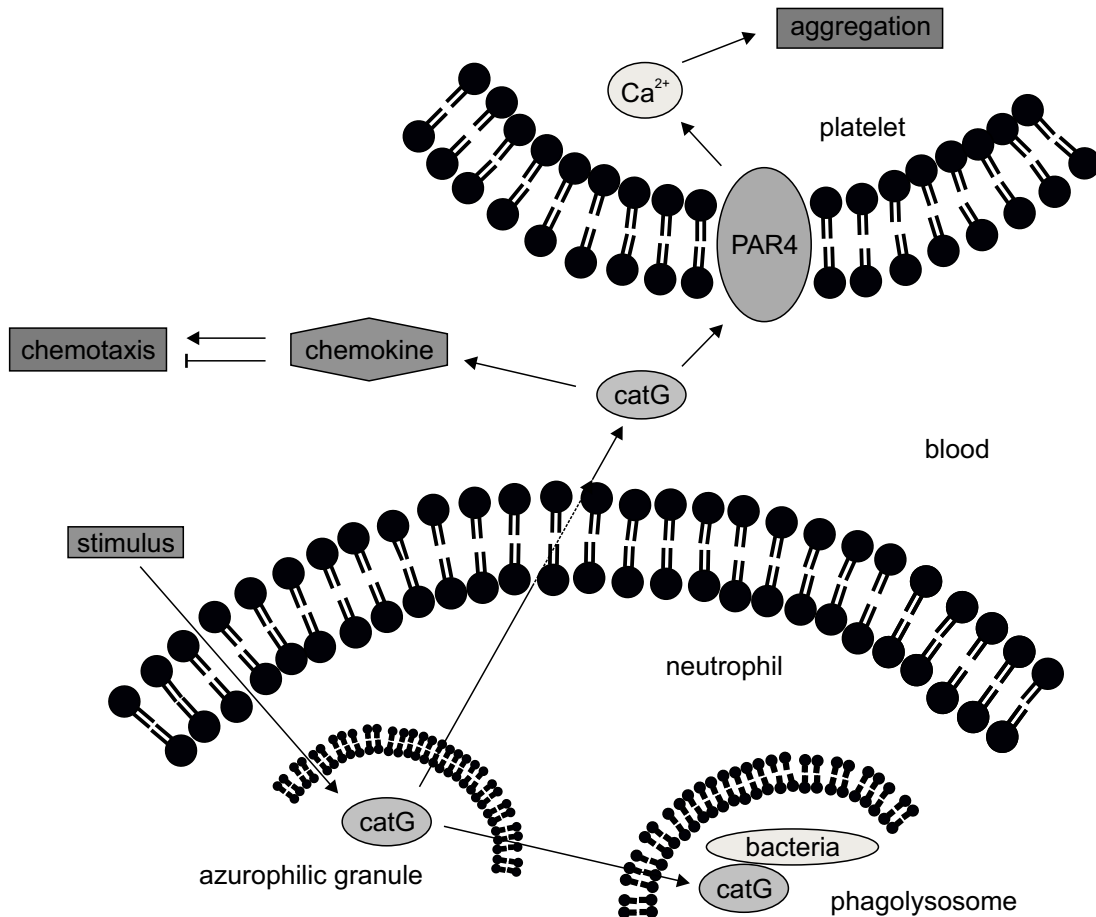
Fig. 2.4: CatG signaling after inflammatory stimulation. *A stimulus leads to the release of catG from azurophilic granules of neutrophils into phagolysosomes and blood. In phagolysosomes, it can kill phagocytosed bacteria. When catG is released into blood, it modifies chemokine activity and activates the protease-activated receptor 4 (PAR4) receptor on platelets, resulting in a Ca^{2+}-dependent platelet aggregation.*

To some extent, azurophilic granules are exocytosed after inflammatory stimulation [181]. CatG gets released and becomes fully activated in the neutral environment of the plasma. Although there are several protease inhibitors present in the plasma, catG retains its activity [182]. This may be explained by the observation that catG is located near the membrane when it is released and the tight adhesion of neutrophils to the extracellular matrix generates a microenvironment, where high-molecular-weight

protease inhibitors cannot enter [183]. Released catG is known to modulate the immune response. It can cleave different types of chemokines [184-187], leading to an enhancement or a reduction of chemotactic chemokine activity, depending on the type of chemokine cleaved. Proteolytic activation of cellular receptors by catG has been reported as well. CatG was described as a direct activator of proteinase-activated receptor 4 (PAR4) on platelets [188]. PAR4 belongs to the protein family of seven transmembrane receptors. After a proteolytic cleavage, a new N-terminus is generated which acts as a tethered ligand activating the receptor [189,190]. A catG mediated activation of platelets results in platelet aggregation, mediated *via* a Ca^{2+}-dependent signal transduction pathway [188]. Taken together, besides its antimicrobial function, catG plays also an immunomodulatory role. It stimulates some pro-inflammatory as well as some anti-inflammatory responses, indicating a complex regulation of the immune system. Most likely the time course of activating and degrading functions is crucial in the catG-depending immune response.

2.5   The protein family Ras

Ras genes were initially identified as transforming agents of the Harvey and Kirsten murine sarcoma virus [191]. The responsible viral genes turned out to be mutated versions of genes which encode for enzymes belonging to the protein superfamily of small GTPases. Six subfamilies have been identified up to now, the Ras, Rho, Ran, Rab, Arf and Kir/Rem/Rad subfamilies [192]. Among the subgroup of Ras proteins, five groups can be classified: p21 Ras, Rap, M-Ras, R-Ras and Ral.

All members of the Ras superfamily of small GTPases are bound to guanine diphosphate (GDP) or guanine triphosphate (GTP) [192]. If GDP is bound, the enzyme is generally considered as inactive, while a binding to GTP leads to an activation of the enzyme. The slow intrinsic GTPase activity converts GTP to GDP, resulting in an inactivation of the proteins. Guanine-nucleotide exchange factors (GEFs) and GTPase activating proteins (GAPs) regulate the activation status of these small GTPases. GEFs catalyze a nucleotide exchange by releasing the bound nucleotide. The released nucleotide is then replaced by the more abundant GTP, resulting in an activation of the enzyme. The inactivation process can be accelerated by GAPs. These proteins bind to

small GTPases and enhance the low intrinsic GTPase activity greatly, leading to an inactivation of these enzymes.

2.5.1   p21 Ras proteins

The group of p21 Ras proteins in humans comprises H-Ras, K-Ras and N-Ras [192]. K-Ras occurs in two alternative splice forms: K-Ras 4A and K-Ras 4B. All p21 Ras proteins are closely related and share about 85% sequence identity. When compared to the other subfamilies of Ras proteins, they have about 40-50% amino acid identity.

p21 Ras proteins are anchored in the membrane by the help of a farnesyl or a geranylgeranyl moiety [193]. In addition, the p21 Ras members H-Ras, N-Ras and K-Ras 4A are palmitoylated, which supports membrane targeting of these enzymes [194,195]. While H-Ras seems to be positioned in lipid rafts, K-Ras 4B is excluded from them [196,197].

Several effector proteins have been identified for the p21 Ras subfamily, like different RalGEFs (RalGDS, Rgl, Rfl/Rgl2 and RPM/Rgl3 [198-202]). Besides GEFs, there are other effectors of p21 Ras, which are involved in p21 Ras-mediated signal transduction pathways. Raf-1, A-Raf and B-Raf, all members of the Raf family of serine/threonine kinases, were found to be activated by p21 Ras proteins, leading eventually to an activation of ERK [203,204]. In addition, the serine/threonine kinase MAPK/ERK kinase kinase-1 (MEKK-1) was found to bind to the effector domain of activated p21 Ras proteins [205]. MEKK-1 activation results in MEK1/2 and ERK1/2 activation, but it activates also c-Jun N-terminal kinase (JNK) and p38 MAPK [206,207]. Besides its role in MAPK signaling, MEKK-1 was also found in the IKK complex, which is involved in the activation of NF-κB [208]. Phosphatidylinositol (PI)-3 kinase is another effector of the p21 Ras subfamily. It binds directly to GTP-bound Ras and becomes activated. $PI(3,4,5)P_3$, produced by PI-3 kinase, binds to Sos1/2 and Vav, which stimulate nucleotide exchange on Rac [209,210].

Ras has been associated with modulation of growth. Cyclin D1, a positive regulator of cell cycle progression, is upregulated by Ras [211]. When Ras is inhibited, the entry and progression through the G_1 phase is blocked [212]. These findings may contribute to the transforming activities observed from activated Ras. On the other hand, there is some evidence that p21 Ras may also induce apoptosis by induction of p19[ARF] or of cell cycle

inhibitors such as p16^{INK4a}, p21$^{Cip1/WAF1}$ and p27^{Kip1} [192]. The Ras-dependent regulation of cellular growth seems therefore to be complex. In addition to the effects on cellular growth, Ras was found to be involved in cell adhesion processes [213]. Ras-transformed cells have a less adhesive phenotype, which may be explained by a suppression of integrin activation [214]. An overexpression of H-Ras resulted in an activation of integrins, however [215]. The exact mode of action how Ras modulates cell adhesion is therefore still not completely understood.

2.5.2 Rap1

Rap1 belongs to the Ras subfamily of Rap GTPases (see **2.5**). This subfamily is comprised of four members: Rap1A, Rap1B, Rap2A and Rap2B. Rap1 is a known mediator of integrin-regulating cellular signals [216-218]. Integrins are cell surface proteins that are important for cell adhesion processes. While Rap1 was described as a regulator of all integrins which are associated with the actin cytoskeleton (**fig. 2.5**), it does not influence intermediate filament associated integrins [219]. This indicates a specific mode of action, and these observations could be confirmed in mice deficient for the Rap-specific GEF RasGRP2, which show impaired platelet adhesion and aggregation [220]. In addition to integrins, cadherins were identified as adhesion molecules which are regulated by Rap1. Cadherins are components of adherence junctions and stabilize cell-cell contact by Ca^{2+}-dependent interactions [221]. A knockdown of a Rap1GEF (Dock4) resulted in the disruption of adherence junctions in osteoblasts [222]. In osteosarcoma cells deficient for Dock4, the adherence junctions could be restored by addition of Dock4 or Rap1. In Ras-transformed Madin-Darby canine kidney cells, active Rap1 restored cadherin-mediated cell-cell adhesion [223]. Both Rap1GEF Epac and Rap1 were shown to mediate the cAMP-induced tightening of cell junctions in endothelia cells [224,225].
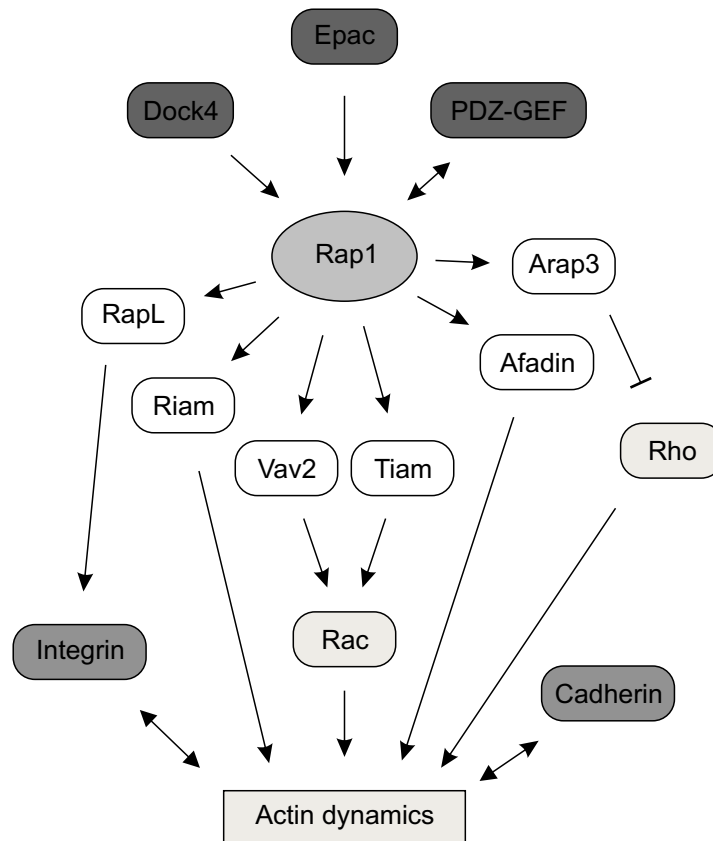
Fig. 2.5: Cellular Rap1 signaling (according to [226]). Rap1 is activated by Epac, Dock4 and PDZ-GEF and activates the effectors RapL, Riam, Vav2, Tiam, Afadin and Arap3. This leads to the modulation of actin dynamics and cell adhesion via integrins and cadherins.

Several Rap1 effectors have been identified up to now, among them Afadin, RapL, Riam, Arap3, Vav2, Tiam1 and PDZ-GEF [226]. Afadin is an adaptor protein that binds to various cell junction proteins [227,228] and was found to be bound by Rap1 [229]. RapL seems to be recruited by Rap1 to activate integrins [230]. Riam was reported to be involved in cell adhesion, and a direct binding of Rap1 was shown to mediate Riam-induced cell spreading and integrin-mediated cell adhesion [231]. Arap3 links Rap1 signaling to Rho signaling. It has a RhoGAP domain and a Rap1 binding domain, and the binding of Rap1 was shown to enhance RhoGAP activity [232]. This may eventually lead to an inhibition of Rho. The RacGEFs Vav2 and Tiam1 were identified as Rap1 effectors as well [233]. Rac is required for Rap1-induced cell spreading, and the activation of RacGEFs may be the link in the signal transduction cascade. PDZ-GEF is besides its function as a Rap1GEF also a Rap1 effector. The activation of PDZ-GEF by Rap1 can be interpreted as a positive feedback control [234]. Taken together, Rap1

proteins seem to be important mediators in controlling cell adhesion processes, as well as other small G proteins.

2.6   Aim of this work

Extracts of the gum resin of *Boswellia* spec. are traditionally used in folk and ayurvedic medicine to treat various diseases since centuries. In the last decades, a growing public interest in medical treatment with natural products became evident. In particular, a great interest in frankincense arose since initial studies proved pharmacological effects *in vivo*. Several animal and clinical studies revealed the efficacy of BEs in the treatment of many inflammatory diseases as bowel diseases (Crohn's disease, ulcerative colitis), chronic arthritis and asthma but also of cancer and cancer-related diseases. In order to develop highly effective drugs, an understanding of the composition of BEs is crucial, as well as the identification of the active principles and their molecular targets. The first active principles identified were BAs, and the identification of 5-LO as a molecular target for BAs provided first knowledge about their molecular mode of action [25]. The growing interest in frankincense resulted in the identification of several other targets besides 5-LO, including HLE, COX-1, IKK, and Akt [235]. Mostly, these targets were identified *in vitro*, while appropriate *in vivo* experiments are still missing. The knowledge of the pharmacokinetic properties of BAs is crucial for the evaluation of the effectiveness of BAs *in vivo*. Several studies analyzed the maximal plasma levels of BAs reached after oral application and demonstrated that AKBA plasma concentrations are considerably lower than the concentration needed for an effective inhibition of many of the identified molecular targets *in vitro*. This led to the question whether an inhibition of these targets by AKBA may actually have *in vivo* relevance. It seemed likely that there are additional targets present for either AKBA or other BAs that reach higher plasma levels. In addition, there may be other active principles present besides BAs which may contribute to the overall anti-inflammatory properties of BEs.

Based on the work of Dr. Lars Tausch (Goethe University, Frankfurt, Germany), who identified catG, hCAP18, Ras and Rap1B as potential BA-binding proteins [40], the study aims to evaluate the pharmacological relevance of these targets. The binding mode was identified (direct/indirect binding), and functional assays were performed to answer the question of a functional consequence. The moieties responsible for target

binding were estimated by structure-activity relationship studies using synthetic BA derivatives. Since it is likely that other compounds from BEs besides BAs might contribute to the anti-inflammatory effect, several additional triterpenes isolated from BEs were tested for their influence on these targets. Furthermore, an additional aim of this study was the identification of novel molecular targets of BAs by utilizing pull-down and functional assays.

BEs as well as BAs possess apoptosis-inducing properties. Different studies identified parts of the underlying signal transduction cascades which are influenced by BEs. However, the exact mode of action mediating this apoptotic effect is still unknown. In order to further investigate the BA-induced apoptosis induction, structure-activity relationship studies were performed using synthetically modified BAs. Although BAs are the best analyzed principles of frankincense, it is reasonable that additional compounds might contribute to the apoptotic effects of BEs as well. Therefore, several triterpenes derived from frankincense were evaluated for their apoptosis-inducing properties.

Taken together, the identification and characterization of new molecular targets, as well as the elucidation of the apoptosis-inducing mechanisms should provide new insights into the molecular mechanisms by which frankincense exert its anti-inflammatory and pro-apoptotic activities.

3.   Material and Methods

3.1   Materials

The following chemicals and materials were obtained from the stated manufacturers.

5-HETE (5-hydroxyeicosatetraenoic acid)	Cayman Chemical (Tallin, Estonia)
Acrylamide solution 30% (37.7:1)	AppliChem GmbH (Darmstadt, Germany)
α-Amyrin	Extrasynthese (Genay, France)
Agar-Agar	Merck KGaA (Darmstadt, Germany)
Ammonium persulfate	AppliChem GmbH (Darmstadt, Germany)
Anti-β-actin (rabbit) antibody	Santa Cruz Biotechnology, Inc. (Heidelberg, Germany)
Anti-caspase-3 (mouse) antibody	Prof. Wesselborg (Tübingen, Germany)
Anti-caspase-8 (mouse) antibody	Prof. Wesselborg (Tübingen, Germany)
Anti-iNOS (rabbit) antibody	Cell Signaling Technologies (Danvers, USA)
Anti-Rap1B (rabbit) antibody	Santa Cruz Biotechnology, Inc. (Heidelberg, Germany)
Anti-CatG (rabbit) antibody	Enzo Life Sciences GmbH (Lörrach, Germany)
Anti-LL-37 (rabbit) antibody	PANATecs GmbH (Tübingen, Germany)
Anti-Ras (rabbit) antibody	Cell Signaling Technologies (Danvers, USA)
Anti-phospho-p44/42 (pERK1/2, mouse) antibody	Cell Signaling Technologies (Danvers, USA)
Anti-phoshpo-p38 MAPK (rabbit) antibody	Cell Signaling Technologies (Danvers, USA)
Anti-cleaved PARP (rabbit) antibody	Cell Signaling Technologies (Danvers, USA)

2-mercaptoethanol	Carl Roth GmbH + Co. KG (Karlsruhe, Germany)
BAs	Prepared as described [236,237]
BCIP (5-bromo-4-chloro-3-indolylphosphate toluidine salt)	AppliChem GmbH (Darmstadt, Germany)
Bromphenol blue (3',3'',5',5''-tetrabromophenolsulfonphthalein)	Merck KGaA (Darmstadt, Germany)
Calcein-AM	Invitrogen GmbH (Karlsruhe, Germany)
Calcium chloride	AppliChem GmbH (Darmstadt, Germany)
λ-carrageenan (type IV)	Sigma-Aldrich (Milan, Italy)
catG	AppliChem GmbH (Darmstadt, Germany)
catG inhibitor I	Calbiochem (Bad Soden, Germany)
Chemotx® plates	Neuroprobe, Inc. (Gathersburg, USA)
Coomassie brilliant blue G250	AppliChem GmbH (Darmstadt, Germany)
Cytochalasin B	AppliChem GmbH (Darmstadt, Germany)
DMEM (Dulbecco's modified Eagle medium, high glucose, 5.4 g/l)	PAA (Coelbe, Germany)
DMSO (dimethyl sulfoxide)	Carl Roth GmbH + Co. KG (Karlsruhe, Germany)
EAH-Sepharose 4B	GE Healthcare Bio-Sciences (Freiburg, Germany)
FCS (fetal calf serum)	PAA (Coelbe, Germany)
Fura-2/AM (acetoxymethylester)	Alexis Corp. (Lausen, Switzerland)
Glycerol	Caesar & Lorentz GmbH (Hilden, Germany)
(L)-Glycine	AppliChem GmbH (Darmstadt, Germany)
GSH-Sepharose (Glutathione Sepharose 4B)	GE Healthcare Bio-Sciences (Freiburg, Germany)

HEPES (4-(2-hydroxyethyl)-1-piperazineethanesulfonic acid)	PAA (Coelbe, Germany)
H-Ras	Jena Bioscience GmbH (Jena, Germany)
Interferon-γ (mouse)	Peprotech GmbH (Hamburg, Germany)
IPTG (isopropyl-β-D-thiogalactopyranoside)	AppliChem GmbH (Darmstadt, Germany)
Leupeptin	AppliChem GmbH (Darmstadt, Germany)
LL-37	PANATecs GmbH (Tübingen, Germany)
Methanol	Merck KGaA (Darmstadt, Germany)
Milk powder (blotting degree)	Carl Roth GmbH + Co. KG (Karlsruhe, Germany)
NBT (nitro-blue tetrazolium chloride)	Roche Diagnostics (Mannheim, Germany)
NP-40 (Nonidet® P40)	AppliChem GmbH (Darmstadt, Germany)
Nycoprep	PAA (Coelbe, Germany)
Penicillin	PAA (Coelbe, Germany)
peqGOLD prestained protein marker IV	PEQLAB Biotechnologie GmbH (Erlangen, Germany)
Polymyxin B	Enzo Life Sciences GmbH (Lörrach, Germany)
Pyrogene® Recombinant factor C endotoxin detection system	Lonza (Basel, Switzerland)
RPMI 1640 (Roswell Park Memorial Institute medium 1640)	PAA (Coelbe, Germany)
SDS (sodium dodecyl sulfate)	Carl Roth GmbH + Co. KG (Karlsruhe, Germany)
Streptomycin	PAA (Coelbe, Germany)
Staurosporine	Calbiochem (Bad Soden, Germany)
TEMED (Tetramethylethylenediamine)	Carl Roth GmbH + Co. KG (Karlsruhe, Germany)
Thrombin	GE Healthcare Bio-Sciences (Freiburg,

	Germany)
Tricin (N-[Tris(hydroxymethyl)methyl]glycine)	AppliChem GmbH (Darmstadt, Germany)
Tris (2-amino-2-(hydroxamethyl)-1,3-propanediol)	AppliChem GmbH (Darmstadt, Germany)
Triton X-100	Carl Roth GmbH + Co. KG (Karlsruhe, Germany)
Trypsin/EDTA (ethylenediaminetetraacetate) solution	PAA (Coelbe, Germany)
Tween®-20	Carl Roth GmbH + Co. KG (Karlsruhe, Germany)
Urea	AppliChem GmbH (Darmstadt, Germany)

Plastic material such as cell culture flasks, microplates and additional cell culture materials were obtained from Greiner bio-one (Frickenhausen, Germany).

All other chemicals not listed were obtained from Sigma-Aldrich (Deideshofen, Germany), unless stated otherwise.

3.2   Cell culture

All cells were cultured in a cell incubator at 37 °C and 6% CO_2 (Heracell, Heraeus, Hanau, Germany).

3.2.1   RAW264.7

RAW264.7 is a mouse leukemic monocyte cell line. It was isolated from an ascites of an induced tumor (*i.p.* injection of Abselon Leukemia Virus) in a male mouse [238]. RAW264.7 cells were cultured in DMEM medium supplemented with fetal calf serum (FCS, 10%), penicillin (100 U/ml) and streptomycin (100 µg/ml). After adherent cells reached a confluence of around 70%, the supernatant was exchanged by fresh medium.

Then, cells were scraped, diluted to 3×10^5 cells/ml in fresh medium and transferred into a new cell culture flask.

3.2.2 Jurkat A3

Jurkat T lymphocytes were isolated from the blood of a 14 year old boy with acute lymphoblastic leukemia [239]. Jurkat A3 cells were provided by Dr. John Blenis, Boston, MA. Cells were cultured in RPMI 1640 with 10% FCS, 10 mM HEPES, penicillin (100 U/ml) and streptomycin (100 µg/ml). After three days of growth, cells were diluted to 2×10^5 cells/ml in fresh medium.

3.2.3 HL60

The HL60 cell line was isolated from the blood of a woman with acute myeloid leukemia [240]. These cells are mainly premyeloid cells, which are able to differentiate after stimulation into granulocytes or monocytes/macrophages [240,241]. HL-60 cells were obtained from the American Type Culture Collection (ATCC). Cells were cultured in RPMI 1640 supplemented with 10% FCS, penicillin (100 U/ml) and streptomycin (100 µg/ml). After three days of growth, cells were diluted to 2×10^5 cells/ml in fresh medium.

3.3   Isolation of neutrophils from buffy coats

Venous blood was collected from healthy human donors by the University Hospital Tübingen (Germany). Leukocyte concentrates (buffy coats) were obtained by centrifugation at $4,000 \times$ g for 20 min. The concentrates were diluted in an equal volume of phosphate-buffered saline (PBS, 1 mM KH_2PO_4, 3 mM Na_2HPO_4, 154 mM NaCl, pH 7.4) before dextran solution (5%, in PBS, w/v) was added in a ratio of 4:5. After 30 min, the supernatant was carefully collected and centrifuged ($800 \times$ g, 10 min, room temperature (RT)) on Nycoprep cushions. At this stage, the blood cells are separated in fractions. The supernatant consists of platelets, the peripheral mononuclear blood cells are located in the interphase, and neutrophils are pelleted.

The supernatant as well as the interphase was discarded and the pelleted cells were washed in PBS. For the lysis of erythrocytes, 10 ml H_2O was added and incubated for 45 sec. The lysis was stopped by addition of 40 ml PBS. Finally, cells were washed two times with PBS and resuspended in PBS supplemented with glucose (1 mg/ml).

3.4   Isolation of platelets from buffy coats

Venous human blood was separated in fractions by dextran sedimentation and centrifugation on Nycoprep cushions as described in **3.3**. The supernatant (platelet-rich plasma) was collected and mixed with PBS (pH 5.9, 3:2, w/v). After centrifugation $(2,100 \times g, 15 \text{ min})$, cells were washed with PBS/NaCl 0.9% (1:1, v/v) and resuspended in PBS (pH 5.9) supplemented with glucose (1 mg/ml).

3.5   Isolation of PBMCs and monocytes from buffy coats

After dextran sedimentation of blood and centrifugation on Nycoprep cushions (see **3.3**), the interphase containing peripheral blood mononuclear cells (PBMCs) was collected. Cells were washed two times in PBS containing EDTA (2 mM), and in case of the peripheral blood mononuclear cell isolation, they were resuspended in PBS and counted (see **3.6**). For the isolation of monocytes, the cells were resuspended in RPMI 1640 supplemented with 2 mM glutamine, 20% FCS, penicillin (100 U/ml) and streptomycin (100 µg/ml). Cells were transferred into cell culture flasks and left for 3 h at 37 °C and 6% CO_2. Then, cells in suspension (mainly lymphocytes) were removed. Adherent monocytes were detached and resuspended in PBS supplemented with glucose (1 mg/ml) and $CaCl_2$ (1 mM). Finally, cells were counted (see **3.6**).
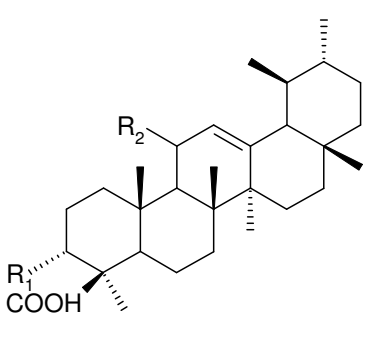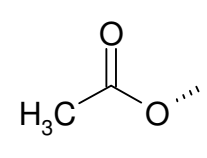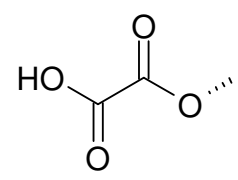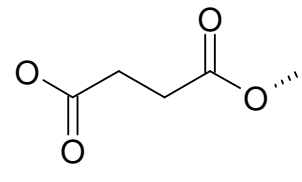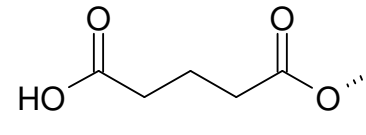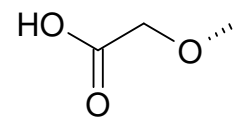
3.6   Cell counting

In order to determine cell numbers, cells were mixed with trypan blue (0.2%, 1:1, v/v) and counted on a Bürker hemocytometer under a light microscope. Viable cells appear unstained while dead cells are stained blue.

3.7   Isolation of BAs and synthesis of BA derivatives
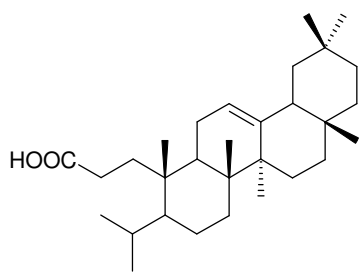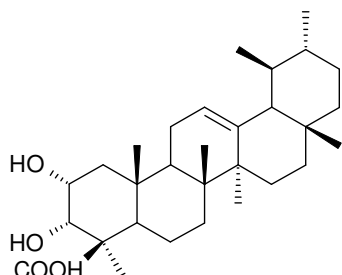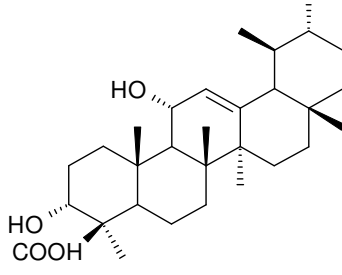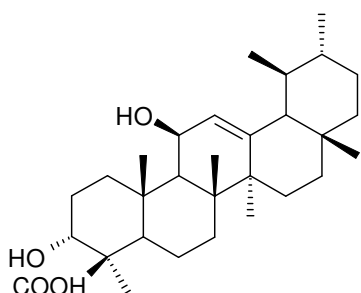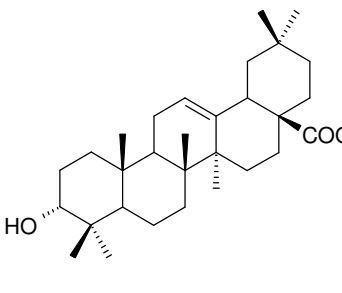
The isolation of naturally occurring BAs and triterpenes were carried out as previously described [236]. Syntheses of new BA derivatives as well as of new triterpenes were performed as previously described [237]. Both isolation and syntheses were carried out by Dr. Nicole Kather (University of Saarland, Saarbrücken). Molecular structures of synthetic BAs modified at the C-3 and C-11 position are shown in **tab. 3.1**.

Tab. 3.1: Structures of naturally occurring and synthetic BAs.

Structure	R₁	R₂	name
	HO⁗	H	β-BA
		O	KBA
	H₃C—C(=O)—O⁗	H	ABA
		O	AKBA
	HO—C(=O)—C(=O)—O⁗	H	oxBA
		O	oxKBA
	O—C(=O)—CH₂—CH₂—C(=O)—O⁗	H	sucBA
		O	sucKBA
	HO—C(=O)—CH₂—CH₂—CH₂—C(=O)—O⁗	H	gluBA
		O	gluKBA
	HO—C(=O)—CH₂—O⁗	H	ether-BA (eBA)
		O	ether-KBA (eKBA)

Besides C-3- and C-11-modified BA derivatives, additional derivatives from triterpenes derived from frankincense were synthesized (**tab. 3.2**). Both synthesis and isolation of all triterpenes were carried out by Dr. Nicole Kather (University of Saarland, Saarbrücken).

Tab. 3.2: Structures of diverse triterpenes and BA derivatives derived from frankincense extracts.

Structure	Structure	Structure
4(23)-dihydro-nycthanthinic acid (DH-nyc)	cis-diol-BA	11α-OH-BA
11β-OH-BA	oleanolic acid	

3.8   Determination of protein concentration

Protein concentrations were analyzed by using a colorimetric protein assay (DC Protein Assay, Biorad). Different concentrations of BSA (0.2 mg/ml – 1.5 mg/ml) were used as protein standards. 5 µl of standards and samples were transferred into a 96-well microplate. 25 µl reagent A' and 200 µl reagent B were added and the plate was mixed. After 15 min, absorptions at 750 nm were measured in a microplate reader (VersaMax^{TM}, Molecular Devices Inc., Sunnyvale, CA, USA). The absorption was plotted against the standard concentrations. The concentrations of unknown samples were calculated with the help of a linear regression.

3.9   Electrophoresis

To separate proteins with molecular masses greater than 20 kDa, a discontinuous electrophoresis system was used [242]. Polyacrylamide was used as a matrix with densities between 8 and 16% acrylamide, depending on the separated samples.

In order to separate proteins with molecular masses smaller than 20 kDa, a tricine gel system was used [243]. A running gel (8 - 16% acrylamide/N,N-methylenebisacrylamide, 33% glycerol, 0.07% APS, 0.07% TEMED, 1 M Tris, 6% SDS, pH 8.45) was cast below a spacer gel (10% acrylamide/N,N-methylenebisacrylamide, 0.1% APS, 0.1% TEMED, 1 M Tris, 6% SDS, pH 8.45) and a stacking gel (4% acrylamide/N,N-methylenebisacrylamide, 0.1% APS, 0.1% TEMED, 3.3% APS, 3.3% TEMED, 1 M Tris, 6% TEMED, pH 8.45).

The electrophoresis was carried out in a Mini Protean system (Bio-Rad, Hercules, CA, USA). All samples were separated for 15 min at a constant current of 80 V and 120 V afterwards.

3.10   Western Blotting

Western blotting was performed after electrophoretic separation of samples (see **3.9**). Proteins were transferred to nitrocellulose membranes (Amersham Pharmacia, Little

Chalfont, UK) by using an electroblotting system (90 V, 90 min, in transfer buffer (48 mM Tris, 40 mM glycine, 0.1 mM SDS, 20% methanol (v/v), tank blotting method, BioRad Mini Trans-Blot® cell, BioRad Powerpac™ Basic, Hercules, CA). Transferred proteins were fixed and stained by transferring the membrane in a Ponceau-S solution (5% Ponceau S in 5% acetic acid). After scanning the membranes (AGFA SnapScan 1236, AGFA Graphics Germany GmbH & Co. KG, Germany), the staining solution was washed out by shaking the membranes in TBS (50 mM Tris, 100 mM NaCl, pH 7.4) for 10 min.

Free binding sites were blocked by 5% dry milk (w/v) and 0.1% Tween-20® in TBS, or 5% bovine serum albumin (w/v) and 0.1% Tween-20® in TBS, respectively. After 1 h of constant shaking, membranes were washed with TBS for three times and transferred into specific antibody solutions (primary antibodies produced in rabbits or mice, diluted 1:1,000 in TBS and 0.1% Tween-20®) over night at 4 °C with constant agitation. Membranes were then intensively washed three times with TBS, before they were transferred into the secondary antibody solutions (dilution 1:1,000 to 1:20,000 in TBS-Tween® (0.1%), depending on the detection system used). The secondary antibodies bind to rabbit or mice proteins and are coupled to horseradish peroxidase or alkaline phosphatase. After three washing steps with TBS-Tween® (0.1%), secondary antibodies were detected in an ECL chemiluminescence system (GE Healthcare Bio-Sciences, Freiburg, Germany) or by a colorimetric method.

The ECL detection system was used according to manufacturer's instructions. Briefly, proteins were visualized by addition of horseradish peroxidase (HRP)-substrate Amersham™ ECL Western Blotting detection reagent (GE Healthcare Bio-Sciences, Freiburg, Germany). Then, the membranes were placed in an X-ray film cassette. A sheet of autoradiography film was placed above the membrane, and after an exposure time of 5 sec to 60 min, the film was developed in a development machine (CP 1000 AGFA Healthcare N.V., Mortsel, Belgium).

For the colorimetric detection, membranes were first equilibrated in detection buffer (100 mM Tris (pH 9.5), 100 mM NaCl and 50 mM $MgCl_2$). Then, nitro blue tetrazolium chloride (NBT) and 5-bromo-4-chloro-3-indolyl phosphate (BCIP, 0.03%, w/v, each) were added. The colorimetric reaction was stopped by washing with TBS and EDTA (2 mM) when bands became visible.

3.11 Coomassie staining of SDS-Gels

Proteins in SDS-Gels were stained with Coomassie brilliant blue G-250. Following SDS-polyacrylamide gelelectrophoresis (SDS-PAGE) (see **3.9**), gels were washed three times with water. Then, staining solution (Coomassie brilliant blue G-250, 70 mg/l, in 35 mM HCl) was added. The gels were heated in a microwave (without boiling) until stained bands became visible. The unbound dye was washed out with water afterwards.

3.12 Mass spectrometric analysis

Following protein-pull down experiments and electrophoretic separation of precipitated proteins (see **3.13** and **3.9**), protein bands were excised and digested. Matrix-assisted laser desorption ionization-time of flight-mass spectrometry (MALDI-TOF-MS) experiments were performed in cooperation with Dr. Lars Tausch (University of Frankfurt) and Prof. Dr. Michael Karas (University of Frankfurt, Germany) on an Ultraflex TOF/TOF mass spectrometer (Bruker Daltonics Inc., Manning Park Billerica, MA) [40]. Samples were dissolved in water/acetonitrile/TFA (29.5/70/0.5, v/v/v). As matrix, 3 mg/ml α-cyano-4-hydroxycinnamic acid (Bruker Daltonics Inc., Manning Park Billerica, MA, USA) dissolved in water/acetonitrile/TFA (29.5/70/0.5, v/v/v) was used. Analyte and matrix were spotted consecutively (1:1) on a stainless steel target before they were dried at room temperature. In order to reduce salt contamination, samples were washed with ice-cold formic acid (5%). Resulting spectra were externally calibrated using a Sequazym^{TM} Peptide Mass Standard Kit (Applied Biosystems, Foster City, CA, USA). An internal calibration was performed by usage of a tryptic auto digestion peptide (*m/z* 2163.0564). Processing of the spectra were done in flexAnalysis 2.2 (Bruker Daltonics Inc., Manning Park Billerica, MA, USA) using the SNAP algorithm (maximal peak number: 150, quality factor threshold: 40, signal to noise threshold: 3). Using the NCBInr database, proteins were identified by Mascot (peptide mass tolerance: 100 ppm, maximum missed cleavages: 1; Matrix Science, Boston, MA, USA). Proteins with a score of 76 or higher were considered significant ($p < 0.05$).

3.13   Immobilization of BAs and pull-down assays

For pull-down experiments, KBA and β-BA were linked *via* the C3-OH-moiety and a glutaric acid linker to EAH sepharose 4B beads as previously described [237]. The resulting constructs are shown in **fig. 3.1**. Immobilizations were performed by Dr. Nicole Kather (University of Saarland, Saarbrücken). In order to identify unknown binding partners of BAs, the immobilized molecules were incubated with isolated proteins or with cell lysates. Bound molecules were analyzed by a modified LAL assay (see **3.14**) or SDS-PAGE (see **3.9**) in conjunction with MALDI-TOF (see **3.12**) or Western blotting (see **3.10**).
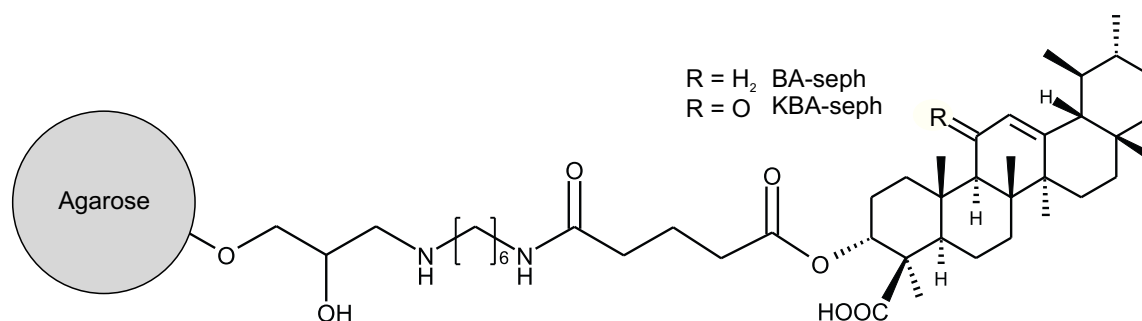
Fig. 3.1: Structure of immobilized β-BA (BA-seph) and KBA (KBA-seph).

LPS (1 µg), LL-37 (0.5 µg), catG (0.5 µg/ml), H-Ras (1 µg) or Rap1B (2 µg) were solubilized in 375 µl binding buffer (50 mM HEPES (pH 7.4), 200 mM NaCl, 1 mM EDTA) supplemented with Triton-X 100 (1%) and BSA (0.02%). Alternatively, cell lysates were prepared. For platelets and HL60 cells, cells (2×10^8 platelets, 1.25×10^7 HL60) were centrifuged ($850 \times g$, 3 min, 4 °C) and resuspended in 75 µl lysis buffer (45 mM HEPES, pH 7.4; 180 mM NaCl; 0.9 mM EDTA; 1% Triton-X 100). After sonification (2×8 sec, Branson B-12, Branson Ultrasonics Corporation, Danbury, CT), lysates were centrifuged ($15,800 \times g$, 10 min, 4 °C) and the supernatants were collected. Finally, binding buffer was added to a total volume of 100 µl. For analysis of catG from neutrophils, cells (1×10^8/ml, 100 µl) were prewarmed for 2 min at 37 °C. Then, cytochalasin B (20 µM) was added for 5 min, followed by an addition of fMLP (5 µM) for 5 min. Samples were rested for 5 min on ice, before cells were spun down ($2,500 \times g$, 10 min, 4 °C) and the supernatant was collected. Lysis buffer was added to a total volume of 100 µl. 150 µl sepharose slurry (50% in H_2O, v/v) was added to isolated protein solutions or cell lysates and incubated overnight at 4 °C under slow constant

rotation. Then, the supernatants were collected and the sepharose beads were intensively washed for three times with binding buffer. Precipitated molecules were either eluted by addition of an equal volume of urea (4 M) or SDS-loading buffer (20 mM Tris (pH 8.0), 2 mM EDTA, 10% 2-mercaptoethanol (v/v), 5% SDS (v/v)). In case of urea elution, eluted LPS as well as LPS in the incubation supernatant were quantified as described in chapter **3.14**. Samples which were eluted by SDS-loading buffer were heated (5 min, 95 °C) and spun down (15,800 × g, 10 min, 4 °C). Supernatants were collected and frozen before they were analyzed by electrophoretic (see **3.9**), mass spectrometric (see **3.12**) and Western blot (see **3.10**) methods.

3.14   Measurement of LPS activities

LPS activities were quantified by using a modified LAL assay kit (Pyrogene®) according to the manufacturer's instructions. Briefly, 100 µl LPS (10 endotoxin units (EU)/ml, from *E. coli* O55:B5) was incubated with 2 µl testing solutions at 37 °C for 10 minutes. Then, 100 µl of a mixture of buffer, substrate and recombinant factor C were added. Generated fluorescence (excitation: 355 nm, emission: 460 nm) was measured in a fluorescent plate reader (Victor[3], PerkinElmer, Rodgau-Jügesheim, Germany) directly and after 60 minutes of incubation.

3.15   Measurement of LL-37 generation

Neutrophils (5×10^7/ml) were incubated with cytochalasin B (10 µM) and BAs for 5 min at 37 °C. Then, fMLP (1 µM) was added. The incubation was stopped after 1 min. by addition of SDS-loading buffer (40 mM Tris (pH 8), 4 mM EDTA, 10% SDS (w/v), 20% 2-mercaptoethanol) in a ratio of 1:3. Samples were heated (95 °C, 5 min) and frozen, before the LL-37 and hCAP18 levels were analyzed by electrophoretic (see **3.9**) and Western blot (see **3.10**) methods.

3.16   Determination of LL-37 activity

In order to determine LL-37 activities, its LPS-inhibiting potential was utilized. In a cellular assay, 2.5×10^7 neutrophils were dissolved in 1 ml PG buffer (PBS + 1 mg/ml glucose). Then, the cells were stimulated with cytochalasin B (10 µM) for 5 min and fMLP (1 µM) for 5 min at 37 °C. In parallel, 1 ml of citrated blood was collected from donors (University Hospital, Tübingen). Similarly, the blood was incubated with cytochalasin B (10 µM) for 2 minutes and fMLP (2.5 µM) for additional 5 minutes at 37 °C. Afterwards, both neutrophil and blood samples were centrifuged (600 × g, 5 minutes, 4 °C) before the supernatant and the plasma were collected.

LPS (10 EU/ml, 100 µl, from *E. coli* O55:B5) was preincubated for 10 minutes at 37 °C with LL-37 (0.1 µM), neutrophil supernatant (1 µl) or blood supernatant (0.4 µl) and testing compounds. Then, buffer, substrate and recombinant factor C was added and the LPS activities were determined as described in **3.14**.

3.17   Determination of released nitrite

The amount of nitrite in cell culture supernatants was determined *via* the Griess reaction [244]. RAW264.7 macrophages (2.5×10^6/ml, 100 µl) were incubated with LPS (1 µg/ml, from *E. coli* O111:B4) and test compounds at different concentrations for 20 h. Then, the supernatant was collected and mixed with an equal volume of napthylethylenediamin-dihydrochloride (1 mg/ml) and sulfanilamide (10 mg/ml in 5% H_3PO_4). After 15 minutes, the absorption at 540 nm was measured in a microplate reader (VersaMax^{TM}, Molecular Devices Inc., Sunnyvale, CA, USA).

3.18   Analysis of iNOS expression

RAW264.7 macrophages (2.5×10^5, in 100 µl) were incubated with LPS (1 µg/ml, from *E. coli* O111:B4) or interferon-γ (IFN-γ, 10 ng/ml) and test compounds at different concentrations for 20 h. Then, 75 µl of the supernatant was replaced by lysis buffer (20 mM Tris (pH 7.4), 150 mM NaCl, 2 mM EDTA, 1% Triton X-100 (v/v), 0.5% NP-40 (v/v)). Cells were lysed on ice while shaking for 10 minutes. SDS-loading buffer (40 mM Tris (pH 8.0), 4 mM EDTA, 20% 2-mercaptoethanol (v/v), 10% SDS (v/v)) was

added and the sample was heated for 5 minutes at 95 °C. Samples were frozen before they were analyzed by Western blotting (see **3.10**)

3.19 Cathepsin G activity assay

CatG activity was measured in a photometric assay. In order to obtain a catG-rich solution [245], neutrophils (2.5×10^7/ml) or venous blood were stimulated with cytochalasin B (10 µM) for 5 min and fMLP (2.5 µM) for additional 5 min at 37 °C. After centrifugation at $1,200 \times g$ (10 min, 4 °C), the supernatant was collected as a source of catG. In a 96-well plate, buffer (180 µl, 100 mM HEPES (pH 7.4), 500 mM NaCl) was mixed with N-suc-ala-ala-pro-phe-pNA (20 µl, 1 mM) and the testing compounds. The photometric reaction was started by addition of 10 µl enzyme solution (neutrophil/blood supernatants or isolated enzyme (1 µg/ml), respectively). The absorption at 405 nm was measured in a microplate reader (Victor^3, PerkinElmer, Rodgau-Jügesheim, Germany) for 110 min. The enzymatic activity of catG was determined by the progress curve method. The activity of catG in presence of a testing substance was compared to the catG activity in presence of the vehicle control.

3.20 Quantification of intracellular Ca^{2+} concentrations

In order to quantify intercellular Ca^{2+} concentrations, blood cells (1×10^8 platelets, 1×10^7 neutrophils or 1×10^6 monocytes) were probed with fura-2-AM (2 µM) for 30 minutes at 37 °C in the dark. Then, cells were washed with PG buffer (PBS + 1 mg/ml glucose), resuspended in 1 ml PG buffer and incubated with testing substances for 10-15 minutes at 37 °C. The whole sample was transferred into a fluorimeter cuvette in a spectrofluorimeter (Aminco-Bowman series 2, Thermo Spectronic, Rochester, NY). $CaCl_2$ (1 mM) was added, and after one minute of constant stirring, the measurement was started by recording fluorescence emission at 510 nm after excitation at 340 and 380 nm. The basal fluorescence was measured for 30 sec, before a specific stimulus was added (100 nM cathepsin G or 1 µM fMLP). After 40 sec, Triton X-100 (5%) was added and after additional 15 sec, EDTA (10 mM) was added. The measurement was stopped after the signal reached a constant level. The intracellular Ca^{2+} concentration was calculated as described [246].

3.21 Chemotaxis assay

Chemotactic activity was analyzed by using a chemotaxis assay kit (Chemotx[®], Neuroprobe, Inc., Gaithersburg, USA). Neutrophils (4×10^7/ml) were incubated with calcein-AM (2.5 µg/ml) for 30 min at 37 °C. Cells were intensively washed with PBS and resuspended in chemotaxis medium (RPMI with HEPES (10 mM) and 10% FCS (v/v)), leading to cell densities of 2×10^6 cells/ml. Chemotaxis medium (29 µl) and different stimuli (fMLP, BAs or LL-37) were added to the wells of a 96-well-Chemotx[®] plate. For quantification, neutrophils (25 µl) were transferred at different cell densities (up to 2×10^6 cells/ml) in additional wells. Then, a filter plate with 8 µm pores was mounted on top of this plate. Neutrophils (25 µl) were added to the top side of the filter above the wells containing media with a stimulus, but not on top of the quantification wells. The whole plate was transferred to an incubation chamber (6% CO_2, 37 °C) for 1 h. Afterwards, the remaining fluid on top of the filter was washed away with PBS. Cells that were attached to the top side of the filter were gently scraped away by a cotton bud. Fluorescence was detected by a fluorescence plate reader (Victor[3], PerkinElmer, Rodgau-Jügesheim, Germany) (excitation: 485 nm, emission: 535 nm). For quantification, cell densities of the quantification wells were plotted against fluorescent emission. A linear regression was made, and the number of migrated cells in the sample wells was calculated by using the obtained regression formula.

3.22 Cell migration assay

Cell culture inserts (8 µm pore size, BD Biosciences, Heidelberg) were coated by addition of matrigel (0.15 mg/insert) and incubated over night at 4 °C. Then, the inserts were washed with RPMI and transferred into 24-well plates (BD Biosciences, Heidelberg). The wells were filled with 350 µl RPMI supplemented with 10% FCS and fMLP (0.1 µM), before neutrophils (100 µl, 1×10^6 cells/ml) were transferred into the inserts. The plates were incubated for 40 min at 37 °C and 6% CO_2. Then, the cell suspension of the inserts was removed and the upper side of the membrane was carefully cleaned by a cotton bud. The bottom side of the membrane was washed with PBS before the membrane was stained with crystal violet (0.25%). After 10 min, the membrane was washed with PBS and dried afterwards. Cells migrated into the membrane were counted under a light microscope.

3.23   Carrageenan-induced pleurisy

The efficacy of BA derivatives on carrageenan-induced pleurisy was analyzed in an *in vivo* model of inflammation. Animal care complied with the European Economic Community regulations (Official Journal of E.C. L358/1 12/18/1986) and with Italian protocols (Ministerial Decree 116192). GluBA and oxBA were dissolved in a saline (0.9%, v/v) / DMSO (4%, v/v) solution. These solutions were injected *i.p.* (1 mg/kg or 5 mg/kg animal weight) in male Wistar Han rats (200-220 g, Harlan, Milan, Italy). Then, the rats were anesthetized with 4% enflurane mixed with 0.5l/min O_2 and 0.5 l/min N_2O. At the level of the sixth intercostal space, the skin was incised and saline or λ-carrageenan (0.2 ml, 1% (w/v), dissolved in 0.9% NaCl) was injected into the pleural cavity. The wound was closed by a suture clip. After 4 h, the animals were killed by inhalation of CO_2 and the chest was opened carefully. 2 ml saline solution (0.9% NaCl, 5 U/ml heparin) was transferred into the pleural cavity, before the whole volume of fluid in the cavity was collected. The amount of exudate was calculated by subtracting the volume of added saline solution from the total collected volume. The collected fluid was centrifuged (800 × g, 10 min, 4 °C) and the supernatant was collected and frozen (-80 °C) for a subsequent determination of PGE_2, 6-keto-prostaglandin 1α (6-keto-$PGF_{1\alpha}$) and LTB_4 (see below). The pellet was resuspended in saline solution (0.9% NaCl, 1 ml) and an additional dilution (1:50) was prepared. The cell number in this dilution was counted (see **3.6**).

The amount of PGE_2, 6-keto-$PGF_{1\alpha}$ and LTB_4 in the exudate supernatant were determined by different assays. PGE_2 was detected by a radioimmunoassay (Assay Designs, Inc., Ann Arbor, MI), while 6-keto-$PGF_{1\alpha}$ and LTB_4 levels were determined by enzyme immuno assay kits (Cayman Chemical Company, Ann Arbor, USA) according to the manufacturer's instructions.

3.24   Ras activation assay

The amount of GTP-bound Ras as a marker for Ras activity was analyzed by utilizing an affinity chromatography method as previously described [247]. Neutrophils (2 × 10^7/ml) or HL60 cells (1 × 10^6/ml) were incubated for 1.5 min with BAs. In some experiments, 5-hydroxyeicosatetraenoic acid (5-HETE, 1 ng/ml) was added afterwards

for additional 1 min. Cells were lysed on ice by addition of lysis buffer (25 mM Tris, pH 7.4, 5% glycerol, 0.5% NP-40, 2.5 mM $MgCl_2$, 200 mM NaCl, 60 µg/ml soybean trypsin inhibitor, 0.5 µg/ml leupeptin, 0.5 mM phenylmethylsulfonyl fluoride) for 10 min. Samples were centrifuged at 10,000 × g for 10 min (4 °C) before the supernatants (750 µl) were transferred to new tubes containing the Ras-binding domain of Raf-1 (Raf-1-RBD) coupled to GSH-sepharose beads (50 µl). The tubes were rotated for 1 h at 4 °C and centrifuged (8,000 × g, 1 min, 4 °C) afterwards. The beads were washed four times with lysis buffer. Bound proteins were eluted by addition of SDS-loading buffer (20 mM Tris (pH 8.0), 2 mM EDTA, 10% 2-mercaptoethanol (v/v), 5% SDS (v/v)) and heating (96 °C, 5 min). After an additional centrifugation (21,000 × g, 1 min, 4 °C), the supernatant was collected and analyzed by Western blotting (see **3.10**)

3.25   Generation of competent bacteria

In order to generate competent *E. coli* bacteria, an overnight culture (37 °C) was prepared by transferring frozen *E. coli* BL21 into fresh Luria broth (LB) medium supplemented with ampicillin (LB-Amp, 5 ml, 10 mg/ml peptone, 5 mg/ml yeast extract, 10 mg/ml NaCl, pH 7.0, 100 µg/ml ampicillin). On the next day, 1 ml of this culture was transferred into 200 ml LB-Amp medium. The culture was raised until an optical density at 600 nm (OD_{600}) of 0.3 was reached and was put on ice for 15 min. After centrifugation (4,000 × g, 10 min, 4 °C), the cell pellet was resuspended in RF1 buffer (20 ml, 100 mM RbCl, 50 mM MnCl, 30 mM potassium acetate, 10 mM $CaCl_2$, 15% glycerol (w/v), pH 5.8) and kept on ice for additional 5 min. The suspension was centrifuged (4,000 × g, 10 min, 4 °C) and the pellet resuspended in RF2 buffer (2 ml, 10 mM RbCl, 75 mM $CaCl_2$, 10 mM MOPS (3-(N-morpholino)propanesulfonic acid), 15% glycerol (w/v), pH 6.5). Cells were kept on ice for 30 min before they were frozen and stored at -80 °C until further usage.

3.26   Transformation of a Rap1B expression vector into *E. coli*

A Rap1B expression vector was kindly provided by Dr. Smolenski (Frankfurt, Germany). The human rap1B gene was cloned into the pGEX-2T vector (GE Healthcare Bio-Sciences, Freiburg, Germany). In order to generate a Rap1B expression bacterial

strain, competent *E. coli* BL21 (100 µl, see **3.25**) were put on ice for 15 min. Then, pGEX-2T vector (10-50 ng) was added while the cells were kept on ice for additional 20 min. A heat shock was performed by transferring the bacteria onto a heating block (42 °C) for 1 min. Afterwards, the sample was put on ice. LB medium (10 mg/ml peptone, 5 mg/ml yeast extract, 10 mg/ml NaCl, pH 7.0) supplemented with 20 mM glucose (900 µl) was added and the cells were rotated slowly at 37 °C for 1 h. 20 µl of the cell suspension was transferred onto an LB-Amp agar plate (10 mg/ml peptone, 5 mg/ml yeast extract, 10 mg/ml NaCl, 15 mg/ml agar, 100 µg/ml ampicillin), and cell growth was facilitated by incubation over night at 37 °C. Single clones were picked by sterile tooth picks and transferred into fresh LB medium supplemented with 100 µg/ml ampicillin (8 ml).

After incubation over night (37 °C), a glycerol stock of this bacterial strain was prepared. Glycerol (10%) was added and the bacteria were frozen in liquid nitrogen and stored at -70 °C until further usage.

3.27   Expression and purification of human recombinant Rap1B

Rap1B was expressed as a glutathione-S transferase (GST)-fusion protein using transformed *E. coli* BL21 (see **3.26**). Bacteria were transferred by sterile pipette tips from frozen glycerol stocks into 8 ml LB-Amp medium (10 mg/ml peptone, 5 mg/ml yeast extract, 10 mg/ml NaCl, 100 µg/ml ampicillin, pH 7.0). Cells were cultured over night at 37 °C while shaking. Then, LB-Amp medium supplemented with 20 mM glucose (400 ml) was added. When the cell density reached an OD_{600} of 0.3, recombinant protein expression was induced by addition of IPTG (0.1 mM). Bacteria were incubated over night shaking at 37 °C and centrifuged (7,700 × g, 10 min, 4 °C) afterwards. The pellet was resuspended in *E. coli*-lysis buffer (20 mM Tris (pH 8.0), 20% sucrose (w/v), 10% glycerol (v/v), 5 mM dithiothreitol, 5 mM $MgCl_2$, 1 mM phenylmethanesulfonylfluoride (PMSF), 1 µg/ml leupeptin, 2 µg/ml aprotinin) and lysed for 30 min on ice. The lysis was completed by sonification (3 × 15 sec, Branson B-12, Branson Ultrasonics Corporation, Danbury, CT). The lysates were centrifuged (12,000 × g, 10 min, 4 °C) before the supernatants were collected and frozen.

The purification of GST-fusion proteins was accomplished by glutathione sepharose 4B beads (GE Healthcare Bio-Sciences, Freiburg, Germany). Beads were washed with PBS

and resuspended in PBS (1:1, v/v), leading to a 50% bead slurry. 20 ml lysate was added to 200 µl bead slurry, and the binding reaction was started under constant slow rotation for 30 min. The whole approach was centrifuged (500 × g, 5 min) and an aliquot of the supernatant was frozen (-20 °C), while the remaining supernatant was discarded. Then, the beads were washed two times with PBS. In order to elute the bound proteins and to remove the GST-tag from the recombinant Rap1B proteins, thrombin was added (40 U/ml in PBS). The approaches were slowly rotated for additional 2 h before centrifugation (500 × g, 5 min). The supernatant containing Rap1B was collected.

The Rap1B solution still contains thrombin, which is able to destroy many proteins. To remove the thrombin, its binding to benzamidine was utilized by an affinity chromatographic method. The chromatographic separation was done by high performance liquid chromatography (HPLC) methods (Shimadzu Deutschland GmbH, Duisburg, Germany). H_2O was used as the mobile phase, while benzamidine was used as the stationary phase (GE Healthcare Bio-Sciences, Freiburg, Germany). First, the column was rinsed with H_2O for 5 min with a flow rate of 1 ml/min. Then, it was equilibrated by benzamidine buffer (50 mM Tris (pH 7.4), 500 mM NaCl) for 5 min. Rap1B solution was injected, and the flow-through (purified Rap1B) was collected.

In order to concentrate the purified Rap1B solution, ultrafiltration columns were used (Vivaspin 6, MWCO 5,000 Da, Sartorius Stedim Biotech S.A., Aubagne, France). The columns were loaded with 6 ml Rap1B solution and centrifuged for 30 min at 1,600 × g. The concentrated purified Rap1B solution was frozen. In order to monitor the success of the purification, an aliquot of this solution was analyzed by Western blotting (see **3.10**).

3.28   Loading of mant-nucleotides to Rap1B

In order to exchange Rap1B-bound nucleotides by mant-GppNHp, Rap1B (6.7 µM) was incubated with 200 mM ammonium sulfate, 13.3 µM mant-GppNHp, 1.44 µM $ZnCl_2$ and 0.27 U/ml alkaline phosphatase. Alkaline phosphatase degrades GDP but not mant-GppNHp, so that nucleotide exchange leads to mant-GppNHp-loaded Rap1B (mRap1B). The mixture was rotated over night at 4 °C in the dark. On the next morning, the sample was purified by transferring it to an illustra NAP-5^{TM} gel filtration column. PBS was added and the flow-through was collected in fractions. The absorption at 280

nm was determined photometrically, before the fractions that showed absorbance at 280 nm were combined. The protein concentration was determined as described in **3.8**.

3.29   Analysis of Rap1B-nucleotide exchange

The exchange of nucleotides of Rap1B was monitored fluorimetrically by incubating fluorescent mRap1B (see **3.28**) in a solution containing an excess of GDP and test compounds (i.e., AKBA). GDP (20 µM) and AKBA (0.1 - 2.5 µM) or GDP and DMSO as a control were dissolved in buffer (20 mM Tris, 100 mM NaCl, 10 mM EDTA, 5 mM $MgCl_2$, pH 8.0). The exchange reaction was started by rapid addition of mRap1B (30 nM), and the change in fluorescence was recorded by a fluorescence plate reader (excitation: 366 nm, emission: 408 nm; Victor[3], PerkinElmer, Rodgau-Jügesheim, Germany).

3.30   Cytotoxicity analysis

In order to analyze cytotoxicity of substances, a colorimetric test (MTT assay) was used. Jurkat A3 (3×10^5/ml) or RAW264.7 cells (2.5×10^6/ml) were transferred into a 96-well plate. Test compounds were added (not exceeding a final DMSO concentration of 0.5%, v/v), and the plate was incubated for 20 to 48 h at 37 °C and 6% CO_2. Then, MTT (3-(4,5-dimethylthiazol-2-yl)-2,5-diphenyltetrazolium bromide, 5 mg/ml, in PBS) was added for additional 30-120 min. The reaction was stopped by addition of lysis buffer (20 mM HCl (pH 4.5), 10% SDS (w/v)) and strong constant shaking for 16 h in the dark. The absorbance at 595 nm was measured in a microplate reader (Victor[3], PerkinElmer, Rodgau-Jügesheim, Germany).

3.31   Analysis of MAPK activation, caspase- and PARP-cleavage

In order to determine the activation status of different MAPKs (ERK-1, ERK-2 and p38) and apoptotic parameters (caspases and poly-ADP-ribose polymerase (PARP)), Jurkat A3 cells (2×10^5 - 2×10^6/ml), RAW264.7 cells (2×10^5 – 1×10^7/ml), neutrophils (2×10^6/ml) or monocytes (1×10^6) were incubated with either test

compounds or test compounds premixed with LPS (10 min, 37 °C) for 10 min to 24 h (never exceeding a final DMSO concentration of 0.3%). Then, cells were spun down (1,600 × g, 10 min) and washed with PBS. After centrifugation at 1,600 × g for 3 min, lysis buffer (20 mM Tris (pH 7.4), 150 mM NaCl, 2 mM EDTA, 1% Triton X-100 (v/v), 0.5% NP-40 (v/v); 4 µl/ml cell suspension used) was added. The samples were mixed and lysed for 10 min on ice. Afterwards, samples were centrifuged (10,000 × g, 10 min, 4 °C), the supernatants were collected and mixed with SDS-loading buffer (40 mM Tris (pH 8.0), 4 mM EDTA, 20% 2-mercaptoethanol (v/v), 10% SDS (v/v), in a ratio 3:1). After heating (5 min, 95 °C), the samples were frozen before they were analyzed by electrophoretic (see **3.9**) and Western blotting (see **3.10**).

3.32   DNA-fragmentation tests

The measurement of DNA fragmentation is based on a method developed by Nicoletti *et al.* [248]. Jurkat A3 cells (2×10^5/ml) were incubated with DMSO, BAs or BA derivatives (never exceeding a final DMSO concentration of 0.2%) for 24 h at 37 °C and 6% CO_2. Then, 500 µl cell suspension was centrifuged (4,200 × g, 5 min) and the pellet was washed with PBS. After an additional centrifugation (200 × g, 5 min) the supernatant was discarded. 100 µl hypotonic propidium iodide (PI)-lysis buffer (0.1% sodium citrate, 0.1% Triton X-100 and 50 µg/ml PI) was added and the cells were carefully resuspended. After 10 min, the samples were analyzed in a FACScalibur (Becton Dickinson) flow cytometer (FL2, 585/42) and plotted logarithmically against cell counts. The fluorescence intensity of cell nuclei from cells in the G_1 phase was set to around 10^3 in the FL2 channel.

3.33   Statistical analysis

Statistical data evaluation was performed by one-way analysis of variance (ANOVA) tests for independent or correlated samples followed by Tukey honestly significant differences (HSD) post-hoc tests. *p* values of <0.05 (*), <0.01 (**) and <0.001 (***) were considered significant.

4.   Results

4.1 Interaction of BAs with hCAP18 and LL-37

4.1.1   hCAP18 and LL-37 are binding partners of BAs

Protein pull-down experiments using immobilized BAs in neutrophil lysates were performed in order to analyze possible binding partners of BAs. A protein with an approximate molecular weight of 16 kDa was precipitated by EAH-sepharose beads coupled to KBA (KBA-sepharose, **fig. 4.1**, **A**) but not by EAH-sepharose beads alone (**fig. 4.1**, **B**). The band was excised, digested and analyzed by MALDI-TOF mass spectrometry. The protein was identified as the human cathelicidin hCAP18 (data not shown). These initial pull-down and MALDI-TOF experiments were performed by Lars Tausch in collaboration with Prof. Dr. Karas (Goethe Univeristy, Frankfurt). Western blot analyses were performed to confirm the mass spectrometric results. To this aim, neutrophil lysates were again incubated with KBA-sepharose or EAH-sepharose. Precipitated proteins were analyzed by Western blotting using an antibody against LL-37, a part of the protein which constitutes the C-terminal part of hCAP18. Both hCAP18 and LL-37 were precipitated by KBA-sepharose but not by the EAH-sepharose control (**fig. 4.1**, **C**). To evaluate whether the binding to LL-37 is direct or involves adaptor proteins, isolated LL-37 was used as a protein source for the pull-down experiment. Under these conditions, LL-37 was precipitated by KBA-sepharose (**fig. 4.1**, **C**) and EAH-sepharose coupled to β-BA (BA-sepharose) (**fig. 4.1**, **D**) but not by unmodified EAH-sepharose, supporting a direct binding of KBA and β-BA to LL-37.

A

B

C

D
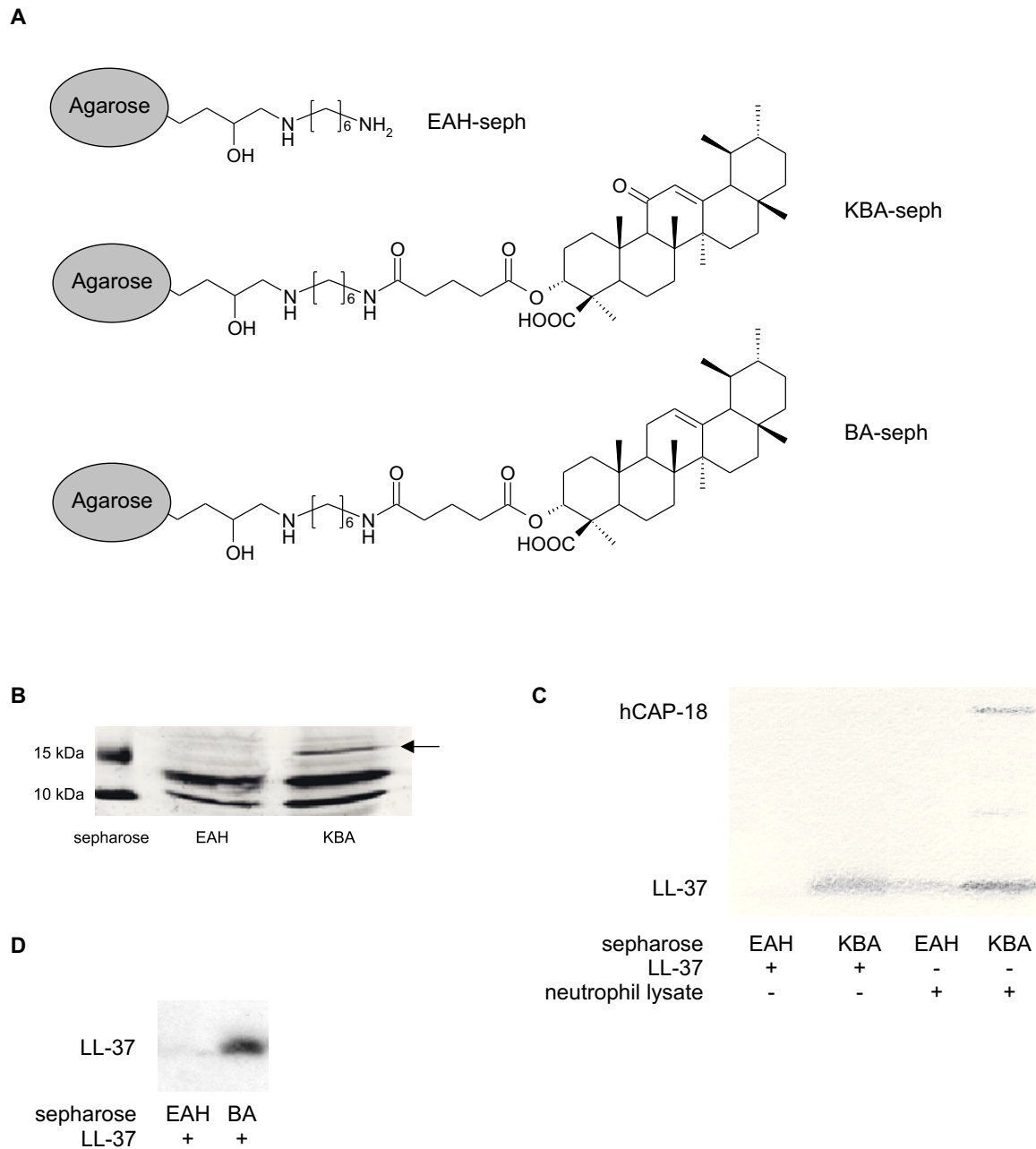
Fig. 4.1: hCAP18/LL-37 pull-down experiments. *(**A**) Structure of EAH-seph, KBA-seph and BA-seph. (**B**) EAH-seph and KBA-seph were incubated with neutrophil lysates. Precipitated proteins were separated by SDS-PAGE and silver-stained. Proteins present in KBA-seph- but not in EAH-seph-approaches are marked by an arrow. This initial pull-down experiment was performed by Lars Tausch. (**C**) EAH-seph and KBA-seph were incubated with isolated LL-37 (1.3 µg/ml) or in neutrophil lysates. Precipitated LL-37 and hCAP18 were detected by Western blotting using anti-LL-37 antibodies. (**D**) Isolated LL-37 (1.3 µg/ml) was incubated with EAH-seph and BA-seph. Precipitated LL-37 was detected in Western blot experiments. Results shown are representative for three independent experiments.*

4.1.2 BAs stimulate LL-37 release

The influence of BAs on the release of the LL-37 precursor hCAP18 from neutrophil granules and on LL-37 generation was analyzed by Western blot experiments. Neutrophils were incubated with BAs and stimulated with cytochalasin B and fMLP. The amount of released LL-37 was determined by Western blotting. AKBA (10 µM) and β-BA (1 and 10 µM) enhanced LL-37 release, while only slight effects were observed on hCAP18 release (**fig. 4.2**).

hCAP18								
LL-37								
cytB/fMLP	-	+	+	+	-	+	+	+
AKBA [µM]	0	0	1	10	-	-	-	-
β-BA [µM]	-	-	-	-	0	0	1	10
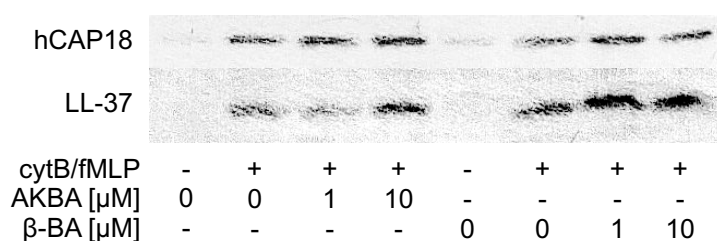
Fig. 4.2: Influence of BAs on LL-37 generation. Neutrophils (5×10^7/ml) were incubated with AKBA or β-BA and cytochalasin B (10 µM, cytB) and fMLP (1 µM). Cells were spun down and the supernatant was analyzed by Western blot experiments using anti-LL-37 antibodies. Results shown are representative for three independent experiments.

4.1.3 BAs restore the inhibition of LPS activities by LL-37

LL-37 is an inhibitor of LPS activity [140]. Measurement of the inhibitory effect of LL-37 on LPS activity (by a modified LAL assay) can therefore by used as a mean to measure functional LL-37 activity. As control, it was first checked whether different BAs directly interfere with LPS activity (see **4.3.2**). Triterpenes from frankincense which did not influence LPS directly (e.g. AKBA or ABA) were incubated with LL-37 and LPS and the remaining LPS activity was determined (**fig. 4.3**). LL-37 reduced LPS activities completely. AKBA and ABA (10 µM, each) potently reversed this inhibition. Synthetic modification of AKBA and ABA by replacement of the acetylic group at the C-3 position by an esterified dicarbonic acid or an etherified ω-hydroxy acid resulted in molecules with lower activities, which were still capable to partially restore LL-37-inhibited LPS activities at 10 µM.

Ac-LA was the only LA derivative with a very potent activity at 10 µM, while both OH-LA and Ac-OH-LA reversed the LL-37 inhibited LPS activities only moderately. All tested RA derivatives displayed an intermediate activity, with LPS activity restoration rates at 41.1% (RA), 45.1% (DH-RA) and 51.3% (DHK-RA) at 10 µM, each. 11-α-OH-BA and 11-β-OH-BA were virtually ineffective.
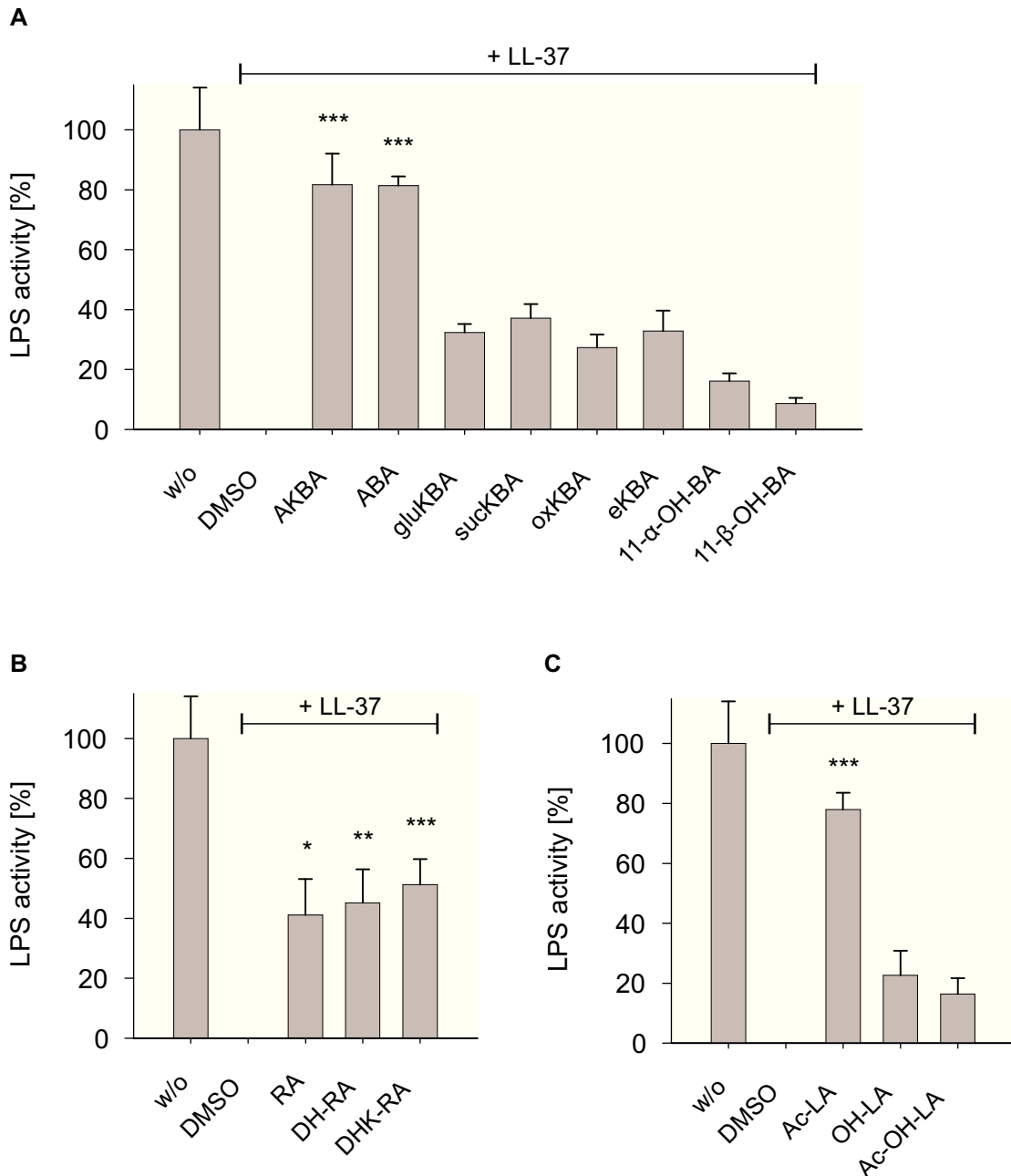
Fig. 4.3: Influence of BAs, RAs and LAs on LL-37-inhibited LPS activity. *LPS (10 EU/ml) was incubated with LL-37 (0.1 µM) and (**A**) BAs, (**B**) RAs or (**C**) LAs (10 µM, each) for 10 min. Incubation of LPS with LL-37 and DMSO served as a vehicle control, LPS activity is completely inhibited under these circumstances. The inhibitory effect of LL-37 is reversed by addition of several triterpenes derived from frankincense. LPS activities were monitored by a modified LAL assay. Data are given as means + s.e.; n = 3. * p < 0.05, ** p < 0.01, *** p < 0.001, vs vehicle (DMSO).*

A concentration-response study revealed a concentration-dependent relationship for the ability of ABA, AKBA and Ac-Lup to reverse LL-37 effects on LPS activities. BAs and LAs restored the LL-37-diminished LPS activities with EC_{50} values of 0.2 µM (ABA, **fig. 4.4**, **A**), 0.8 µM (AKBA, **fig. 4.4**, **B**) and 0.7 µM (Ac-LA, **fig. 4.4**, **C**).
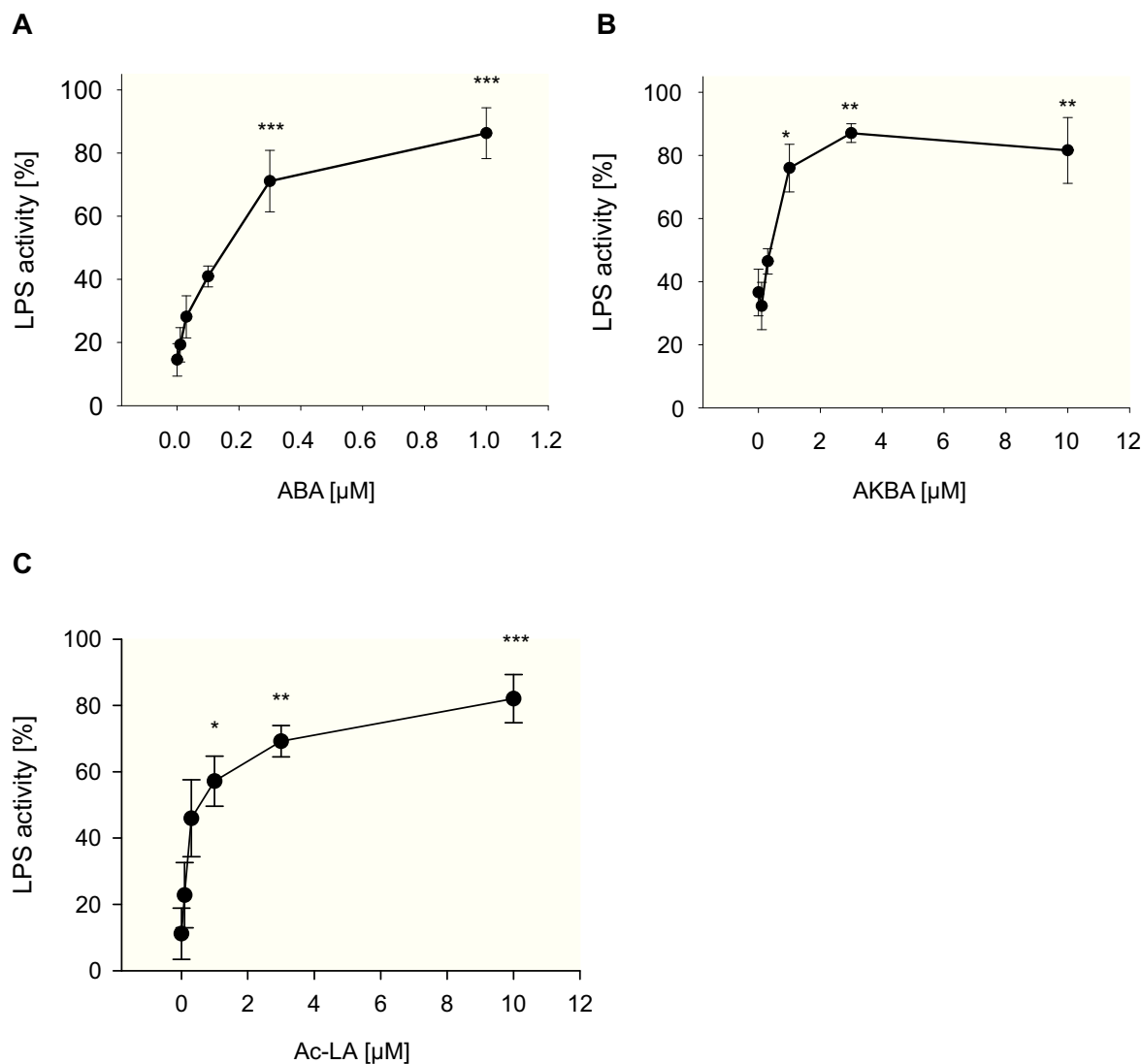
Fig. 4.4: Influence of ABA, AKBA and Ac-LA on LL-37-inhibited LPS activity. *LPS (10 EU/ml) was incubated with LL-37 (0.1 µM) and (**A**) ABA, (**B**) AKBA or (**C**) Ac-LA for 10 min. Incubation of LPS with LL-37 and DMSO as a vehicle leads to maximum inhibition of LPS activity, which is restored by addition of several triterpenes derived from frankincense. LPS activities were monitored by a modified LAL assay. Data are given as means ± s.e.; n = 3. * p < 0.05, ** p < 0.01, *** p < 0.001, vs vehicle (DMSO).*

Next, two different experimental settings were used in order to characterize the effects of BAs on LL-37 in a more physiological context. In the first system, neutrophils were stimulated to degranulate (and to release LL-37). The resulting supernatant after centrifugation of activated neutrophils is supposed to contain LL-37 and was added to an LPS/BA mixture. Supernatants from stimulated cells strongly reduced LPS-activity, apparently due to LL-37 (**fig. 4.5**), which was reversed by addition of ABA (EC_{50} = 1.3 µM, **fig. 4.6**, **A**).
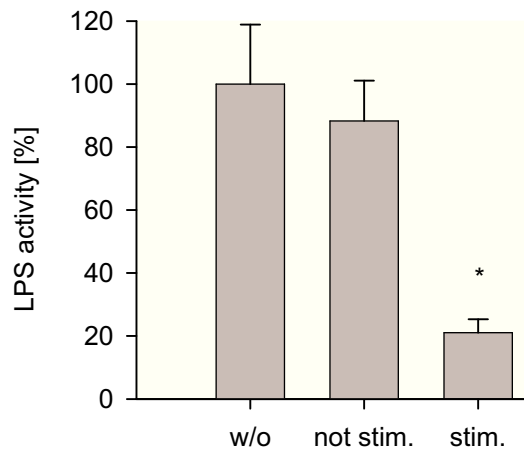
Fig. 4.5: Stimulated neutrophils release LPS-inhibiting compounds. Neutrophils were stimulated to degranulate with cytochalasin B (10 µM) and fMLP (1 µM) or left untreated. After centrifugation, the supernatant was incubated with LPS (10 EU/ml) and ABA for 10 min, before the remaining LPS activity was measured. Data are given as means ± s.e., n = 3. * p < 0.05, vs vehicle (DMSO).

In the second system, citrated human whole blood was stimulated to induce degranulation of blood neutrophils. Blood plasma (that seemingly contains LL-37 when stimulated) was collected and mixed with LPS and ABA. While the plasma from stimulated blood had potent LPS-inhibiting properties (**fig. 4.6**, **B**), ABA was able to reverse this effect (EC_{50} = 3.5 µM).
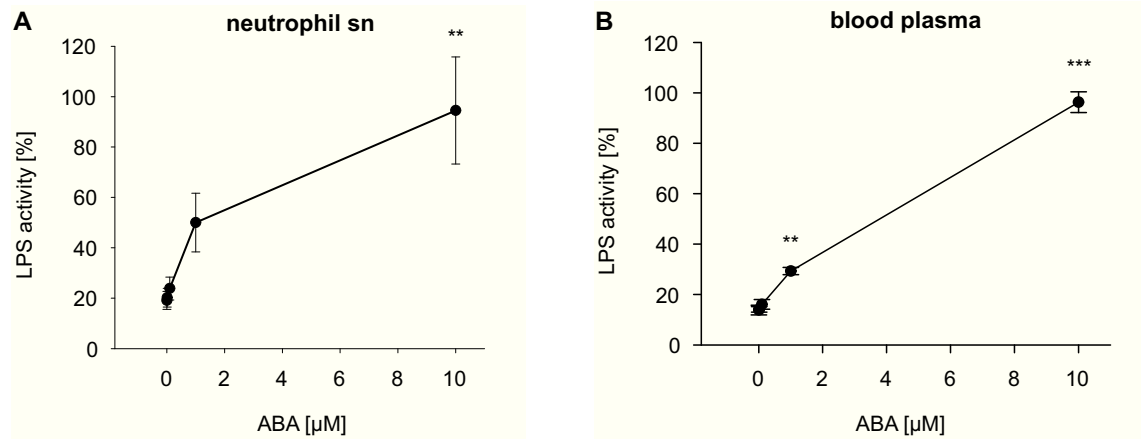
Fig. 4.6: Influence of ABA on degranulated neutrophil supernatant-diminished or plasma-inhibited LPS activity. *(**A**) Neutrophils were stimulated to degranulate with cytochalasin B (10 µM) and fMLP (1 µM). After centrifugation, the supernatant was incubated with LPS (10 EU/ml) and ABA for 10 min before the remaining LPS activity was measured. (**B**) Diluted citrated blood plasma was stimulated with cytochalasin B (10 µM) and fMLP (2.5 µM). The plasma was incubated with LPS (10 EU/ml) and ABA for 10 min. The remaining LPS activity was assayed by a modified LAL testing system. Data are given as means ± s.e., n = 3. ** p < 0.01, *** p < 0.001, vs vehicle (DMSO).*

Taken together, BAs bind to LL-37 and restore inhibition of LPS activities induced by isolated LL-37 as well as by LPS-inhibiting compounds released by stimulation of human neutrophils and whole blood.

4.2 Re-evaluation of LL-37 functions

Next, the effects of BAs on other previously described functions of LL-37 (i.e. cytotoxicity for leukemic T-lymphocytic cells [249], induction of neutrophil chemotaxis [250], activation of ERK2 and p38 MAPKs [138] and increase of intracellular Ca^{2+} concentration in leukocytes [251,252]) were evaluated.

It has been reported that LL-37 is cytotoxic for leukemic T-lymphocytic cells [249]. In order to verify this effect, Jurkat A3 cells were incubated with LL-37 and ABA in different concentrations. However, neither LL-37 (0.01 - 1 µM) nor ABA (1-10 µM) had a significant influence on cell viability (**fig. 4.7**), while cycloheximide (CHX) used as a positive control strongly reduced cell viability.
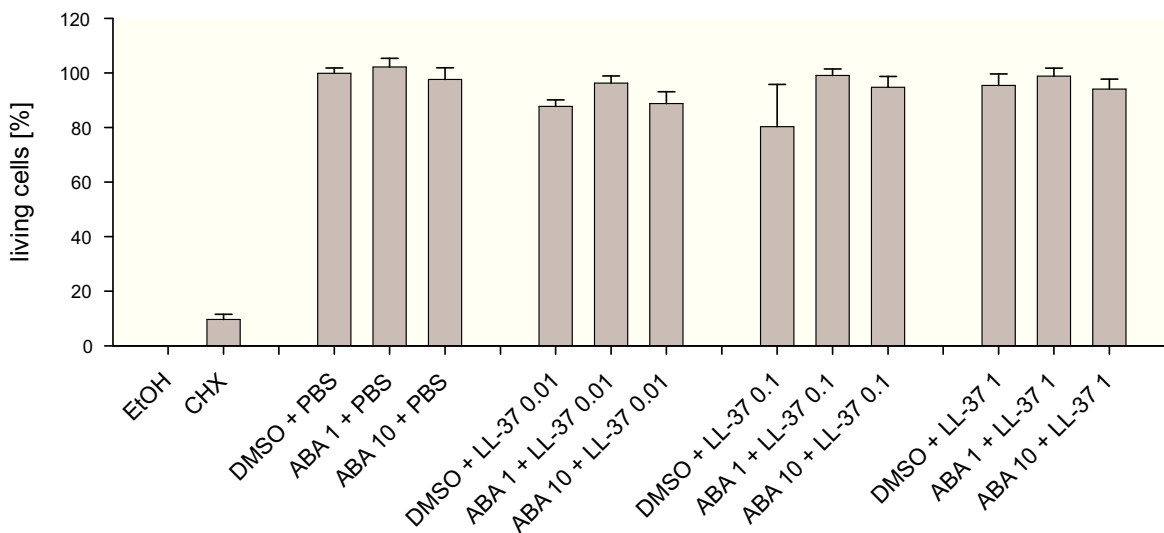
Fig. 4.7: Effects of LL-37 on cell viability and the influence of ABA. *Jurkat A3 (3 × 10^5/ml) were incubated with LL-37 (0.01, 0.1 and 1 µM) with and without ABA (1 and 10 µM) for 48 h. As a control, ethanol (EtOH, 16.7%, v/v) and cycloheximide (CHX, 50 µM) were used. After 48 h, the dye MTT was added and incubated for 30 min. Cells were lysed and the absorption at 595 nm was measured. Data are given as means + s.e.; n = 4.*

LL-37 has also been described to stimulate neutrophil chemotaxis [250]. However, LL-37 (up to 10 µM) did not show a significant chemotactic activity against neutrophils in an established chemotaxis assay (**fig. 4.8**).
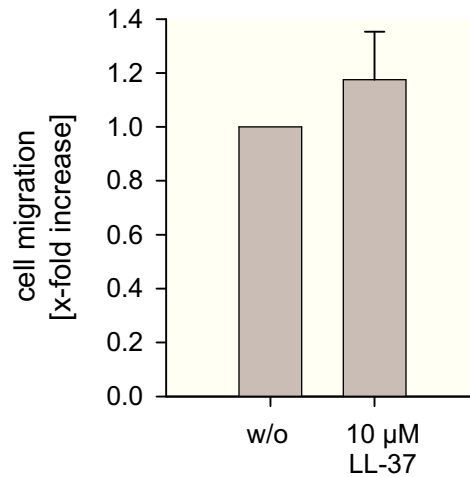
Fig. 4.8: Chemotactic activity of LL-37 in neutrophils. LL-37 was dissolved in medium and added to the lower compartment of a modified Boyden chamber. A membrane (8 µm pore size) was mounted and calcein-AM-stained neutrophils (5×10^4) were placed on the top side. After 1 h, the fluid on the top side of the membrane was washed away and the number of migrated neutrophils was determined by fluorescence measurement (ex. 485 nm, em. 535 nm) of the lower compartment and the membrane. Data are given as means + s.e.; n = 3.

Similarly, LL-37 (5 µM; 0.5-30 min) did not influence the activation status of ERK1, ERK2 and p38 MAPKs (**fig. 4.9**). In contrast, the chemotactic peptide fMLP was an effective inductor of ERK1, ERK2 and p38 MAPKs as expected.
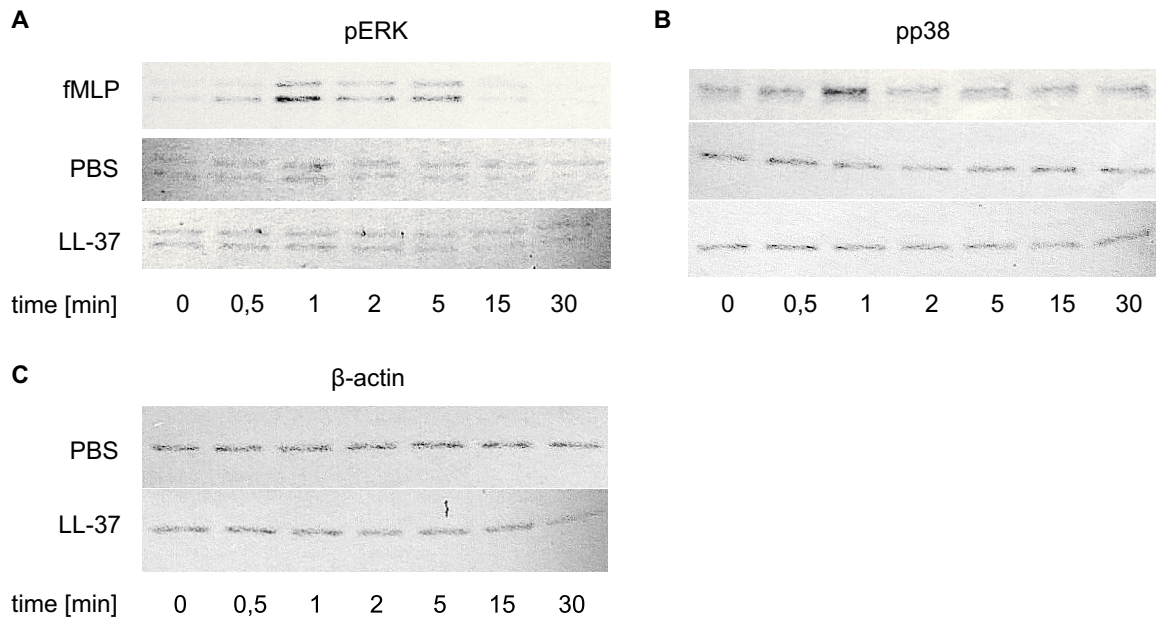
Fig. 4.9: MAPK activation is not influenced by LL-37. *Neutrophils (2 × 10^6/ml) were incubated with LL-37 (5 µM), fMLP (0.1 µM) or PBS (negative control) for 15 min at 37 °C. Cells were lysed and lysates were analyzed by Western blotting using (A) anti-phospho-ERK, (B) anti-phospho-p38 MAPK or (C) anti-β-actin antibodies. Results shown are representative for three independent experiments.*

In addition, LL-37 had no effect on Ca^{2+} influx in leukocytes. Fura-2-loaded neutrophils (**fig. 4.10**, **A**) and monocytes (**fig. 4.10**, **B**) were incubated with LL-37. The presence of LL-37 had no influence on the intracellular Ca^{2+} levels, neither in neutrophils nor in monocytes, while fMLP, used as a control, was a prominent inductor of Ca^{2+} influx.
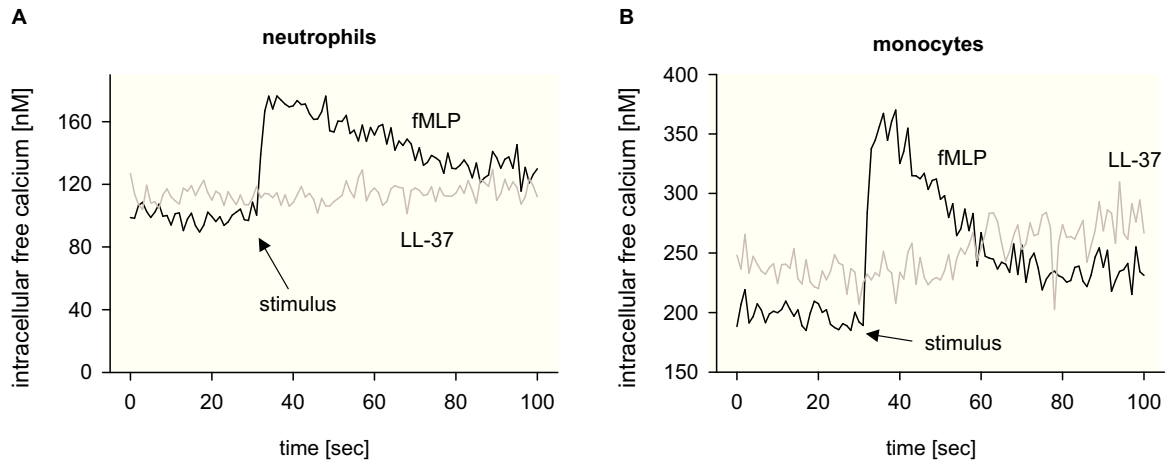
Fig. 4.10: Effects of LL-37 on the intracellular Ca^{2+} concentration. (A) Fura-2-loaded neutrophils (1 × 10^7/ml) or (B) monocytes (1 × 10^6/ml) were incubated with CaCl$_2$ (1 mM) for 1 min before the measurement of intracellular Ca^{2+} concentration started. After 30 sec, LL-37 (10 µM) or fMLP (1 µM) was added. Results shown are representative for three independent experiments.

4.3 Interaction of BAs with LPS

4.3.1   BAs bind to LPS

Selected BAs were identified as compounds which restore LL-37-inhibited LPS activities (see **4.1.3**). During this investigation, evidence arose that some other BAs may inhibit LPS activities by themselves. In order to analyze if BAs bind to LPS, a pull-down assay was performed. BA-sepharose or EAH-sepharose without a coupled β-BA (**fig. 4.1**, **A**) was incubated with LPS before bound molecules were eluted and analyzed for their LPS content. LPS could be precipitated by BA-sepharose but not by EAH-sepharose, accompanied by a concomitant decrease of LPS in the supernatant (**fig. 4.11**). Thus, the direct influence of BAs and other compounds from frankincense on LPS activity was evaluated.
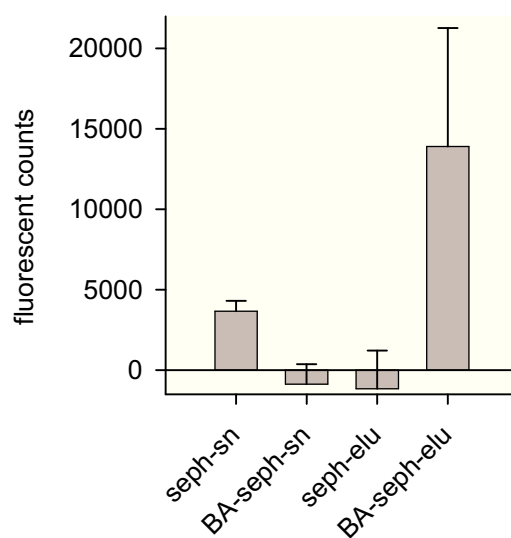
Fig. 4.11: LPS pull-down experiments with immobilized β-BA. EAH-sepharose (seph) and BA-sepharose (BA-seph) were incubated with LPS (2.7 µg/ml). Precipitated molecules were eluted and LPS levels of the eluates (elu) and supernatants (sn) were analyzed by a fluorimetric modified LAL assay. Data are given as means + s.e..; n = 4.

4.3.2 LPS activity is inhibited by selected BAs

The influence of different compounds from frankincense on LPS activity was measured by a modified LAL assay. LPS was incubated with the testing compounds and LPS activity was determined afterwards. Certain BAs displayed a very potent inhibition of LPS activity, while others were virtually ineffective (**fig. 4.12**). Especially eBA, oxBA, gluBA and sucBA proved to be very potent with a maximal inhibition (0-5% remaining activity) reached already at 10 µM. β-BA, cis-diol-BA, α-BA and 11-β-OH-BA were slightly less potent, leading to remaining LPS activities (at 10 µM) of 31, 19, 42 and 40%, respectively. None of the 11-keto-BAs tested proved to be effective at 10 µM (KBA, AKBA, eKBA, oxKBA, gluKBA and sucKBA), and neither RA derivatives (RA, DH-RA and DHK-RA) nor LA derivatives (Ac-OH-LA, Ac-LA, OH-LA) showed any effects. ABA was the only BA without an 11-keto moiety without effects on the LPS activity. 11-α-OH-BA and oleanolic acid failed to inhibit LPS activities at 10 µM as well.
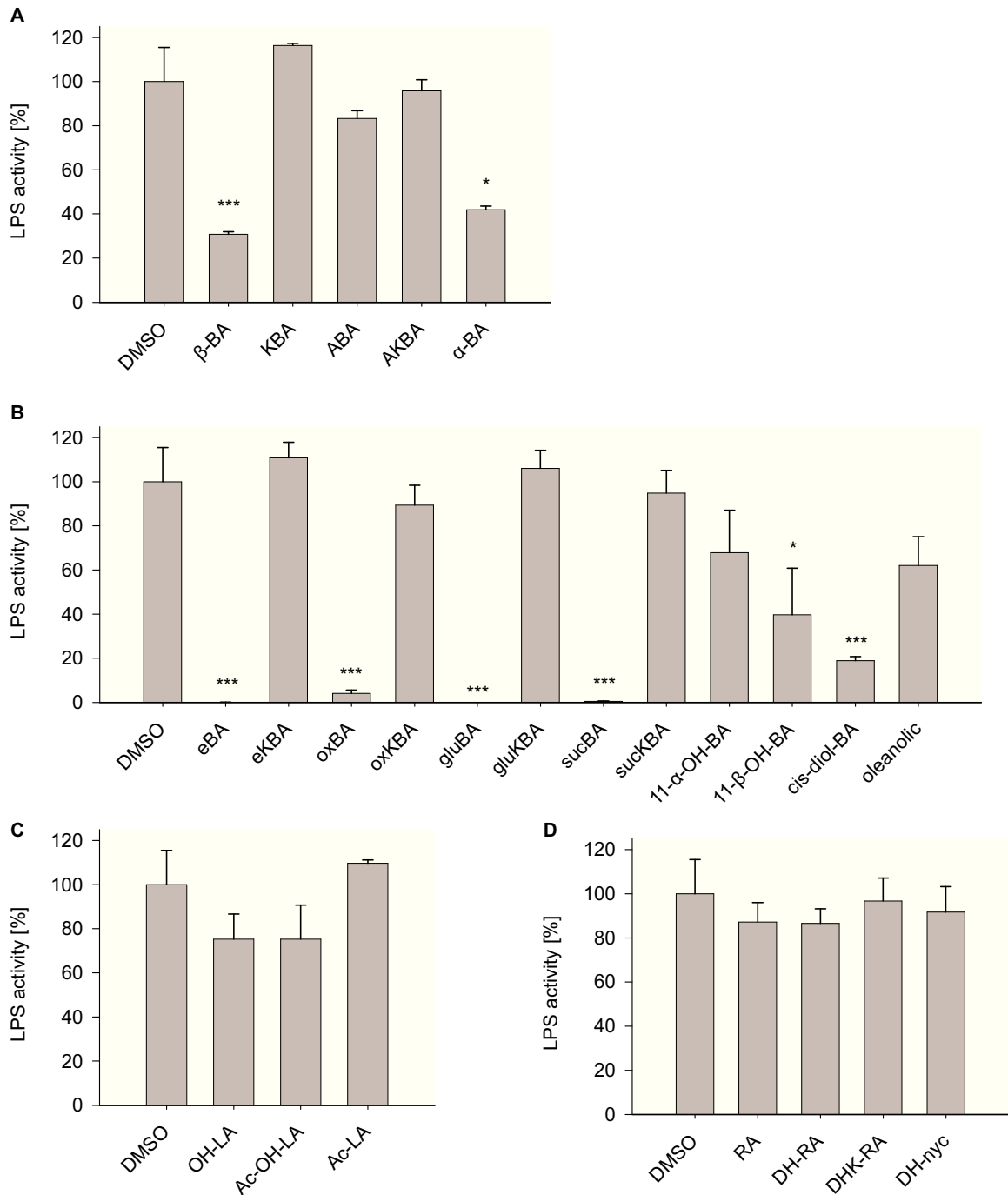
Fig. 4.12: Influence of BAs, LAs, RAs and DH-nyc on LPS activities. *(A) Naturally occurring BAs, (B) synthetic BAs, (C) LAs and (D) RAs and DH-Nyc were incubated with LPS (10 EU/ml) for 10 min at 37 °C. Then, fluorogenic substrate, buffer and recombinant factor c were added. LPS activity was determined by measuring the activity directly and after 60 min at 37 °C. Final LPS activity was calculated by subtracting the fluorescence at the beginning from the fluorescence after 60 min. Data are given as means + s.e.; n = 3. *,p < 0.05, ** p < 0.01, *** p < 0.001, vs vehicle (DMSO).*

A concentration-response analysis revealed IC_{50} values for the inhibition of LPS activities (**fig. 4.13**). BAs which inhibited LPS activities at 10 µM very potently displayed a similar concentration-response behavior, with IC_{50} values of 1.9 µM (eBA and gluBA) and 2.5 µM (sucBA). LPS activity was completely suppressed at 10 µM (gluBA, sucBA). β-BA, which also had similar potency ($IC_{50} = 1.8$ µM), showed a maximal inhibition of only 60-70%. AKBA, on the other hand, had no influence on LPS activities at concentrations up to 10 µM. As a control, a known LPS-neutralizing compound (polymyxin B) was tested which displayed total inhibition of LPS at 1 µM as expected.
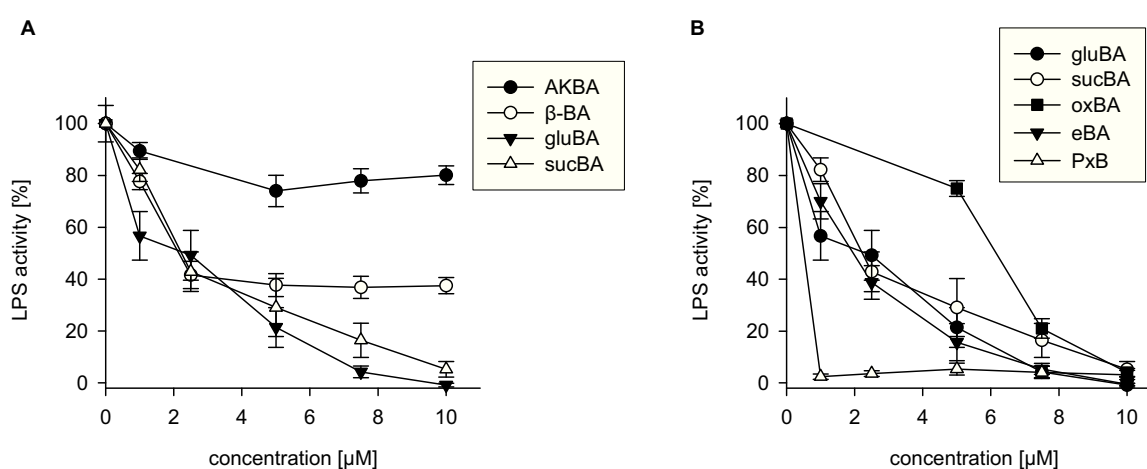
Fig. 4.13: Concentration-dependent influence of BAs on LPS activities. (A) Naturally occurring BAs and (A, B) synthetic BAs were incubated with LPS (10 EU/ml) for 10 min at 37 °C. Then, fluorogenic substrate, buffer and recombinant factor c were added. LPS activity was determined by measuring the activity directly and after 60 min of incubation at 37 °C. PxB = polymyxin B. Data are given as means ± s.e.; n = 3.

4.3.3 LPS-induced iNOS-expression and NO formation are inhibited by selected BAs

In order to investigate if the inhibition of LPS activity by BAs has an influence on LPS-induced cellular events, iNOS expression levels were analyzed. LPS strongly induced iNOS expression in RAW264.7 cells (**fig. 4.14**). This induction was inhibited by certain BAs. β-BA displayed a moderate inhibition at 3 µM and a strong inhibition at 10 µM. Similarly, gluBA and sucBA were somewhat more potent than β-BA and inhibited the LPS-induced iNOS expression efficiently at 10 µM. AKBA, which did not significantly influenced LPS activity in the LAL assay, had also no effect on LPS-induced iNOS

expression. Polymyxin B, used as a positive control, displayed a weaker potency than gluBA and sucBA while being equipotent to β-BA.
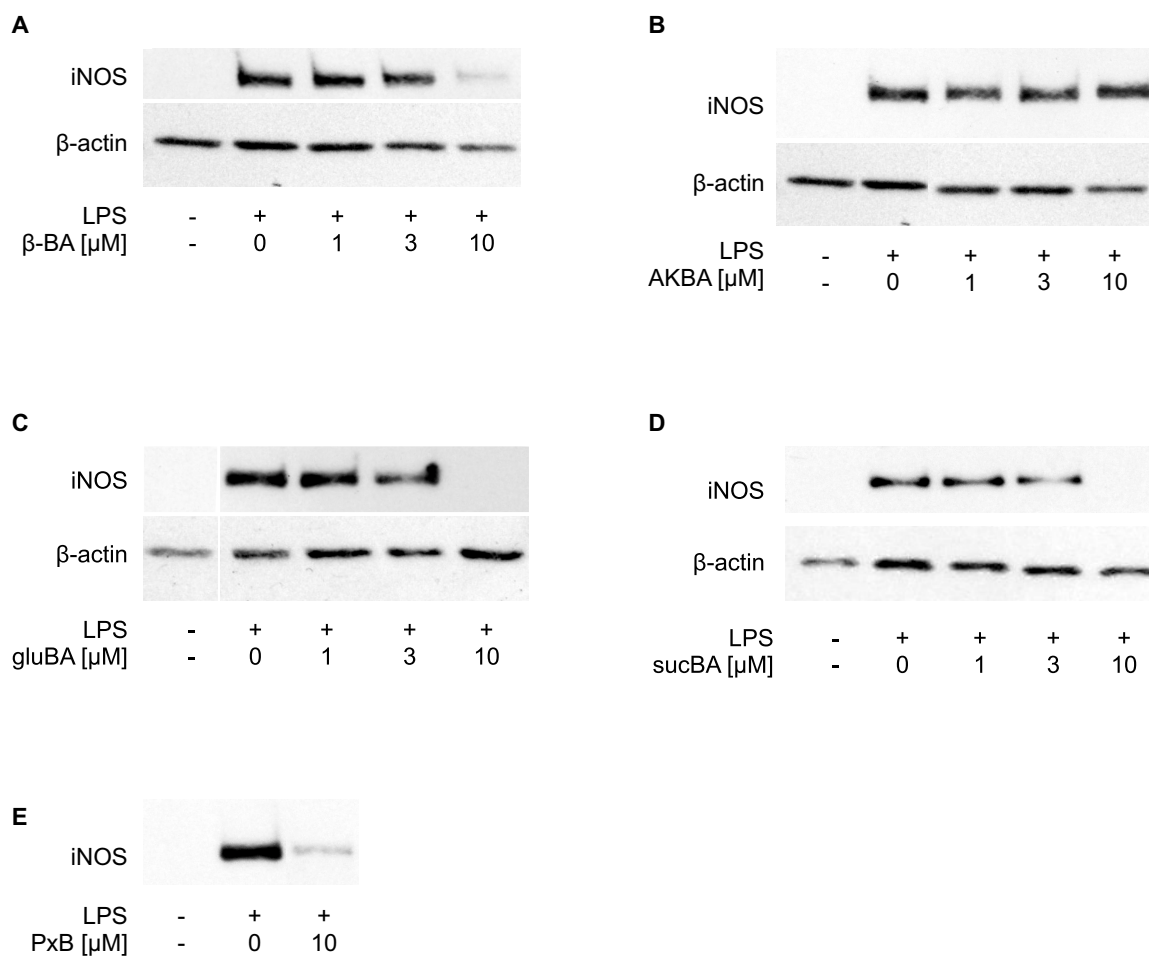
Fig. 4.14: Effects of BAs on LPS-induced iNOS expression. RAW264.7 cells (2.5 × 10^6/ml) were incubated with LPS (1 µg/ml, from E. coli O111:B4) and (A) β-BA, (B) AKBA, (C) gluBA, (D) sucBA or (E) polymyxin B (PxB) for 20 h. Cells lysates were analyzed by Western blotting using anti-iNOS and anti-β-actin antibodies. Results shown are representative for three independent experiments.

To evaluate whether inhibition of iNOS expression results in lower NO formation, the influence of BAs on LPS-induced NO generation was analyzed using the measurement of nitrite levels by the Griess reaction as a marker [244]. RAW264.7 cells were incubated with LPS and BAs for 20 h before the amount of nitrite in the medium was analyzed. All BAs tested (BA, AKBA, oxBA, gluBA and sucBA) were ineffective at concentrations below 3 µM (**fig. 4.15**, **A**). β-BA displayed a tendency for a slight inhibition (17%) of nitrite generation at 10 µM, while AKBA was completely ineffective. GluBA was slightly more active than sucBA, with moderate inhibition

(24%) at 3 µM and potent inhibition at 10 µM (95%). sucBA displayed no inhibition at 3 µM but a strong inhibition (77%) at 10 µM.

In order to evaluate if the inhibition of nitrite generation is due to by cytotoxic effects, cell viability of RAW264.7 cells stimulated by the same conditions as in the LPS-induced nitrite generation experiments was analyzed by MTT experiments (**fig. 4.15**, **B**). β-BA, AKBA and sucBA were not cytotoxic up to 10 µM. GluBA was the only BA with cytotoxic properties, with no cytotoxic activity at 3 µM and a moderate activity at 10 µM.
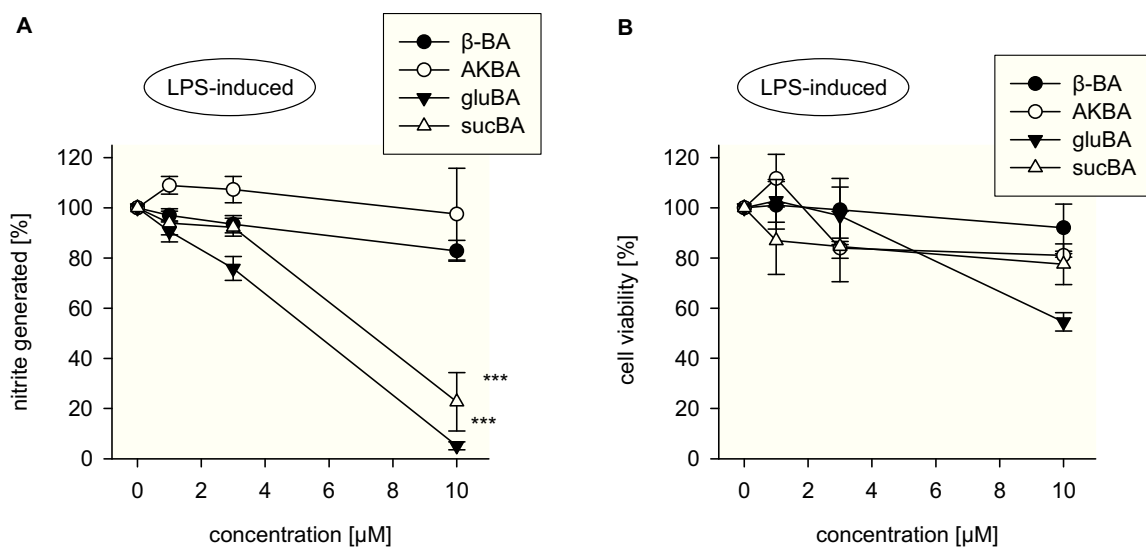
Fig. 4.15: Effects of BAs on LPS-induced NO generation and cytotoxicity. (A) *Influence of BAs on nitrite levels after LPS-stimulation. RAW264.7 (2.5×10^6/ml) were incubated with LPS (1 µg/ml) and BAs for 20 h. Nitrite concentration of the extracellular medium was determined by addition of Naphtylethylenediamin-dihydrochloride (1 mg/ml) and sulfanilamide (10 mg/ml in 5% H_3PO_4) for 15 min (Griess reaction). The absorbance at 540 nm was measured. (**B**) Cytotoxicity of BAs. RAW264.7 cells (2.5×10^6/ml) were incubated with LPS (1 µg/ml) and BAs for 20 h. Viable cells were stained for 2 h by MTT addition (5 mg/ml) and lysed. Absorption at 595 nm was measured as a marker for viable cells. Data are given as means ± s.e.; n = 3. *** p < 0.001, vs vehicle (DMSO).*

4.3.4 IFN-γ-induced iNOS expression and NO generation are not inhibited by BAs

Inhibition of LPS-induced iNOS expression and NO formation by selected BAs might be the result of the direct inhibition of LPS activity, but it might also be due to modulation of related cellular events. In order to investigate this issue, the effects of BAs on iNOS and NO were evaluated when a different stimulus was used, i.e. IFN-γ (**fig. 4.16**). All BAs tested (BA, AKBA, gluBA and sucBA) as well as polymyxin B did not inhibit IFN-γ-induced iNOS expression at concentrations up to 10 µM. This indicates that the reduction of LPS-induced iNOS levels is likely not related to interference with the transcriptional apparatus or other cellular events but rather suggests that the compounds suppress iNOS expression due to direct interference with LPS.
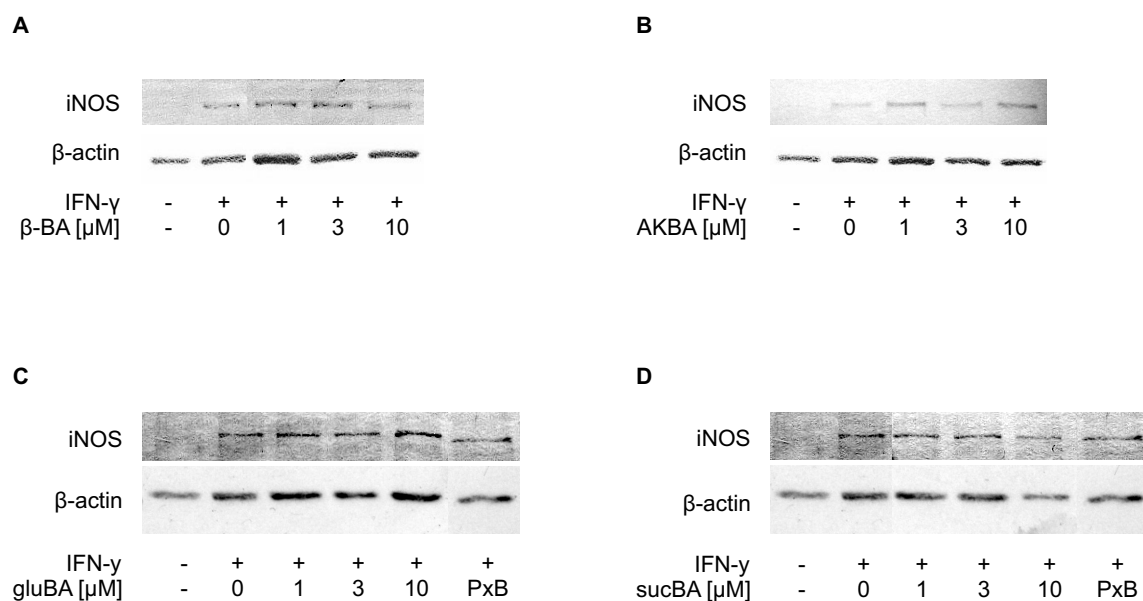
Fig. 4.16: Effects of BAs on IFN-γ-induced iNOS expression. RAW264.7 cells (2.5 × 10⁶/ml) were incubated with IFN-γ (10 ng/ml) and (A) β-BA, (B) AKBA, (C) gluBA, (D) sucBA or (C-D) polymyxin B (PxB) for 20 h. Cells lysates were analyzed by Western blot analysis using anti-iNOS and anti-β-actin antibodies. Results shown are representative for three independent experiments.

Neither β-BA nor AKBA reduced IFN-γ-induced nitrite levels (**fig. 4.17**, **A**). GluBA was active at 10 µM (69% inhibition, **fig. 4.17**, **B**), but not at lower concentrations. Also, sucBA displayed moderate inhibition at 10 µM (44%).
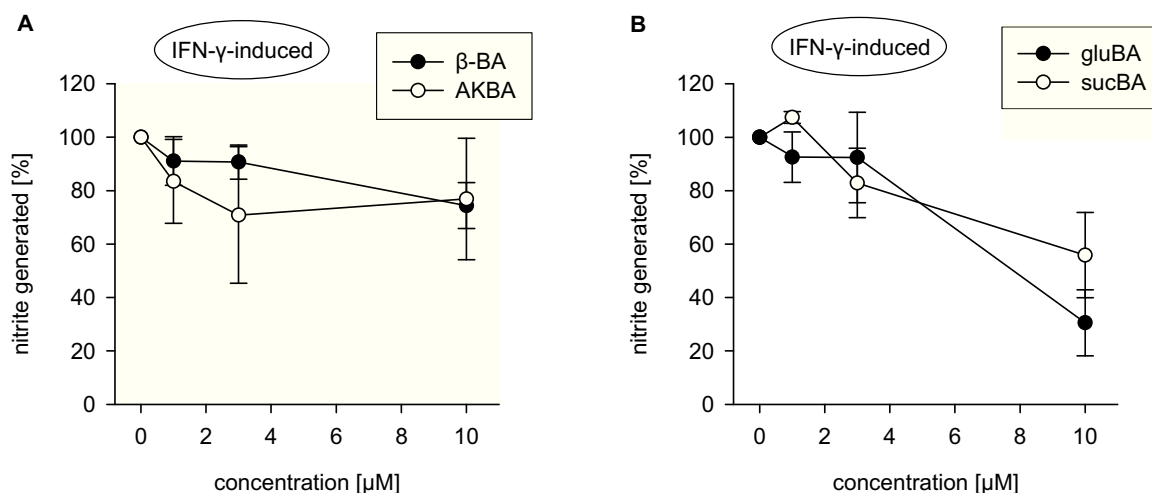
Fig. 4.17: Effects of BAs on IFN-γ-induced NO generation. *(**A**) Impact of β-BA and AKBA on nitrite levels after stimulation with IFN-γ. RAW264.7 cells (2.5 × 10^6/ml) were incubated with IFN-γ (10 ng/ml) and BAs for 20 h. Nitrite concentrations were determined by the Griess reaction. (**B**) Influence of gluBA and sucBA on nitrite levels after stimulation with IFN-γ. RAW264.7 cells (2.5 × 10^6/ml) were incubated with IFN-γ (10 ng/ml) and BAs for 20 h. Nitrite concentrations were determined by the Griess reaction. Data are given as means ± s.e.; n = 3. *** p < 0.001, vs vehicle (DMSO).*

4.3.5   Influence of BAs on LPS-induced p38 MAPK activation

LPS is a well described activator of p38 MAPK [253]. Therefore, the influence of BAs on additional LPS-induced subcellular pathways was analyzed by determination of the p38 MAPK activation status. RAW264.7 cells were incubated with LPS and BAs, lysed and the amount of phosphorylated p38 MAPK was detected as an activation marker by Western blot analysis. LPS increased the amount of phosphorylated p38 MAPK (**fig. 4.18**). Addition of β-BA resulted in an inhibition of p38 MAPK activation. β-BA and AKBA gave similar results, with β-BA being slightly more active than AKBA. Both BAs were ineffective at 0.5 µM, but displayed a quite potent inhibition at 1.7 and 5 µM. A higher concentration (17 µM) resulted in increased amounts of activated p38 MAPK. SucBA and gluBA failed to inhibit p38 MAPK activation. GluBA slightly enhanced p38 MAPK activation at 0.5 - 5 µM, but decreased it to 100% levels at

17 µM. sucBA led to a concentration-dependent potent activation of p38 MAPK, starting already at 0.5 µM, which was further enhanced with higher concentrations. These results indicate that BAs interfere with the p38 MAPK activating pathway in a more complex manner which may not solely be related to a simple direct binding and inhibition of LPS activity.

A

LPS	-	+	+	+	+	+	+	+	+	+	+	+
β-BA [µM]	-	-	0	0.5	1.7	5	17	-	-	-	-	-
AKBA [µM]	-	-	-	-	-	-	-	0.5	1.7	5	17	PxB5

B

LPS	-	+	+	+	+	+	+	+	+	+	+	+
gluBA [µM]	-	-	0	0.5	1.7	5	17	-	-	-	-	-
sucBA [µM]	-	-	-	-	-	-	-	0.5	1.7	5	17	PxB5
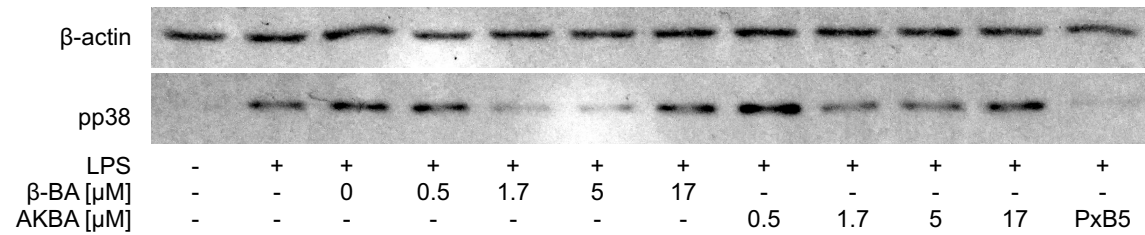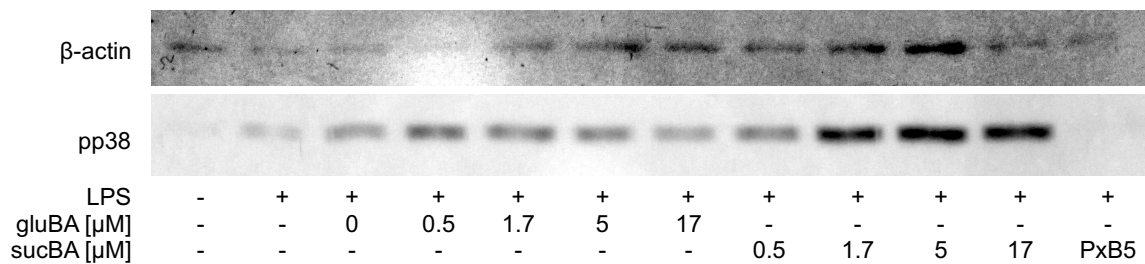
Fig. 4.18: Influence of BAs on LPS-induced p38 MAPK activation. *LPS was premixed with BAs or polymyxin B (PxB) for 10 min at 37 °C. Then, this mixture was added to RAW264.7 cells (1 × 10^7/ml), leading to a final LPS concentration of 0.1 µg/ml and (**A**) 0.5-17 µM β-BA, AKBA, (**B**) 0.5-17 µM gluBA, sucBA or (**A-B**) 5 µM PxB. Cells were incubated for 15 min at 37 °C, lysed and the amount of phosphorylated p38 MAPK (pp38) and β-actin were detected by Western blot experiments. Results shown are representative for three independent experiments.*

4.4 Interaction of BAs with catG

4.4.1   CatG is a binding partner of BAs

Similarly to LL-37, the serine protease catG was identified as a possible binding partner for BAs [40]. In order to characterize binding and possible functional effects, pull-down experiments as well as functional assays were performed.

In protein pull-down experiments, immobilized BAs were incubated with isolated catG. Precipitated proteins as well as proteins from the supernatant were analyzed by Western blotting. CatG could be specifically precipitated by BA-sepharose but not by the EAH-sepharose control (**fig. 4.19**). Addition of dissolved β-BA reversed this effect, as well as addition of a specific catG inhibitor (cathepsin G inhibitor I, CGI), suggesting similar binding sites. The catG level in the supernatant was diminished after precipitation. Again, this effect was reversed by addition of dissolved β-BA or CGI.

bead sn						
eluate						
EAH-seph	+	+	+	-	-	-
BA-seph	-	-	-	+	+	+
catG	+	+	+	+	+	+
β-BA [mM]	0	1	CGI	0	1	CGI
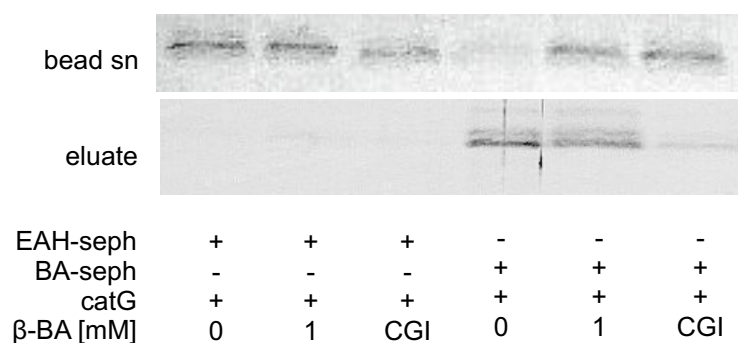
Fig. 4.19: CatG pull-down experiments with immobilized β-BA. EAH-sepharose (EAH-seph) and BA-sepharose (BA-seph) were incubated with catG (0.5 µg/ml) and DMSO, β-BA (1 mM) or catG inhibitor I (CGI, 0.5 µM). Precipitated proteins (eluate) as well as pull-down supernatants (bead sn) were analyzed by Western blotting using anti-catG antibodies. Results shown are representative for three independent experiments.

4.4.2   CatG activity is inhibited by BAs

In order to investigate if BAs inhibit catG activity, a catG-rich solution was freshly prepared from neutrophils by stimulation with cytochalasin B and fMLP. CatG activity was analyzed by addition of a colorimetric substrate and BAs. Several BAs displayed catG inhibiting activities (**fig. 4.20**). All β-configured BAs lacking an 11-keto moiety (ABA, eBA, gluBA and sucBA) inhibited catG efficiently at 10 µM, while at least a tendency of inhibition was detectable at 1 µM. Most potent were gluBA (24.5% remaining activity), ABA (28.1% remaining activity), eBA (28.8% remaining activity) followed by sucBA (59.4% remaining activity) at 10 µM, each. The corresponding synthetic 11-keto-BAs (eKBA, gluKBA and sucKBA) did not inhibit catG activity, neither at 1, nor at 10 µM. However, the naturally occurring 11-keto BA AKBA was quite active at 1 µM and 10 µM (36.4% and 14.7%, respectively), and KBA was also active at 10 µM (29.4 remaining activity).

Ac-LA was the only LA derivative which inhibited catG activity (**fig. 4.20**). While it was inefficient at 1 µM, an inhibition of 51% was determined at 10 µM. All RA derivatives tested were virtually ineffective, as well as α-BA, cis-diol-BA, oleanolic acid, 11-α-OH-BA and 11-β-OH-BA.
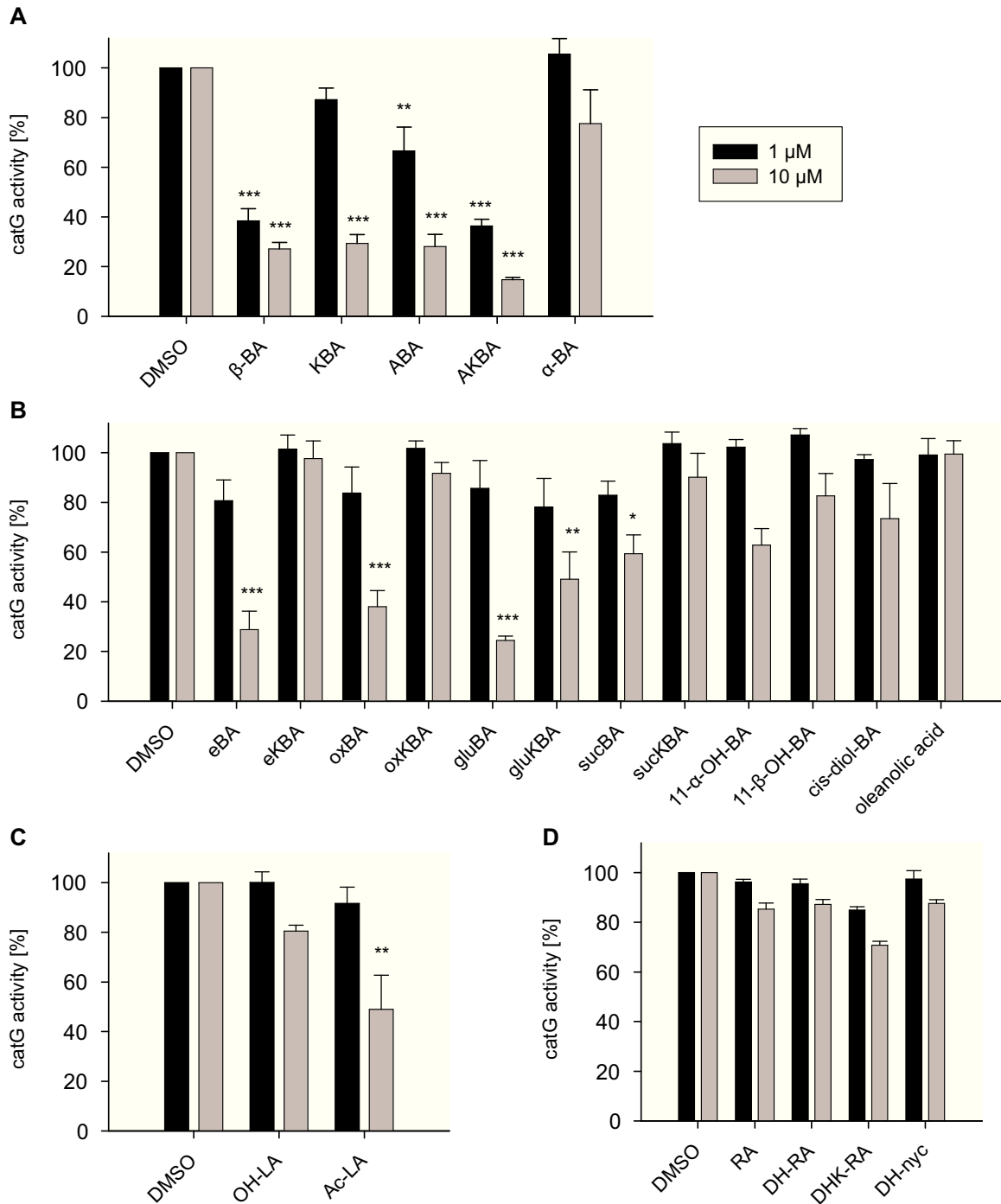
Fig. 4.20: Influence of BAs, LAs, RAs and DH-nyc on catG activity. *Neutrophils (2.5 ×10⁷/ml) were stimulated with cytochalasin B (10 μM) for 5 min and fMLP (2.5 μM) for additional 5 min at 37 °C to degranulate. After removal of cells by centrifugation, the supernatant was incubated with catG substrate (1 mM) and (**A**) naturally occurring BAs, (**B**) synthetic BAs, (**C**) LAs, (**D**) RAs and DH-Nyc for 110 min. The converted substrate was measured in a spectrophotometer at 405 nm. Data are given as means + s.e.; n = 3-7. * p < 0.05, ** p < 0.01, *** p < 0.001, vs vehicle (DMSO).*

4.4.3   AKBA inhibits the cathepsin G-induced Ca^{2+} influx

CatG-stimulation leads to an intracellular Ca^{2+} influx in platelets [188]. Platelets were preincubated with AKBA, CGI or DMSO and stimulated with catG. The amount of intracellular Ca^{2+} was monitored during the experiments. Addition of catG resulted in a prominent Ca^{2+}-influx in vehicle (DMSO)-treated platelets (**fig. 4.21**). Intracellular Ca^{2+} concentrations rose continuously for approx. 1 min. Afterwards, the intracellular Ca^{2+} concentrations decreased until they reached the initial level. Preincubation with AKBA resulted in an inhibition of this stimulation. When AKBA-preincubated platelets were stimulated with catG, a small, but continuous increase in intracellular Ca^{2+} levels was monitored. The slope was much lower than in the vehicle control. Addition of CGI led to a similar result as observed for AKBA.
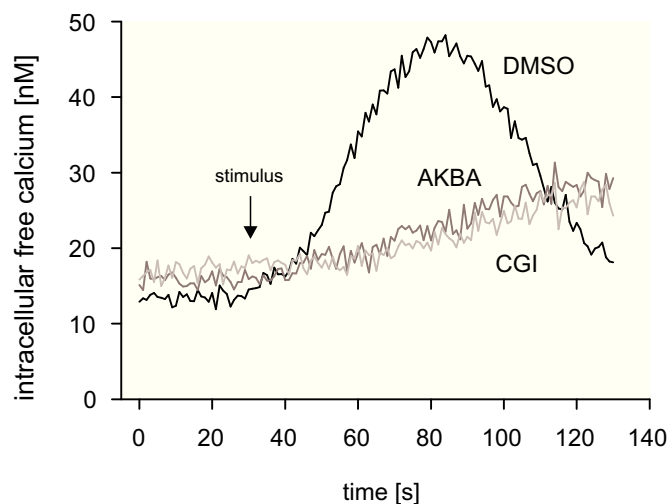
Fig. 4.21: Influence of AKBA on catG induced Ca^{2+} influx in platelets. *Fura-2 loaded platelets (1 × 10^8/ml) were pre-incubated with catG-inhibitor I (CGI, 0.2 μM), AKBA (5 μM) or DMSO for 15 min at 37 °C. Then, the measurement of intracellular Ca^{2+} levels was started. After 30 sec, catG (100 nM) was added. Curves are representative for three independent experiments.*

4.4.4 BAs inhibit fMLP-induced migration, but not chemotaxis

The protease catG is a mediator of neutrophil migration [254]. Thus, the influence of BAs on fMLP-induced motility was analyzed in neutrophils. ABA, AKBA and CGI inhibited the fMLP-induced cell migration through matrigel, while the chemotaxis in the absence of matrigel was not influenced by either of these compounds (**fig. 4.22**). Cell migration assays were performed by Lars Tausch.
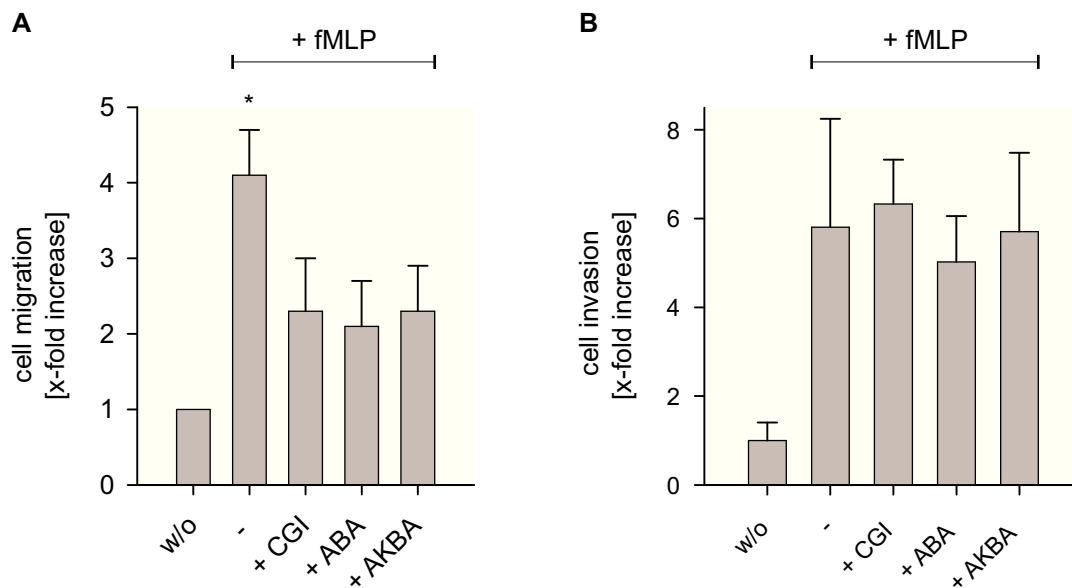
*Fig. 4.22: BAs inhibit cell migration through matrigel but not chemotaxis in absence of matrigel. (A) Cell migration was analyzed in a modified Boyden chamber system. Neutrophils (1 × 10^5 cells/ml) preincubated with BAs (10 µM, each) or catG inhibitor I (0.1 µM, CGI) were placed into matrigel-coated cell culture inserts (8 µm pore size). The inserts were transferred into wells filled with medium, FCS (10%) and fMLP (0.1 µM) or vehicle, alternatively. After 40 min, migrated cells in the matrigel layer were stained by crystal violet and counted under a light microscope. Cell migration assays were performed by Lars Tausch. (B) Chemotactic activity was analyzed. Experimental settings were the same as described above, except that the membranes of the cell culture inserts were left uncoated. Data are given as means + s.e.; n = 3. * p < 0.01, vs unstimulated cells.*

In order to analyze if BAs influence chemotaxis themselves, isolated BAs were tested for their ability to induce chemotaxis. While the non-acetylated BAs KBA and β-BA had only little effects on neutrophil chemotaxis, ABA and AKBA displayed chemotactic effects at higher concentrations ($\geq$ 30 µM, **fig. 4.23**). Thus, ABA (30 µM) led to a six-fold increase in migrated cell numbers. The potency of AKBA was intermediate, and resulted in an increase of migrated neutrophils by the factor 3.4 at 30 µM.
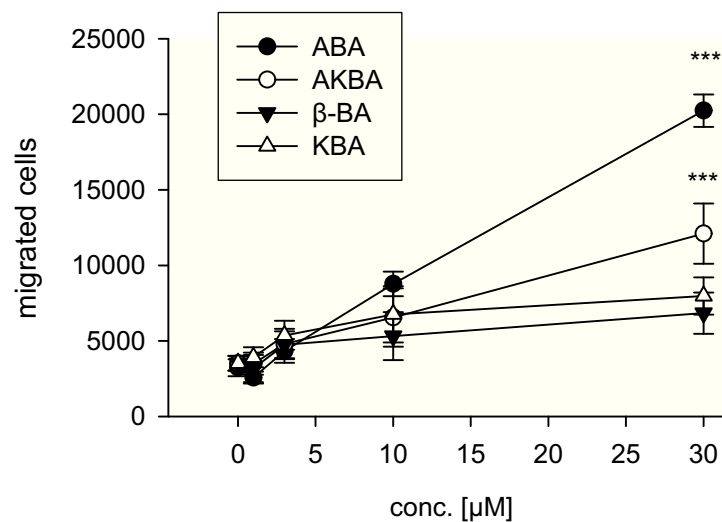
Fig. 4.23: Chemotactic activities of BAs. BAs were dissolved in medium and added to a lower compartment of a modified Boyden chamber. A membrane (8 µm pores) was mounted and calcein-AM-stained neutrophils (5 × 10^4) were placed on the top side. After 1 h, the fluid on the top side of the membrane was washed away and the number of migrated neutrophils was determined by a fluorescence measurement (ex. 485 nm, em. 535 nm) of the lower compartment and the membrane. Data are given as means ± s.e.; n = 3. *** p < 0.001, vs vehicle (DMSO).

4.4.5   BAs inhibit catG activity in the blood of BE-treated patients

In a phase II-III clinical trial, BE (3 × 800 mg/day) or placebo was administered to Crohn's disease patients. CatG activity of the blood was determined *ex vivo* before and after treatment for four weeks (**fig. 4.24**). Treatment with BE significantly reduced catG activity, while placebo treatment did not result in catG inhibition.
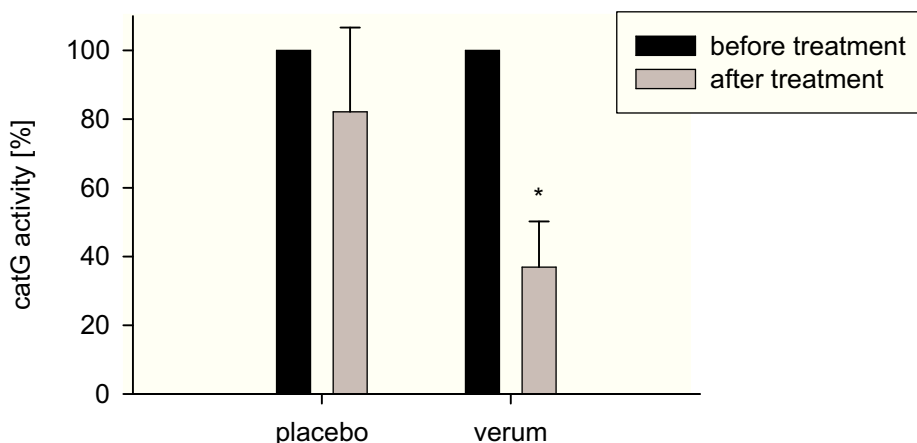
*Fig. 4.24: Inhibition of catG activity in the blood of BE-treated patients. In a phase II-III trial, blood was taken from Crohn's disease patients prior medication and after four weeks of continuous administration of either BE (3 × 800 mg/day) or placebo. Venous blood was collected and stimulated with 10 µM cytochalasin B and 2.5 µM fMLP for 5 min. Plasma was prepared and added to a buffer solution containing catG substrate N-suc-ala-ala-pro-phe-pNA (1 mM). The absorption at 405 nm was measured for 110 min as a marker for catG activity. Data are given as means + s.e.; n = 3. * p < 0.01, vs catG activity before treatment. Data were assessed in together with Lars Tausch.*

4.4.6   GluBA and oxBA do not inhibit inflammatory parameters in a pleurisy inflammation model

In order to analyze if a reduced cell migration (see **4.4.4**) might have *in vivo* relevance, a rat model of pleurisy inflammation was utilized. Previously, β-BA was shown to reduce inflammatory cell numbers in the pleural exudate of λ-carrageenan-treated rats, in addition to inhibition of other inflammatory parameters of the exudate [255]. Since synthetic BAs as gluBA and oxBA are potent catG-inhibitors (see **4.4.2**), the influence of these compounds in λ-carrageenan-induced pleurisy was analyzed. Both BAs were *i.p.* injected into male mice. Then, λ-carrageenan was injected in the pleural cavity before mice were killed 4 h later. Several inflammation parameters in the pleural

exudate were analyzed, including the exudate volume, the number of inflammatory cells in the exudate, prostaglandin E_2 (PGE_2) and LTB_4 formation. Both PGE_2 and LTB_4 are well described mediators of several inflammatory processes [256] and their generation was found to be inhibited by β-BA in the same animal model [255]. Therefore, these parameters were chosen as inflammatory markers.

When 1 mg/kg BAs were injected, oxBA reduced the exudate volume as a tendency (but not significantly), while gluBA had no effect (**fig. 4.25**, **A**). Cell number (**fig. 4.25**, **B**), PGE_2 (**fig. 4.25**, **C**) and LTB_4 formation (**fig. 4.25**, **D**) in the exudate were not influenced by gluBA and oxBA.
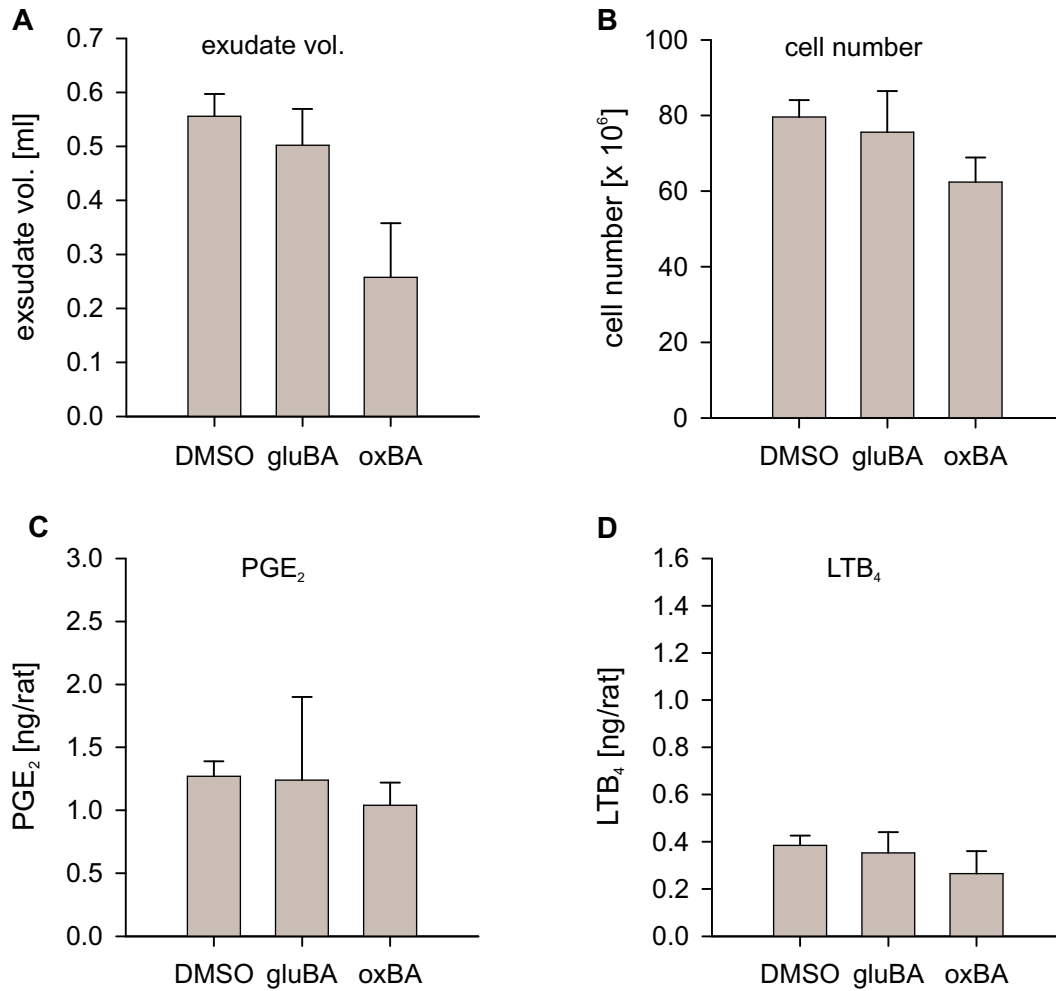
Fig. 4.25: oxBA (1 mg/kg) slightly influences exudates volume in a pleurisy inflammation model. *GluBA, oxBA or DMSO (1 mg/kg) were injected i.p. into male Wistar Han rats. Then, λ-carrageenan (1%) was injected into the pleural cavity. After 4 h, the animals were killed and the exudates from the pleural cavity were collected. (**A**) The exudate volume was determined. (**B**) Cells in the exudates were counted. (**C**) PGE$_2$ levels were determined by a radioimmunoassay. (**D**) LTB$_4$ levels in the exudates were detected by an enzyme immuno assay. Data are given as means + s.e.; n = 5.*

When 5 mg/kg weight BAs were injected into rats, none of the inflammatory parameters tested was influenced. Exudate volume (**fig. 4.26**, **A**), cell number (**fig. 4.26**, **B**), PGE$_2$ (**fig. 4.26**, **C**) and LTB$_4$ (**fig. 4.26**, **D**) formation were at the same levels as the vehicle control.
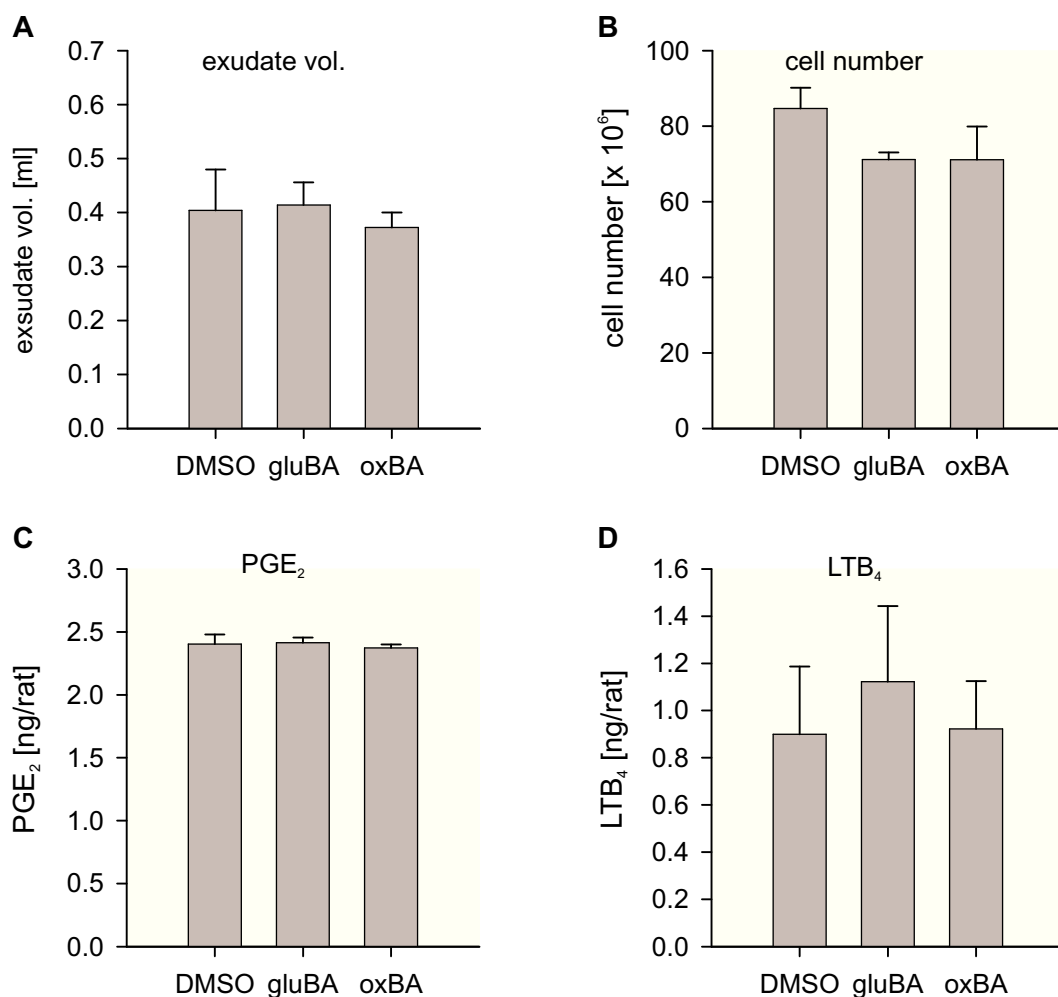
Fig. 4.26: BA derivatives (5 mg/kg) do not influence several inflammatory parameters in a murine pleurisy inflammation model. *GluBA, oxBA or DMSO (5 mg/kg) was injected i.p. into male Wistar Han rats. Then, λ-carrageenan (1%) was injected into the pleural cavity. After 4 h, the animals were killed and the exudates from the pleural cavity were collected. (**A**) The exudate volume was determined. (**B**) Cells in the exudates were counted. (**C**) PGE$_2$ levels were determined by a radioimmunoassay. (**D**) LTB$_4$ levels in the exudates were detected by an enzyme immuno assay. Data are given as means + s.e.; n = 5.*

4.5 Interaction of BAs with p21 Ras

4.5.1   BAs bind to p21 Ras in a direct manner

Besides LL-37 and catG, p21 Ras was identified in initial protein pull-down experiments as a potential binding partner of BAs [40]. In the present study, the interaction of BAs and p21 Ras was investigated in detail. First, a possible binding of BAs to H-Ras was analyzed in protein pull-down experiments. HL60 lysates as well as isolated H-Ras were used as a source of Ras and incubated with immobilized BAs. H-Ras could be precipitated by KBA-sepharose but not by EAH-sepharose in both lysate and isolated protein approaches (**fig. 4.27**).

Ras						
Sepharose	EAH	KBA	EAH	KBA	EAH	KBA
Ras	+	+	+	+	-	-
HL60	-	-	+	+	+	+
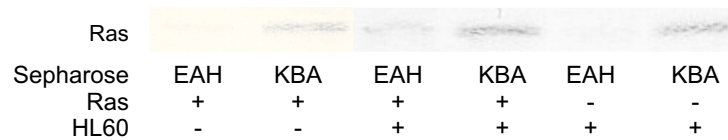
Fig. 4.27: Binding of KBA to H-Ras. KBA-sepharose and EAH-sepharose were incubated with H-Ras (2.7 µg/ml), HL60 lysates or a mixture of both. Precipitated proteins were analyzed by Western blotting using anti-Ras antibodies. Results shown are representative for three independent experiments.

4.5.2 Influence of BAs on p21 Ras activity

The influence of BAs on the amount of GTP-bound p21 Ras was determined as a marker for p21 Ras activity. When neutrophils were incubated with AKBA (30 µM) and stimulated with 5-HETE, an increase of Ras-GTP levels were detected (**fig. 4.28**, **A**). A lower AKBA concentration of 10 µM as well as β-BA (up to 30 µM) did not enhance Ras-GTP amounts. AKBA and β-BA alone did not stimulate endogenous Ras-GTP concentrations in neutrophils (**fig. 4.28**, **B**) or in HL-60 cells (**fig. 4.28**, **C**).

A

Ras-GTP					Ras-GTP			
AKBA [µM]	0	10	30		β-BA [µM]	0	10	30
5-HETE	+	+	+		5-HETE	+	+	+

B

Ras-GTP						Ras-GTP				
AKBA [µM]	0	10	30	-		β-BA [µM]	0	10	30	-
5-HETE	-	-	-	+		5-HETE	-	-	-	+

C

Ras-GTP					Ras-GTP			
AKBA [µM]	0	0.1	1	10	β-BA [µM]	0	0.1	1	10
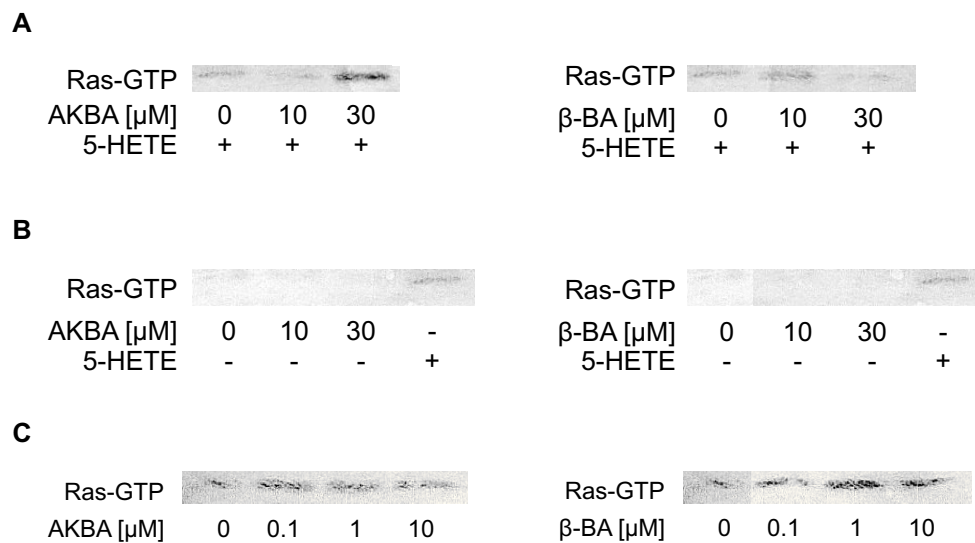
Fig 4.28: Influence of AKBA and β-BA on Ras activation. (A) Neutrophils (2 × 10^7/ml) were incubated with BAs for 1.5 min and stimulated afterwards with 5-HETE (1 ng/ml) for additional 1 min. Cell were lysed and lysates were transferred onto Raf-RBD coupled sepharose-beads. After incubation for 1 h, the beads were washed. Bound proteins were eluted and analyzed by Western Blotting using a Ras-specific antibody. (B) Neutrophils (2 × 10^7/ml) or (C) HL-60 cells (1 × 10^6/ml) were incubated with BAs for 1.5 min. Cell lysates were incubated with Raf-RBD coupled sepharose beads and the bound proteins were washed, eluted and analyzed by Western Blotting. Results shown are representative for three independent experiments.

4.6 Interaction of BAs with Rap1B

4.6.1   Recombinant Rap1B expression

To analyze possible binding to Rap1B, a method for expression and purification of Rap1B was established. The bacterial expression strain *E. coli* BL21, transformed with Rap1B-GST-fusion-protein expression vectors (obtained from A. Smolenski, University of Frankfurt, Germany) was used as a producing organism. After induction of expression by IPTG, Rap1B-GST-fusion proteins were produced and detected in Western blotting experiments of bacterial lysates (**fig. 4.29**). In order to isolate Rap1B-GST-proteins, immobilized glutathione (GSH-sepharose) was used to precipitate fusion proteins. After elution by proteolytic cleavage, Rap1B was liberated. Thrombin was removed by affinity chromatography columns and purified Rap1B could be detected in the flow-through.
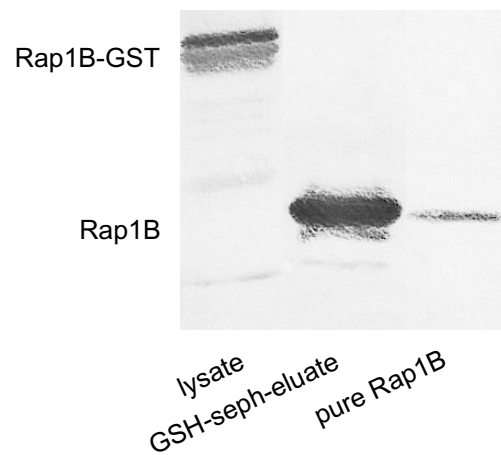
Fig. 4.29: Recombinant expression and purification of Rap1B. E. coli *BL21, transformed with a Rap1B-GST-expression vector (pGEX-2T-rap1B), were induced overnight at 20 °C by IPTG (0.1 mM) to express Rap1B-GST fusion proteins. Cell lysates were analyzed by Western blotting using anti-Rap1B antibodies. Rap1B-GST was precipitated with GSH-sepharose (GSH-seph) and eluted by a proteolytic cut in front of the GST-domain with thrombin. Thrombin was removed by affinity chromatography using benzamidine columns, and an isolated Rap1B solution was obtained.*

4.6.2   Rap1B is a binding partner of BAs

In protein pull-down experiments the binding characteristics of BAs and Rap1B were analyzed. Purified Rap1B as well as platelet lysates were incubated with KBA-sepharose or EAH-sepharose. Rap1B could be specifically precipitated in isolated protein and in lysate approaches (**fig. 4.30**).

	EAH	KBA	EAH	KBA
Sepharose	EAH	KBA	EAH	KBA
Rap1B	+	+	-	-
Platelets	-	-	+	+
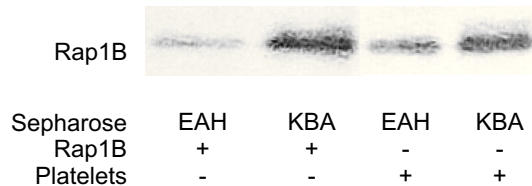
Fig. 4.30: Binding of Rap1B to KBA. KBA-sepharose and EAH-sepharose were incubated with isolated Rap1B (5.3 µg/ml) or in platelet lysates. Precipitated proteins were analyzed by Western blotting using anti-Rap1B antibodies. Results shown are representative for three independent experiments.

4.6.3 Nucleotide exchange of Rap1B is not influenced by AKBA

The influence of AKBA on nucleotide exchange speed was analyzed by incubating mRap1B (Rap1B loaded with mant-GppNHp) with AKBA and an excess of GDP. The binding of mant-GppNHp leads to a fluorescent labeling of Rap1B. Nucleotide exchange can be monitored by measuring fluorescence of mant-nucleotide-loaded proteins in a solution with an excess of free unlabeled nucleotides: the fluorescence of mant-nucleotides is quenched if they are not bound to proteins [257]. As shown in **fig. 4.31**, AKBA does not influence nucleotide exchange behavior in concentrations up to 2.5 µM.
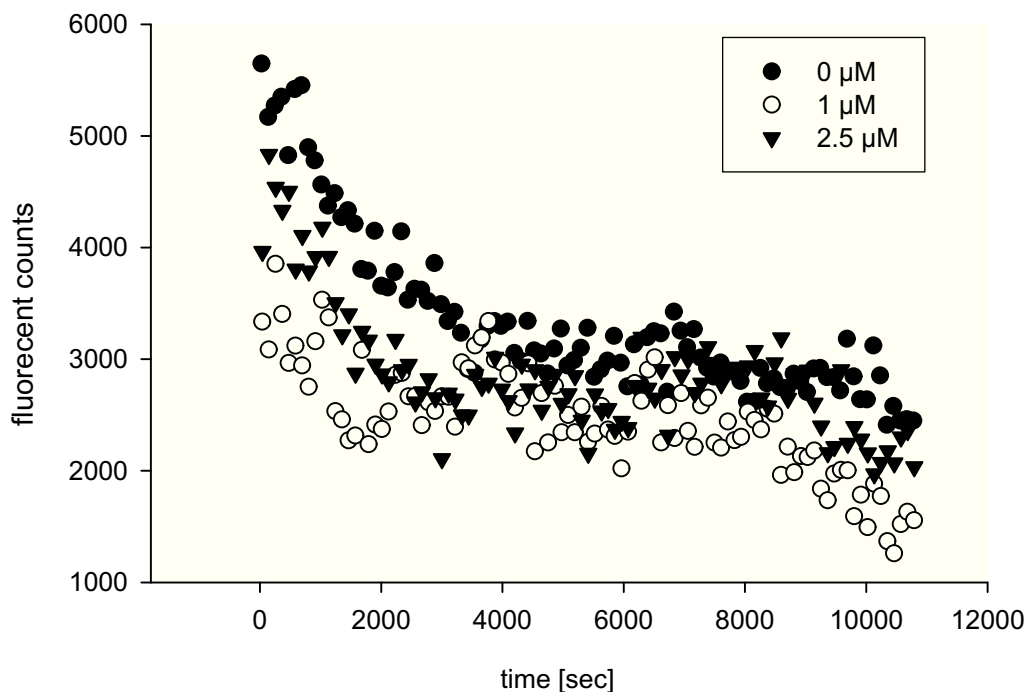
Fig. 4.31: AKBA has no influence on nucleotide exchange of Rap1B. Rap1B (30 nM) was loaded with fluorescent mant-GppNHp. GDP (2 mM) and AKBA was added and the fluorescence change (ex. 366 nm, em. 408 nm) was recorded. Curves shown are representative for three independent experiments.

Taken together, both p21 Ras and Rap1B were identified as direct binding partners of BAs. However, functional assay showed only slight effects on p21 Ras and Rap1B activity.

4.7 Influence of BAs on cell viability and apoptosis

4.7.1   Selective BAs induce apoptosis in Jurkat cells

Previous studies showed that BEs and BAs, in particular AKBA, induced apoptosis in a number of cancer cells [235]. In order to investigate whether synthetic BA derivatives and other triterpenes derived from frankincense may induce apoptosis and to identify the potential molecular mechanism, Jurkat T-lymphocytes were chosen as a testing system. A *B. caterii* Birdw. extract was previously shown to induce apoptosis in Jurkat cells [258], and a contribution of BAs and triterpenes derived from frankincense seemed likely. First, cell viability of triterpene-stimulated Jurkat A3 cells was analyzed. After two days of incubation with triterpenes, surviving cells were stained and quantified *via* an MTT cytotoxicity assay. The naturally occurring BAs KBA, β-BA and α-BA did not show cytotoxic effects at 10 µM, while both ABA and AKBA decreased the number of viable cells (ABA: 21% viable cells, AKBA: 65%, **fig. 4.32**). The only synthetic BAs with cytotoxic activity were eKBA (64.3% viable cells at 10 µM), oxBA (67.4%), gluBA (10.4%) and sucBA (31.8%), while eBA, oxKBA, gluKBA and sucKBA did not influence cell viability. The LA derivatives OH-LA and Ac-OH-LA were quite cytotoxic (17.4% and 25.1% viable cells at 10 µM, respectively), while Ac-LA itself had no impact on the number of viable cells. All RAs were moderately cytotoxic at 10 µM, while DH-RA was the most potent RA (50.9% viable cells), followed by RA (72.9%) and DHK-RA (78.3%).

The most cytotoxic compound analyzed was ursolic acid, with 8.7% viable cells at 10 µM. Amyrin and oleanolic acid were not cytotoxic.

A

B

C

D
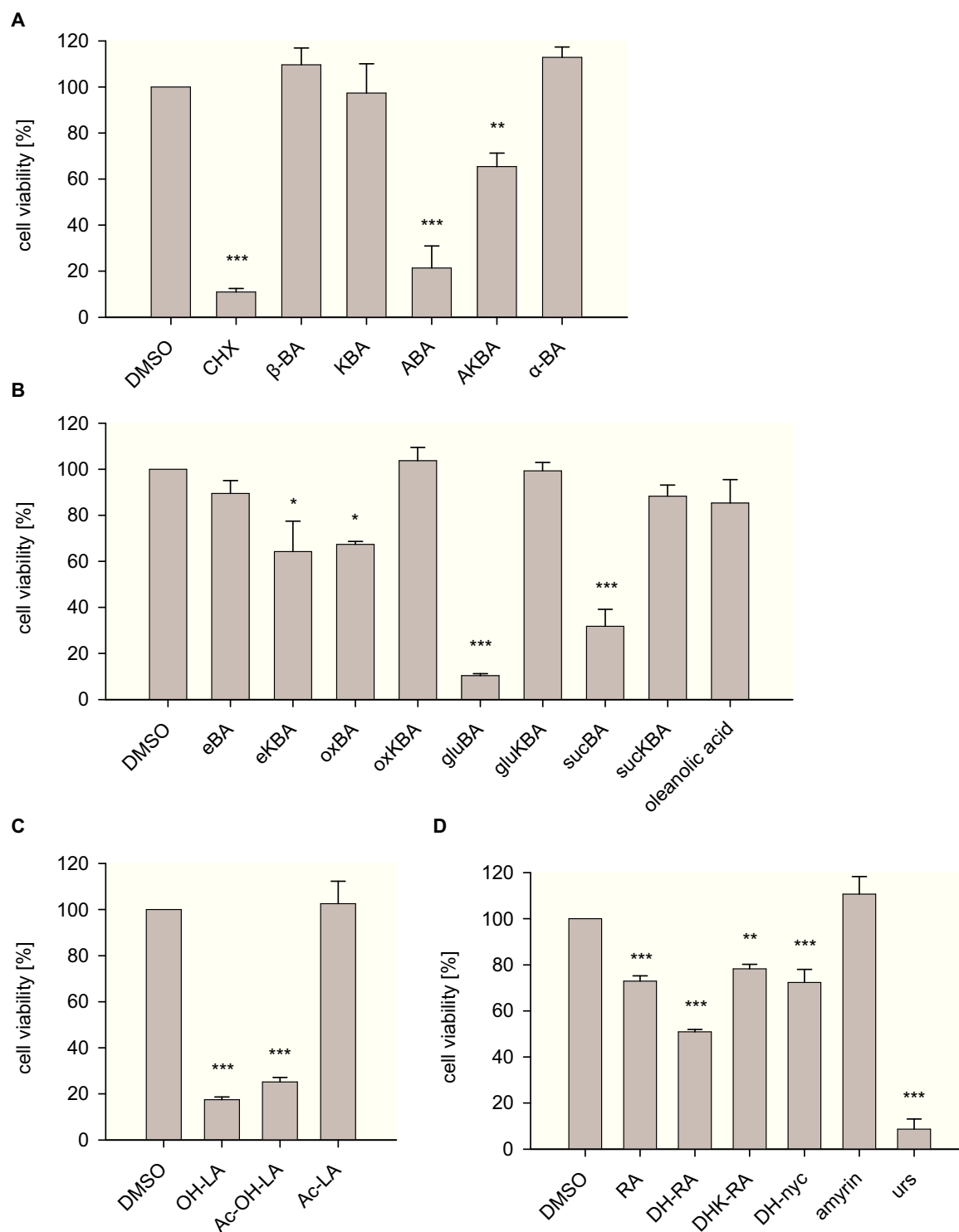
Fig. 4.32: Cytotoxicity of triterpenes derived from frankincense in Jurkat T lymphocytes. *Jurkat A3 (3×10^5/ml) were incubated with (**A**) naturally occurring BAs, (**B**) synthetic BAs, (**C**) LAs and (**D**) RAs and other triterpenes derived from frankincense (10 μM, each) for 48 h at 37 °C and 6% CO_2. Then, the dye MTT was added for additional 30 min. Only viable cells are able to reduce the yellow MTT to a purple product. Cells were lysed overnight and the absorption at 595 nm was measured. Data are given as means + s.e.; n = 3. * p < 0.05, *** p < 0.001, vs vehicle (DMSO).*

A concentration-response analysis was performed to achieve EC_{50} values regarding the cytotoxicity. Surprisingly, ABA was the most potent triterpene tested (EC_{50} = 2.8 µM, **fig. 4.33**, **A**) and AKBA was much less efficient (EC_{50} = 9.8 µM). The synthetic BAs sucBA and gluBA showed EC_{50} values of 9.8 µM and 5.2 µM, respectively, while oxBA was only slightly cytotoxic (up to 30 µM, **fig. 4.33**, **B**). OH-LA and Ac-OH-LA were cytotoxic with EC_{50} values of 6.3 µM and 9.7 µM, respectively (**fig. 4.33**, **C**). Ac-LA itself had no effect on the cell viability. RA and DH-RA are only slightly cytotoxic (**fig. 4.33**, **D**), with EC_{50} values of 16.9 µM (RA) and 10.1 µM (DH-RA). DHK-RA displayed very little cytotoxic effects ($EC_{50} > 30$ µM). 3-α-Ac-TA reduced cell viability moderately (EC_{50} = 14.7 µM), while other TAs (3-oxo-TA, 3-α-OH-TA, 3-β-OH-TA and 3-α-OH-7,24-dien-TA) had only slight cytotoxic properties ($EC_{50} > 30$ µM, **fig. 4.33**, **E**). Ursolic acid was quite toxic with an EC_{50} value of 4.5 µM.
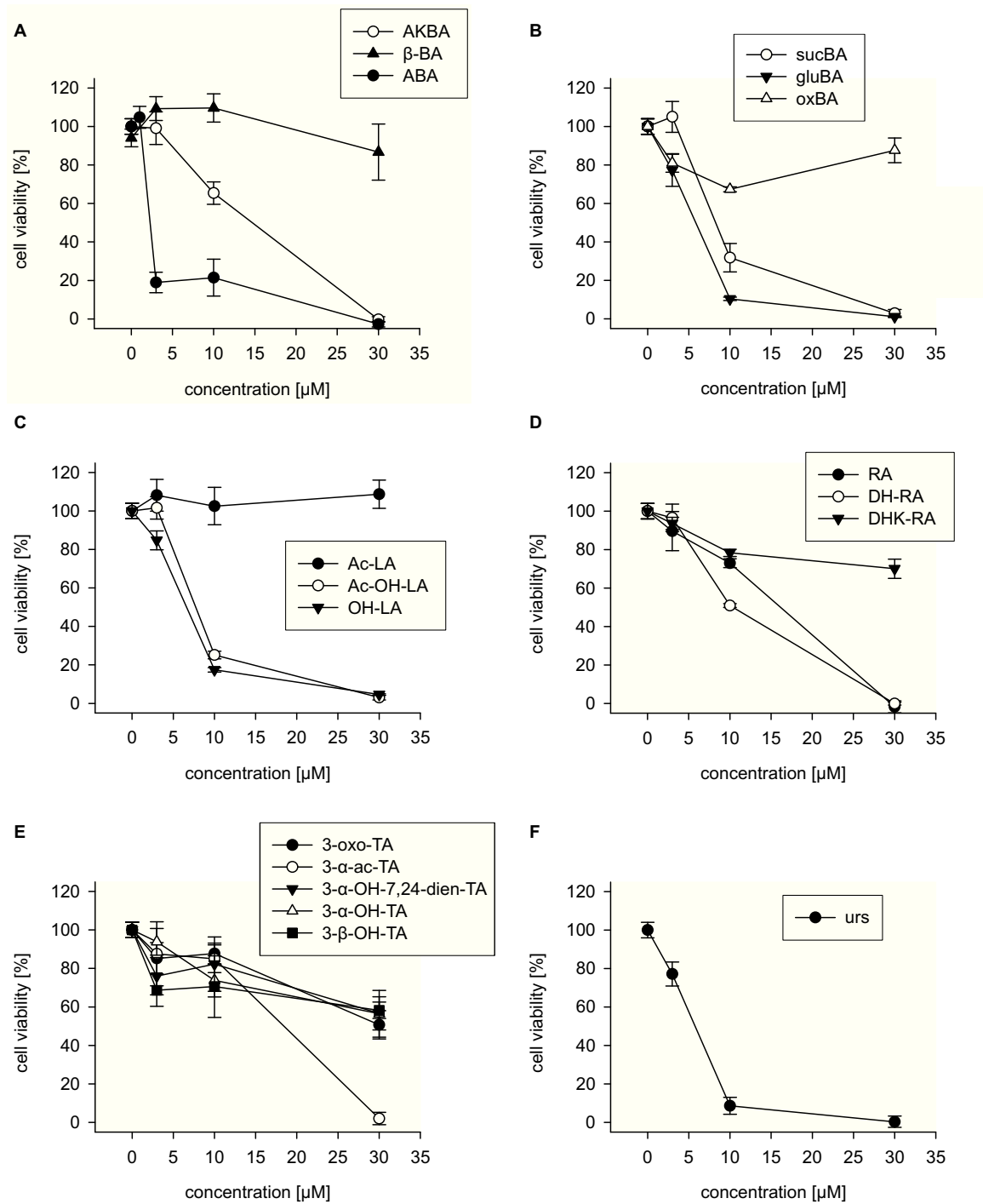
Fig. 4.33: Concentration-dependent cytotoxicity of BAs, LAs, RAs, TAs and urs.
*Jurkat A3 (3×10^5/ml) were incubated with (**A**) naturally occurring BAs, (**B**) synthetic BAs, (**C**) LAs, (**D**) RAs, (**E**) TAs or (**F**) urs for 48 h at 37 °C and 6% CO_2. Then, the dye MTT was added for additional 30 min. Only viable cells are able to reduce the yellow MTT to a purple product. Cells were lysed overnight and the absorption at 595 nm was measured. Data are given as means ± s.e.; n = 3. * p < 0.05, *** p < 0.001, vs vehicle (DMSO).*

In order to analyze if the viability of non-cancer cells is affected by compounds from frankincense, peripheral blood mononuclear cells (PBMCs) were investigated in the MTT cytotoxicity assay (**fig. 4.34**). AKBA was the only naturally occurring BA tested which displayed a cytotoxic effect at 25 µM (31.8% viable cells). GluBA and sucBA were cytotoxic as well (13.5% and 28.4% cell viability), while the other synthetic BAs (eBA, eKBA, oxBA, oxKBA, gluKBA and sucKBA) did not influence cell viability. Both OH-LA and Ac-OH-LA were cytotoxic at 25 µM (28.8% and 51.7% viable cells, respectively). Ac-LA showed no cytotoxic effects. RA and DH-RA decreased the number of viable cells (51.9% and 34.0% viable cells), while DHK-RA had no effect. Finally, DH-nyc was cytotoxic (43% viable cells), and oleanolic and amyrin had no impact on the cell number.
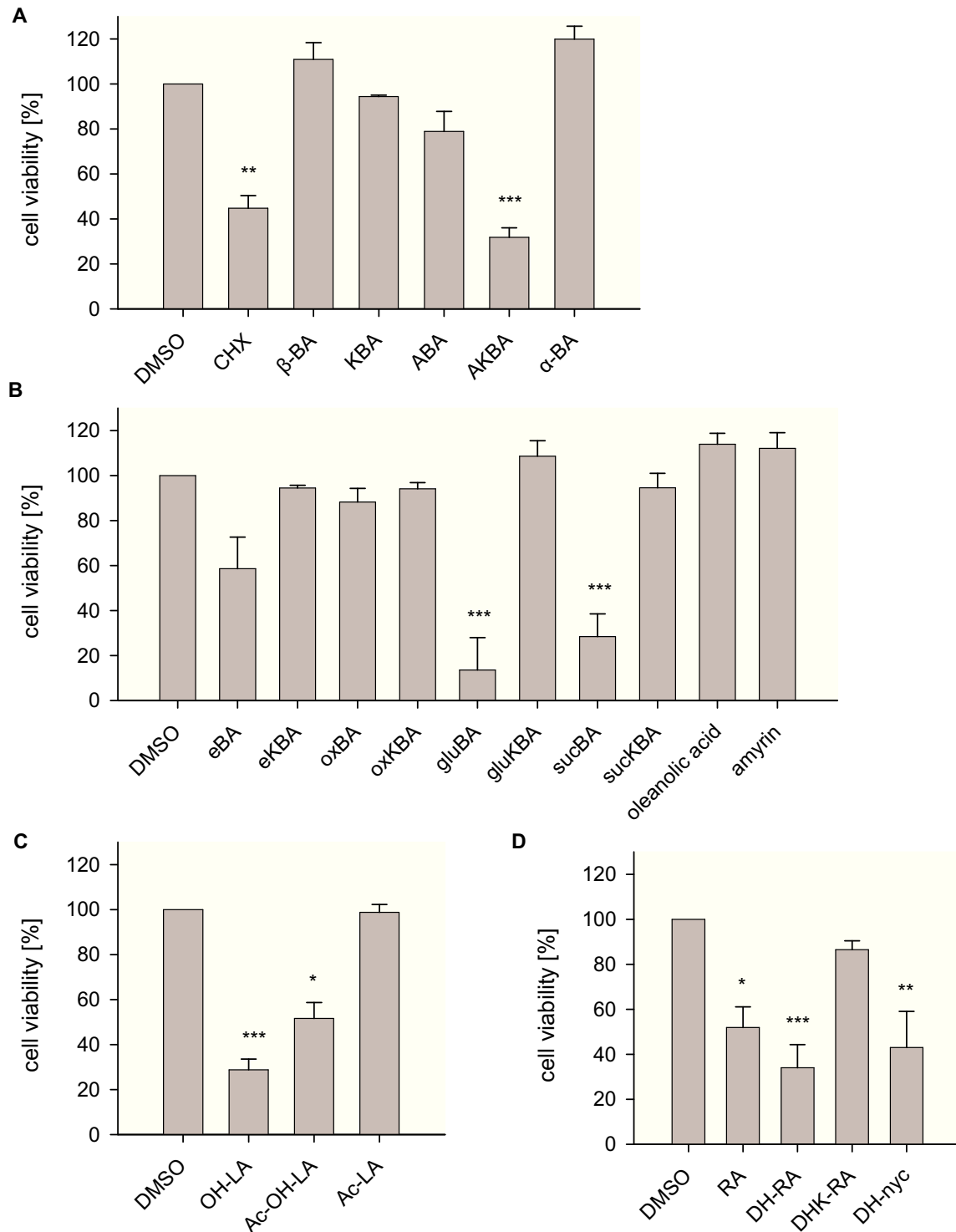
Fig. 4.34: Cytotoxicity of BAs, LAs, RAs and DH-nyc in PBMCs. *PBMCs (2 × 10⁶/ml) were incubated with (A) naturally occurring BAs, (B) synthetic BAs, (C) LAs and (D) RAs and DH-nyc (25 μM, each) for 48 h at 37 °C and 6% CO₂. Then, the dye MTT was added for additional 30 min. Only viable cells are able to reduce the yellow MTT to a purple product. Cells were lysed overnight and the absorption at 595 nm was measured. Data are given as means + s.e.; n = 3. * p < 0.05, ** p < 0.01, *** p < 0.001, vs vehicle (DMSO).*

4.7.2   BAs induce PARP-, caspase-3 and caspase-8 cleavage

Reduction of cell viability can be related to apoptosis or necrosis. Additional experiments were performed in order to investigate which of those two modes of actions are responsible for the cytotoxic effects of BAs and LAs. During apoptosis, caspases are activated by proteolytic cleavage [259]. In addition, PARP is a well described apoptosis marker, which is cleaved during programmed cell death [260]. Jurkat A3 were incubated with BAs and lysed. The cellular amount of uncleaved caspase-3, caspase-8, as well as the amount of cleaved PARP, was analyzed by Western blotting. AKBA, gluBA, sucBA and OH-LA decreased procaspase-3 and procaspase-8 levels at 10 µM, while the amount of cleaved PARP rose in a concentration-dependent manner (**fig. 4.35**). A slight reduction of procaspase levels and a slight increase of cleaved PARP levels were detected already at 3 µM, while lower concentrations had no effects.

A

B

C

D

E

F
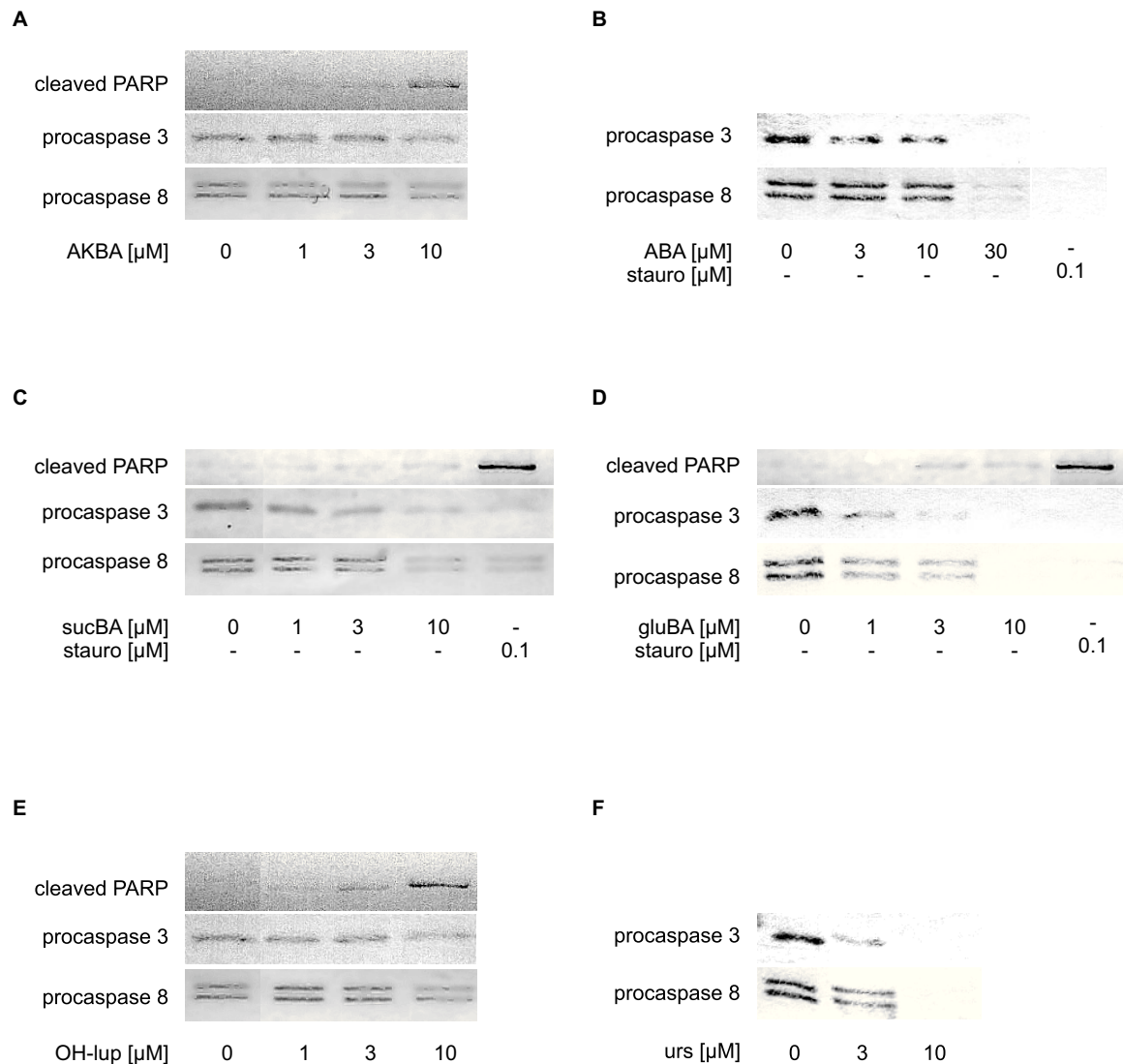
Fig. 4.35: Influence of triterpenes derived from frankincense on caspase-3, caspase-8 and PARP. Jurkat A3 cells (2 × 10⁵/ml) were incubated with (A) AKBA, (B) ABA, (C) sucBA, (D) gluBA, (E) OH-LA, (F) urs and (B-D) staurosporine (stauro, 0.1 µM) for 24 h at 37 °C and 6% CO₂. Cells were lysed and lysates were analyzed by Western blotting using anti-caspase-3-, anti-caspase-8 and anti-cleaved-PARP-antibodies. Results shown are representative for three independent experiments.

4.7.3 DNA fragmentation is induced by BAs

DNA fragmentation occurs during apoptosis [261]. To evaluate the effects of BAs on DNA fragmentation in Jurkat A3, cells were incubated with BAs, lysed and DNA was stained by propidium iodide.

The amount of cells with low fluorescence (sub-G1) was increased by rising concentrations of AKBA, sucBA and gluBA (fig. 4.36). GluBA was the most potent BA tested and at 30 µM equally effective as staurosporine at 1 µM. AKBA displayed intermediate DNA-fragmentation, while the activity of sucBA was slightly lower than the activity of AKBA.
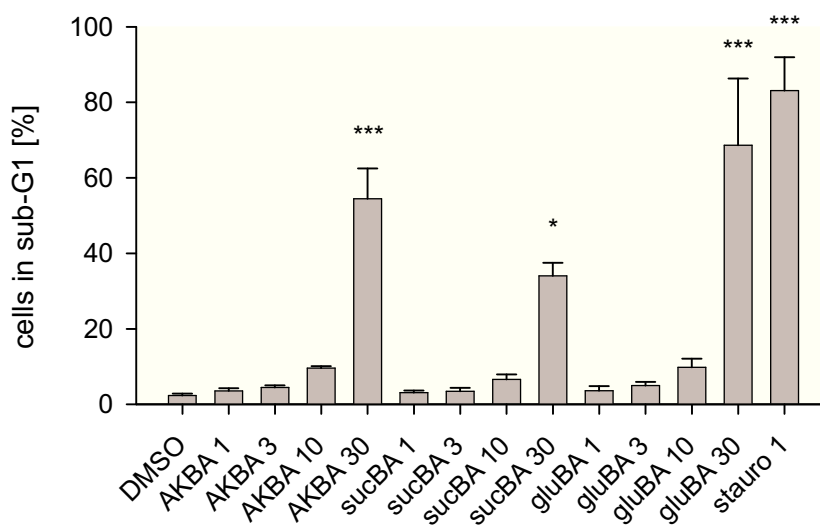
*Fig 4.36: Influence of BAs on DNA fragmentation. Jurkat A3 cells (2×10^5/ml) were incubated with BAs (1-30 µM), staurosporine (1 µM) or DMSO for 24 h. Cells were lysed with lysis buffer containing propidium-iodide, before fluorescence intensities of cell nuclei were measured in a flow cytometer (FL2 585/42). Apoptotic nuclei have a lower fluorescence than the 2N peak (sub-G1) and contain hypodiploid DNA. Data are given as means + s.e.; n = 3. * $p < 0.01$, *** $p < 0.001$ vs vehicle (DMSO).*

5.   Discussion

5.1 Identification and evaluation of molecular targets of BAs

The molecular mechanisms underlying the anti-inflammatory effects of frankincense extracts are poorly understood. BAs are the main principles in these extracts, and a contribution of BAs to the observed effects seems likely. Though several targets of BAs were identified up to now (including 5-LO, COX-1, IKK, Akt, HLE and C3-convertase) [235], many of these studies either analyzed solely AKBA or identified AKBA as the compound with the highest activity. However, the bioavailability of AKBA is very low [10,68], and a contribution of BAs with a higher bioavailability to the anti-inflammatory effects of frankincense extracts seems likely. In addition, other active principles of frankincense extracts besides BAs may modulate the inflammatory process.

In the present study, several new targets for triterpenes derived from frankincense were identified by using a pull-down strategy. This strategy was based on linking a triterpene to an insoluble bead. By incubating these triterpene-coupled beads with cellular lysates, potential binding partners (targets) could be identified and further characterized by additional biochemical methods. The interactions of different triterpenes derived from frankincense with each of these identified targets, the effects, the relevance and possible consequences are discussed in detail in the following paragraphs.

5.1.1 hCAP18 and LL-37 are targeted by BAs and other triterpenes

Previous target-fishing studies using BAs as bait performed by Dr. Lars Tausch (Goethe University, Frankfurt) revealed the human cathelicidin hCAP18 as a potential binding partner of KBA [40]. Here, a direct binding mode was demonstrated. Interestingly, the C-terminal antimicrobial peptide liberated from hCAP18, i.e. LL-37, is also a direct binding partner of KBA, implying that the binding to hCAP18 likely occurs through the LL-37 domain. The LL-37 binding effect was not only specific to KBA-sepharose, as LL-37 binds also to BA-sepharose. Importantly, this binding has functional consequences: the LPS-inhibiting potential of LL-37 was diminished. This inhibitory

effect was most prominent for the natural occurring BAs (i.e. ABA and AKBA), but not limited to BAs, as some LAs and RAs were able to restore LL-37-inhibited LPS activities as well (for a summary of the SAR studies, see **tab. 5.1**, **tab. 5.2** and **tab. 5.3**). It seems that an introduction of a carboxylic group connected *via* an alkylic ester or ether at the C-3 position of BAs impairs the bioactivity of the compounds. This may be caused by a modification of the polarity near the C-3 position, or by sterical hindrance at this site (the introduced moieties elongate the molecule at the C-3 position) and it implicates that either the introduced polar group or the elongation at the C-3 position is detrimental for the LL-37 inhibiting effects. The impact of the C-11-keto group could not be analyzed in detail under the testing conditions because many non-11-keto-BAs are prominent direct LPS neutralizing compounds and interfered with the testing system. However, the similar effects of AKBA and ABA implicate that the 11-keto group may be of minor importance.

The inhibition of biological LL-37 activities may have *in vivo* relevance. The low IC_{50} values of BAs, especially of ABA (IC_{50} = 0.2 µM), are in the range of plasma concentrations reached after oral application of *B. serrata* extracts (e.g. ABA: 2.4-4.9 µM) [10,68]. The inhibitory effect was not only limited to isolated LL-37; it was also relevant in the presence of other proteins from neutrophil granules. Upon stimulation, neutrophils degranulate and release proteinase-3 and hCAP18 [97]. hCAP18 is then processed by proteinase-3, resulting in the liberation of LL-37. The LPS-inhibitory effect of degranulated neutrophil supernatant was reversed by ABA and the LPS-inhibitory effect of diluted human blood plasma was impaired by ABA as well. This implicates that the ability of plasma proteins to bind to BAs [262] does not abolish their inhibitory effects on LL-37. However, it should be noted that diluted plasma was used and a higher plasma protein concentration is present in whole blood, therefore a possible interaction with plasma proteins cannot be completely excluded. In general, the reversion of the LPS-inhibiting properties of LL-37 demonstrates the effectiveness of BAs to inhibit LL-37 activity.

Inhibition of LL-37 might explain some of the observed anti-inflammatory effects of BAs. Though both pro- and anti-inflammatory properties of LL-37 have been reported [126], high LL-37 levels were found in certain inflammatory diseases, e.g. psoriasis [113], and a contribution of LL-37 to the course of this disease has been suggested. Interestingly, in the CD18 hypomorphic mouse model of psoriasis [263], systemical and

local treatment with AKBA inhibited several disease parameters like TNF-α production and interleukin-12 and -23 expression [264]. The only murine cathelicidin CRAMP (cathelin-related antimicrobial peptide) is closely related to LL-37 [265], implicating that BAs may influence its activity as well. However, detailed studies about the effects on human psoriasis are still missing, and further evidences are needed to exploit the potential of BAs as novel therapeutics in the treatment of psoriasis. Nonetheless, BAs are virtually the first identified inhibitors of LL-37 and might open a new field for the development of novel drugs against LL-37-mediated diseases.

The main function of LL-37, derived from the only human cathelicidin hCAP18, was initially assumed to be the killing of bacteria [122]. Later on, immunomodulatory effects of LL-37 were identified, and LL-37 cannot be regarded as a solely anti-microbial peptide anymore [129]. Among the pro-inflammatory properties, LL-37 was described as a chemotactic agent for neutrophils [131]. Cellular signaling resulting in chemotactic activity may be related to mobilization of intracellular Ca^{2+} and activation of MAPKs (as ERK1/2 and p38 MAPK) [138]. These effects could not be reproduced in this thesis, however. Even at rather high concentrations (10 µM), LL-37 did not induce neutrophil chemotaxis, ERK1/2 or p38 MAPK phosphorylation or intracellular Ca^{2+} mobilization. Also, in contrast to a previous study [249], the reported apoptosis-inducing abilities of LL-37 in Jurkat T-lymphocytes could not be confirmed. Therefore, the molecular basis of the immunomodulatory mode of action of LL-37 might be carefully re-evaluated.

Though BAs have inhibitory effects on LL-37 activity, selected BAs may also increase LL-37 generation under certain conditions. Both β-BA and AKBA induced a higher release of hCAP18 in cytochalasin B/fMLP-stimulated neutrophils. This is most likely a priming effect which leads to a more extensive degranulation. As a consequence, higher levels of LL-37 were observed, suggesting that the increased release of hCAP18 might completely overcome the reported slight inhibition of the LL-37 liberating protease (proteinase-3) by BAs [40]. Released LL-37 may lead to a higher capacity of killing bacteria and may contribute to the beneficial effect of BEs in diseases where bacteria potentially participate (i.e. Crohn's disease) [266]. However, high concentrations of BAs are needed to upregulate hCAP18 release and therefore the inhibitory effects of BAs on LL-37 activity may dominate and have a higher *in vivo* relevance.

5.1.2   LPS is a target of triterpenes derived from frankincense

Bacterial LPS was identified as a direct binding partner of β-BA in pull-down experiments. The binding of BAs to LPS resulted in an inhibition of LPS activity. From the natural occurring BAs, only β-BA, one of the most abundant BA in frankincense, was able to neutralize LPS (ABA, KBA and AKBA had no effect, see **tab. 5.1**). The absence of an 11-keto group seems necessary for a potent inhibition by the synthetic BA derivatives: all analyzed 11-keto-free BA derivatives displayed very potent LPS-inhibiting properties, while the corresponding 11-keto derivatives had no activity. The only exception to this rule was ABA, which was the only inactive 11-keto-free BA derivative. Replacement of the 11-keto group by a hydroxy group led to somewhat more active compounds compared to their 11-keto variants. Nonetheless, the activity was still reduced when compared to analogues without any substituent at C11. This indicates that a nonpolar C-11 position is necessary for an efficient LPS neutralization.

While ABA had no LPS neutralizing activity, the replacement of the acetylic group by an etherified ω-hydroxy acid or an esterified dicarbonic acid greatly enhanced the inhibitory potential. This may be caused by a change in the steric environment or a change of the polarity near the C-3 position. The polarity has a strong influence: all analyzed compounds with a free hydroxy or acid group near the C-3 position had a high activity against LPS. Both α- and β-configured BAs had a similar potency, indicating that the position of the methyl group at C-19 or C-20 has no impact on the LPS-neutralizing capabilities. The LPS neutralizing effect seem to be specific for BAs, since neither LAs nor RAs were able to inhibit LPS activity (see **tab. 5.2** and **tab. 5.3**).

Inhibition of LPS resulted in an inhibition of LPS signaling. A late downstream event in LPS signaling is the modulation of gene expression. For example, LPS leads to an induction of iNOS expression and in enhanced NO generation. Several 11-keto-free BAs were able to inhibit iNOS expression, while AKBA as an 11-keto BA was ineffective, hence correlating with the ability to neutralize LPS. The inhibition of iNOS expression resulted in lower amount of released NO, most prominent for the C-3 modified synthetic non-11-keto BA derivatives gluBA and sucBA. β-BA itself (up to 10 μM) did not reduce LPS-induced NO release significantly, implicating that higher concentrations might be necessary. Notably, β-BA was also less effective than gluBA and sucBA as a direct LPS inhibitor. The inhibition of NO release seems to be specific for LPS-induced signaling, as IFN-γ-induced NO release was not influenced by most

BAs. The effects of gluBA as the only active compound (but only at high concentrations) may be explained by its cytotoxic activity, while the other BAs were neither cytotoxic nor inhibited IFN-γ-induced NO release.

NO is involved in mediating several immune responses to chronic diseases and cancer [267]. It plays a role in inflammatory bowel diseases like Crohn's disease and ulcerative colitis [268], as well as in osteoarthritis [269]. The causes of these diseases are not completely identified, but there are some speculations that bacteria might be involved in Crohn's disease [266]. The connection of LPS to osteoarthritis still has to be elucidated, but LPS was at least shown to be involved in reactive arthritis [270]. BEs are beneficial for the treatment of both inflammatory bowel diseases (e.g. Crohn's disease) [85] and osteoarthritis [76], therefore an inhibition of NO generation by LPS neutralization might explain some of the anti-inflammatory effects of BEs. Nonetheless, one should keep in mind that an inhibition of LPS signaling may also occur at additional targets downstream of TLR-4. An interference of BAs with IκBα kinases (IKKs) has been reported, but the mode of action on this target (direct binding or indirect regulation) is controversial disputed [39,65]. Therefore, a contribution of a potential direct interaction of BAs with IKKs to the observed inhibitory effects on NO generation cannot be completely excluded at this point.

An additional component of LPS signaling is p38 MAPK [253]. Both β-BA and AKBA inhibited LPS-induced p38 MAPK phosphorylation in mouse macrophages at concentrations between 1 and 17 µM, indicating that this LPS sensitive pathway is also inhibited by BAs. However, the synthetic BA derivatives gluBA and sucBA, which are both very potent LPS inhibitors, led to an unexpected enhancement of p38 MAPK phosphorylation, indicating that additional pathways may be activated by these derivatives. Interestingly, activation of p38 MAPK by BAs has already been reported for neutrophils, platelets and granulocytic HL-60 cells [36,38] and may be responsible for the effects of gluBA and sucBA in mouse macrophages as well. Activation of p38 MAPK occurs independent of NF-κB signaling. Therefore, a possible contribution of an inhibition of IKKs seems unlikely. However, the observation that AKBA was also effective in inhibiting LPS-induced p38 MAPK activation despite no LPS neutralizing activity indicate that the effects on this pathway may be multiple and exploited at different levels.

Taken together, it could be demonstrated that certain non-11-keto BAs bind specifically to LPS and inhibit selected LPS-induced cellular functions. The amounts of β-BA needed for an efficient inhibition (IC_{50} = 1.8-10 µM) are in the range of β-BA blood plasma levels reached after oral application of *B. serrata* extracts (6.35-10.1 µM) [10,68]. LPS plays a role in a variety of diseases. Inhalation of LPS leads to bronchoconstriction [271-273], a change in non-specific airway responsiveness [271,272,274] and in a reduction in alveolar capillary diffusion [275]. A participation of endotoxin in chronic airway diseases as asthma has been suggested [276]. A *B. serrata* extract has been shown to be beneficial for the treatment of asthma [91], this might be explained by inhibition of LPS and reduction of the resulting bronchial inflammation. However, the major LPS-related disorders (e.g. sepsis and septic shock), are diseases which are a major cause of death in critically ill patients [277]. Detailed studies about the influence of BEs and BAs on these diseases are still missing, but the present study provides first evidence that BEs might be beneficial in the treatment of LPS-related diseases.

5.1.3 CatG is a target of BAs and other triterpenes from frankincense

Another molecular target of BAs that was identified by the target-fishing approach is catG. β-BA binds to catG in a direct manner, as demonstrated in protein pull-down experiments using immobilized BAs. This interaction could be antagonized by addition of soluble β-BA as well as by the catG inhibitor CGI. CGI is a potent, selective, reversible and competitive catG inhibitor which binds to catG at the substrate binding site [278]. The antagonism of catG-binding by CGI and β-BA implicate that β-BA may bind to the substrate binding site in a similar manner as CGI. Recently, a model for the proposed binding site was generated in collaboration with Dr. Lars Tausch and Prof. Dr. Gisbert Schneider (Goethe University, Frankfurt) by molecular docking experiments [68]. This model suggest a binding of β-BA to catG at the substrate binding site blocking the S1 binding pocket, similar to the proposed binding mode of CGI. The binding of catG to BAs had functional consequences, as its enzymatic activity was potently inhibited. AKBA acts thereby in a similar fashion as CGI (as a competitive and reversible inhibitor of catG activity [68]). catG-stimulated Ca^{2+} release was impaired by both CGI and AKBA, and fMLP-induced neutrophil migration through a synthetic

extracellular matrix was inhibited but not chemotaxis itself. This implicates that the inhibition of the proteolytic activity impairs the ability of neutrophils to pass through the extracellular matrix.

SAR studies revealed the impact of the 11-keto group (see **tab. 5.1**). Synthetic BA derivatives lacking the 11-keto group were much more potent inhibitors than their respective 11-keto analogs. When the 11-keto group was replaced by a hydroxyl group, the potency is even more diminished. Such a strict correlation between activity and 11-keto group was not observed for the naturally occurring BAs. In fact, while the 11-keto group of KBA decreases the inhibitory activity, similar to the effect observed for synthetic BAs, AKBA had a higher potency than ABA. Therefore, the absence of the 11-keto group seems to be important in many but not in all cases of catG inhibition.

Variations of the C-3 moiety demonstrate the influence of this position. A molecular modeling approach revealed a potential higher efficacy of C-3 modified synthetic BAs [237]. While both a short moiety (as in ABA and oxBA) and a long glutaroyl-moiety (as in gluBA) led to efficient inhibitors, an intermediate length (as in sucBA) was less effective. In addition, a C-2 hydroxy group renders the compound inactive (cis-diol-BA). Besides BAs, several other natural occurring triterpenes derived from frankincense were characterized for their catG inhibiting potency. Among LAs, the absence of a 28-hydroxy group seems to be crucial for catG inhibitory activity (see **tab. 5.3**). RA derivatives displayed only a slight tendency for catG inhibition (see **tab. 5.2**). Taken together, among the analyzed compounds from frankincense, non-11-keto BAs seem to be the most relevant group of catG inhibitors.

As discussed above, inhibition of catG by BAs led to a diminished cell migration. This effect might be explained by inhibition of the proteolytic activity catG, which is responsible for the cleavage of the extracellular matrix [279,280]. In the absence of a migration barrier as matrigel, chemotaxis itself was not negatively influenced by BAs. This demonstrates that BAs are not general inhibitors of chemotaxis but instead influence the proteolytic degradation allowing for migration. The cleavage of the matrix is essential for cell migration into tissues, and the inhibition of the responsible proteases may lead to an inhibition of the innate immune response.

Inhibition of catG by BAs may have *in vivo* relevance as well. The blood of Crohn's disease patients that were orally treated with a BE displayed significant lower catG

activities versus those treated with placebo. This implicates sufficient bioavailability of the active principles, and a participation of BAs like β-BA and ABA, which reach relative high plasma concentrations (2.4-10.1 µM) [68,281], may be reasonable. In addition to catG, an interaction of BAs with other homologue neutrophil serine proteases [282] has been described. Safayhi *et al.* identified HLE as a functional target of AKBA and β-BA [33]. HLE inhibition by BAs is characterized by relative high IC_{50} values (AKBA: 15 µM, β-BA > 15 µM), however. Since maximum plasma levels after oral application of BE do not exceed 0.1 µM (AKBA) or 10.1 µM (BA), respectively [10], catG seems to be a more relevant target.

CatG may play a role in a variety of diseases, in which BEs have beneficial effects. The extracellular matrix is cleaved by catG [283,284], and in an adjuvant induced arthritis model of inflammation, urinary excretion of connective tissue was reduced after BE application [4]. CatG inhibitors have been proposed to be potential therapeutics for the treatment of asthma, psoriasis and arthritis [177,283] and a *B. serrata* extract had beneficial effects on the treatment of bronchial asthma [91] and on arthritic disease parameters in several animal models [2,235]. There are also some *in vivo* similarities between the actions of JNJ-10311795, a catG inhibitor structurally similar to CGI, and BEs. For example, JNJ-10311795 inhibits glycogen-induced rat peritonitis [285], while a *B. serrata* extract impaired λ-carrageenan-induced pleurisy in rats [5]. Taken together, catG is a functional target of BAs, and the inhibition of catG may be responsible for some of the observed anti-inflammatory effects of BEs and BAs.

5.1.4   Interaction of BAs with p21 Ras

In previous studies, p21 Ras was specifically precipitated from cellular lysates by immobilized KBA-seph [40]. However, it was not clear whether p21 Ras proteins are direct binding partners of KBA or an indirect binding mode *via* adaptor proteins takes place. The present study demonstrates that H-Ras directly bind to KBA, since isolated H-Ras could be specifically precipitated by KBA-seph. Nonetheless, this binding does have only a slight impact on the p21 Ras activation status. While neither AKBA nor β-BA was able to activate p21 Ras in neutrophils, a co-stimulation with 5-HETE and AKBA resulted in higher amounts of activated p21 Ras. This implicates that AKBA somehow interferes with the 5-HETE-induced cell signaling, maybe *via* priming effects. BAs are activators of the MAPK ERK1/2 and p38 MAPK [36], but this activation may

be independent of p21 Ras, since BAs have no direct effect on p21 Ras activity in the absence of 5-HETE. The 11-keto and the 3-acetoxy groups seem to be crucial, since β-BA did not enhance the 5-HETE-stimulated p21 Ras activation. Notably, the 11-keto group was also important for BA-induced activation of ERK1/2 MAPK [36] and Ca^{2+} mobilization, as well as for inhibition of agonist-induced 5-LO product formation in neutrophils [24], 12-HHT formation in platelets [31] and nucleotide and protein synthesis in HL-60 cells [45]. However, it was not clear whether p21 Ras is involved in the signal transduction pathways leading to these observed inhibitory and stimulatory effects. Also, it is unknown if this effect might contribute to the overall apoptosis inducing effects of BAs. In fact, upregulation of p21 Ras can result in an induction of apoptosis [286] and AKBA was effective in inducing apoptosis in Jurkat T-lymphocytes, while β-BA had no effect on cell viability. This strengthens the hypothesis that the 11-keto group is crucial for mediating effects on cellular signal transduction pathways. On the other hand, activation of p21 Ras may also induce cellular growth. Constitutively activated forms of p21 Ras proteins were identified in several cancer tissues [287], and Ras is responsible for the progression through the cell cycle [288]. Nonetheless, there are no reports stating a cancerogenic potential of BAs while an apoptosis-inducing mode of action is well analyzed, implicating that an interaction with p21 Ras proteins might preferably address the pro-apoptotic effects of p21 Ras.

Relatively high concentrations of AKBA were needed for activation of p21 Ras, which questions the pharmacological relevance of this interaction. The maximum concentration of AKBA in the plasma after oral application of a *B. serrata* extract is in the range of 0.1 µM [10,68], while an activation of p21 Ras was only detectable at 30 µM. It may be possible that AKBA accumulates in tissues, resulting in the observed very low plasma concentration. However, no studies were performed yet analyzing the distribution of AKBA in different peripheral tissues, but at least an interaction with cells in the blood stream seems unlikely.

5.1.5   Interaction of BAs with Rap1B

The small G protein Rap1B from the Ras family was also precipitated in platelets in pull-down experiments of cell lysates [40]. In order to characterize the binding mode of action, recombinant Rap1B was expressed. A transformation of a *rap1b*-expression vector into *E. coli* BL21 resulted in a bacterial strain expressing a Rap1B-GST fusion

protein. The GST-tag was removed and isolated Rap1B was purified. By using these isolated proteins, a direct binding of Rap1B to KBA was demonstrated. This binding does not seem to influence the nucleotide exchange rate, however. Since Rap1B is generally thought to be activated by nucleotide exchange [289], this result implicates that KBA may not be able to activate Rap1B. Nonetheless, a modulation of Rap1B activity cannot be completely excluded, since binding to Rap1B at different domains than the nucleotide binding domain may influence the activity as well. It might be possible that BAs interact with the effector binding site and influence the downstream signal transduction. An inhibition of active Rap1B might explain the inhibitory effect of AKBA on platelet aggregation [255]. On the other hand, an activation could explain the observed induction of aggregation by β-BA and ABA [40]. However, the regulation of platelet aggregation is complex and might involve Rap1B-independent signal transduction pathways as well.

Taken together, although a direct binding of KBA to Rap1B could be proven, the question whether the biological activity of Rap1B is influenced still needs further investigations. An activating mode of action *via* nucleotide exchange can be excluded, however.

5.2 Elucidation of BE-induced apoptosis

5.2.1 Structure-activity relationship of BAs concerning the mechanism of apoptosis induction

BEs as well as BAs are known to induce apoptosis in different cell lines [46,48-51,53,54,290]. A part of the underlying molecular pathway has been identified and involves the induction of the extrinsic pathway of apoptosis [49,50]. Thus, the BE/BA-dependent induction of apoptosis is characterized by activation of caspase 8, caspase 3 and by cleavage of PARP, accompanied by DNA fragmentation. Since there are indications that BEs may be beneficial in the treatment of tumor and tumor-associated diseases [235], a complete understanding of their active principles and the molecular mode of action is essential.

Initial investigations revealed that a *B. carterii* extract induces apoptosis in Jurkat T-lymphocytes [258]. In the present study, several compounds from frankincense extracts have been analyzed for their cytotoxic properties. Although AKBA is generally considered the most potent apoptotic inductor [235], it has only moderate cytotoxic properties in Jurkat cells as compared to other BAs. In fact, ABA was identified as the most potent cytotoxic agent among the natural occurring BAs. A structure-activity relationship analysis revealed that compounds with an 11-keto group possess less potent cytotoxic activities (see **tab. 5.1**). Cytotoxicity is also influenced by modification of the C-3 position. A hydroxy group leads to a loss of efficiency, while esterification with acetylic acid or a dicarbonic acid with a backbone consisting of at least four carbon atoms leads to highly toxic compounds.

The mechanisms by which C-3-modified synthetic BAs cause cytotoxicity are similar to AKBA. Cleavage of procaspases-3 and -8 as well as PARP was demonstrated, and all of the compounds induced DNA fragmentation. Notably, the synthetic derivatives as well as ABA displayed an enhanced potency over AKBA. This result is in line with the observation of an enhanced cytotoxicity of ABA, while AKBA is only moderately cytotoxic.

The identification of ABA as a more potent analogue than AKBA might help explaining the anti-neoplastic effects of BEs. Since AKBA has very poor absorption rates [69] and reaches only low plasma levels after oral application [10,68], the contribution of ABA with much higher plasma levels as a potent principle might be reasonable. The absorption rates of ABA still have to be elucidated, but plasma levels indicate a considerably higher bioavailability. In addition, ABA was cytotoxic for the Jurkat cancer cell line, but not for healthy PBMCs, which might be of interest for the development of novel anti-cancer agents.

5.2.2 Novel triterpenes as apoptosis inducing agents

Besides BA derivatives, other triterpenes derived from frankincense could be identified as apoptosis inducing compounds. Two LAs were identified, as well as two RA derivatives and ursolic acid. These compounds have a similar potency than the most potent natural occurring BA (i.e. ABA). However, detailed studies about the relative amount of LAs and RAs in frankincense extracts are still missing, as well as

pharmacokinetic studies. Several investigations have demonstrated the anti-neoplastic potential of BEs in animal models. Besides BAs, LAs, RAs and ursolic acid might contribute to the tumor growth inhibiting effects. While apoptosis inducing effects of ursolic acid [291] and some LA derivatives are reported [292], the effects of RAs and of the analyzed LA derivatives were unknown up to now. In contrast to BEs, which are thought to induce apoptosis *via* the extrinsic pathway [49,50], ursolic acid was shown to act *via* the intrinsic pathway [293]. Since BEs are mixtures of different active compounds, it may be possible that the pro-apoptotic effect of isolated ursolic acid may not contribute to the final apoptotic outcome when BEs are applied.

It should be noted that BEs, although efficiently inhibiting tumor growth in different animal models [235], had no influence on brain tumor growth in humans [89,90] with the exception of some tumor-related events, i.e. the reduction of the volume of the associated edema. Notably, the extracts used in different studies were manufactured by different extraction methods, and so the molecular composition was likely different. Due to the different experimental conditions, final conclusions are hard to draw. More detailed analysis about the content of the BEs used in separate experimental settings are required. It may be reasonable that an extract with high amounts of LAs and RAs may possess a higher anti-neoplastic value.

5.3 Additional cellular functions modulated by BAs

The present study demonstrates that BAs are able to induce chemotaxis in neutrophils. This observation is in contrast to a previous study, where neutrophil chemotaxis was found to be inhibited by a mixture of BAs [6]. The inhibitory effects reported previously were however only detectable at very high concentrations (>100 µM) which are much higher than the maximal plasma levels of BAs reached after oral application [10,68] and the concentrations applied in the present study (≤30 µM). Additionally, the authors missed to define the exact composition of the BA mixture used, making an evaluation of these effects very tricky. Thus, due to the very high amounts of BAs needed for inhibition of chemotaxis, a physiological relevance for this effect seems unlikely. On the other hand, induction of chemotaxis by BAs might have *in vivo* relevance, since the concentrations of BAs needed are in the range of the maximal plasma levels reached after oral application. An inhibition of a local inflammation, as observed for several BEs

[2,235], might be explained if BAs are systemically available and inhibit chemotaxis directed to the site of inflammation by activating the same signal transduction pathways as the chemotaxis inducing chemokines. The chemotactic gradient would therefore be disturbed.

However, induction of chemotaxis seems to be based on other mechanisms than those responsible for fMLP-induced chemotaxis: fMLP-induced chemotaxis is not influenced by BAs. This implicates that BAs may act on other pathways than fMLP to induce chemotaxis. Some evidences indicate similarity with the signaling of vascular endothelial growth factor (VEGF), which is inhibited by AKBA [294]. However, in an animal model of pleural inflammation, the synthetic BA derivatives gluBA and oxBA (applied *i.p.*) did not influence the number of inflammatory cells in the exudate of a λ-carrageenan-induced pleurisy in rats. This result strengthens the hypothesis that BAs may only inhibit chemotactic activity induced by a specific stimulus. An orally applied *B. serrata* extract, however, was found to inhibit neutrophil migration into the exudate of λ-carrageenan-induced pleurisy [5]. Besides the fact that a BE is composed of many different potential bioactive substances which might have different effects on chemotaxis, the mode of application might also have a strong impact on the outcome. A systemic administration might inhibit chemotaxis (see above), whereas a local application of BAs might even enhance the number of infiltrating cells. Further studies are needed to evaluate the impact of a potential induction of chemotaxis directed to the site of inflammation. While beneficial effects of higher immune cell numbers in bacterial-induced inflammation might be imaginable, enforced immune cell activity can be destructive as well. This would lead to an increase in inflammation. Therefore, a local application of BAs might enforce inflammation, but whether the induction of chemotaxis is still relevant under *in vivo* conditions still remains to be elucidated.

While AKBA is generally regarded as the most potent active principle, a contribution of other BAs to the observed anti-inflammatory effects of BEs seems likely. In an *in vivo* system of λ-carrageenan-induced pleurisy in rats, a *B. serrata* extract (*p.o.*) inhibited exudate volume and the number of invading cells [5]. β-BA may be responsible for this effect, as it inhibits the exudates volume and the cell counts in a similar manner, while AKBA was ineffective [255]. Notably, β-BA itself had no direct effect on chemotaxis *in vitro*, while AKBA induced neutrophil chemotaxis. CatG might contribute to pleural inflammation, and a molecular modeling approach suggested a stronger binding to catG

if the moiety at the C-3 position contains a hydrophilic group [237]. Therefore the influence of gluBA and oxBA on pleurisy was analyzed. GluBA was completely inactive at a low (1 mg/kg) and high (5 mg/kg) dose, while low-dose oxBA-treatment resulted in a slightly reduced exudate volume. This effect seems to be absent at higher doses, and oxBA had no effect on cell counts or arachidonic acid metabolism, neither at low nor at high doses. Overall, both gluBA and oxBA have a very low or even no potency in inhibiting λ-carrageenan-induced pleurisy. This implicates that the properties of the C-3 position are crucial for the beneficial effects. A modification of the C-3 hydroxyl group impairs the biological activity, as shown for AKBA [255], oxBA and gluBA (this study). CatG seems to be either not a primary inflammatory mediator in this model, or both gluBA and sucBA may be not bioavailable or active *in vivo*.

However, although λ-carrageenan-induced pleurisy in rats can be regarded as a general model system of non-sterile inflammation, it is most likely not dependent on LPS and LL-37. The inhibition of inflammation is presumably based on additional targets, on which the influence of gluBA and oxBA is still unknown. Maybe these compounds would potentially be more efficient in test systems where LPS and LL-37 play a major role, like in sepsis, endotoxic shock models or psoriasis. This implicates that BAs might mediate anti-inflammatory activities in diverse diseases *via* distinct molecular mechanisms. However, effects like low bioavailability might also potentially contribute to the low activity of gluBA and oxBA in the pleurisy model. Bioavailability studies are therefore an important tool to evaluate whether these compounds may be effective in other *in vivo* systems as well or if further modifications are necessary to generate compounds with an enhanced potency.

5.4 Conclusion

The molecular mechanisms underlying the anti-inflammatory effects of frankincense extracts are incompletely understood. BAs are major principles of the extracts, and a contribution of BAs to the observed effects seems likely. Indeed, several targets of BAs were identified up to now, including 5-LO, COX-1, IKK kinases, Akt, HLE and C3-convertase [235]. Many of these studies either analyzed solely AKBA or identified AKBA as the BA with the highest activity. Since the bioavailability of AKBA is very low [10,68], a contribution of BAs with a higher bioavailability to the

anti-inflammatory effects seems reasonable. In addition, there may be other bioactive principles besides BAs which may modulate inflammatory processes.
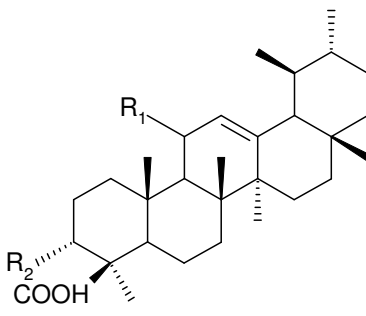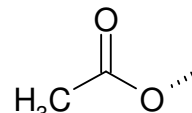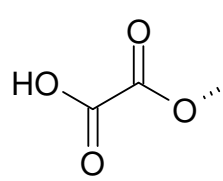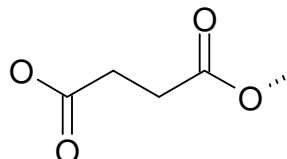
In the present study, several new targets for triterpenes derived from frankincense were identified. The inhibition of LPS and the subsequent LPS-induced cellular signaling by BAs modulates the immunologic reaction in response to this strong inflammatory stimulus. LPS is involved in a variety of diseases where frankincense extracts have beneficial effects, and the identified compounds might contribute to this outcome. However, not all diseases where frankincense extracts are beneficial depend on LPS, so the existence of additional targets is reasonable. The identification of LL-37 as a functional target of BAs, RAs and LAs might help explaining the efficacy of BEs in some (most likely) LPS-independent diseases like psoriasis. LL-37 was shown to be a direct binding partner of BAs, and its activity is inhibited by several triterpenes from frankincense extracts. This may lead to a modulation of the immune response in some diseases in which LL-37 was suggested to participate. Also, catG was identified as a third functional target of BAs. BAs bind directly to catG and inhibit its biological activities. There is evidence that the inhibition of catG might be relevant *in vivo* as well, as blood from patients treated with a BE had lower catG activities compared to placebo-treated patients.

The identification of RAs and LAs as active principles of BEs leads to new insights into the molecular mechanisms by which BEs influence inflammatory disorders. Up to now, most of the effects of BEs have been related to the actions of BAs. Though BAs represent a major group of ingredients in BEs, some of them have a very poor bioavailability. It is reasonable to hypothesize that other triterpenes like RAs and LAs might contribute to the beneficial effects of frankincense extracts, in particular if they reach sufficient plasma levels, despite of their lower contents in BEs. Detailed studies about the bioavailability of RAs and LAs are still missing however.

Treatment of cancer and cancer-related diseases is a part of the traditional use of BEs. Several studies contributed to the understanding of the underlying molecular mechanism by which apoptosis is induced. The present study extends this context to leukemic T-lymphocytes and demonstrates a contribution of LAs which act besides BAs as apoptosis-inducing agents. Among BAs, an evaluation of the impact of the C-3 and C-11 moiety revealed novel synthetic BAs with a higher potency of apoptosis induction. These compounds may have superior capabilities in the treatment of cancer and cancer-

related diseases. Detailed studies about their *in vivo* efficacy in these diseases are still missing, but the obtained *in vitro* data seem to be promising.

Tab. 5.1: Effects of BAs on LPS, LL-37, catG and cell viability. *SAR studies revealed the importance of the C-3- and C-11 position in different testing systems. Natural occurring BAs are marked in light gray, synthetic BAs with a C-3 esterified dicarbonic acid in intermediate gray and synthetic BAs with a C-3 etherified ω-hydroxy acid in dark gray. n.d., not determined.*

name	R_1	R_2	LPS	LL-37	CatG	Cytotoxicity	
						Jurkat	PBMC
β-BA		HO''''	+	n.d.	++	-	-
ABA		H₃C—C(=O)—O''''	-	++	++	++	-
oxBA	H	HO—C(=O)—C(=O)—O'''	++	n.d.	+	+	-
sucBA		O—CH₂—CH₂—C(=O)—O'''	++	n.d.	+	++	++
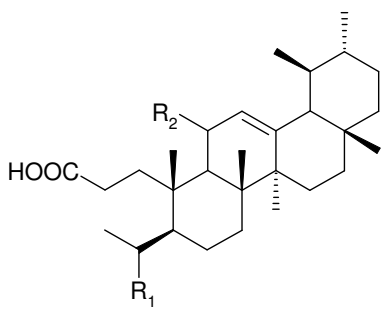
name	R_1	R_2	LPS	LL-37	CatG	Cytotoxicity	
						Jurkat	PBMC
gluBA	H		++	n.d.	+	++	++
eBA			++	n.d.	+	.	.
KBA		HO	-	n.d.	+	-	-
AKBA	O		-	++	++	+	++
oxKBA			-	+	-	-	-
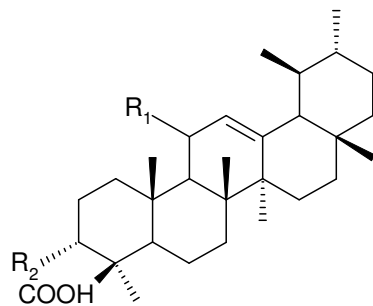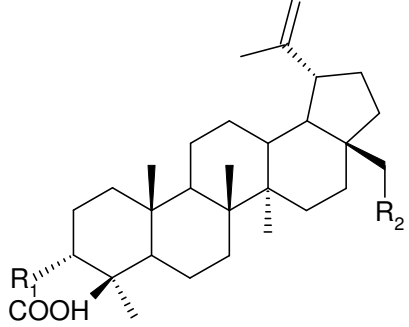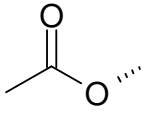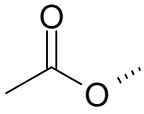
name	R$_1$	R$_2$	LPS	LL-37	CatG	Cytotoxicity	
						Jurkat	PBMC
sucKBA			-	+	-	-	-
gluKBA	O=		-	+	+	-	-
eKBA			-	+	-	+	-

Tab. 5.2: Effects of RAs on LPS, LL-37, catG and cell viability. *SAR studies revealed the importance of the C-3- and C-11 position in different testing systems.*

name	R_1	R_2	LPS	LL-37	CatG	Cytotoxicity	
						Jurkat	PBMC
RA	H_2C		-	+	-	+	+
DH-RA	H_3C	H	-	+	-	+	++
DHK-RA	H_3C	O	-	+	-	+	+

Tab. 5.3: Effects of LAs on LPS, LL-37, catG and cell viability. *SAR studies revealed the importance of the C-3- and C-11 position in different testing systems. n.d., not determined.*

name	R_1	R_2	LPS	LL-37	CatG	Cytotoxicity	
						Jurkat	PBMC
OH-LA	HO''''		-	+	-	++	++
Ac-OH-LA	(acetyl-O''')	HO—	-	+	n.d.	++	+
Ac-LA	(acetyl-O''')	H—	-	++	+	-	-

6.   References

1.   Martinez D, Lohs K, Janzen J. Weihrauch und Myrrhe. Kulturgeschichte und wirtschaftliche Bedeutung: Botanik, Chemie, Medizin: Stuttgart: Wissenschaftliche Verlagsgesellschaft; 1989

2.   Ammon HPT. Boswellic acids in chronic inflammatory diseases. Planta Medica 2006;72:1100-1116

3.   Reddy GK, Dhar SC. Effect of a new non-steroidal anti-inflammatory agent on lysosomal stability in adjuvant induced arthritis. The Italian Journal of Biochemistry 1987;36:205-217

4.   Reddy GK, Dhar SC, Singh GB. Urinary excretion of connective tissue metabolites under the influence of a new non-steroidal anti-inflammatory agent in adjuvant induced arthritis. Agents and Actions 1987;22:99-105

5.   Sharma ML, Khajuria A, Kaul A, Singh S, Singh GB, Atal CK. Effect of salai guggal ex-Boswellia serrata on cellular and humoral immune responses and leucocyte migration. Agents and Actions 1988;24:161-164

6.   Sharma ML, Bani S, Singh GB. Anti-arthritic activity of boswellic acids in bovine serum albumin (BSA)-induced arthritis. International Journal of Immunopharmacology 1989;11:647-652

7.   Reddy GK, Chandrakasan G, Dhar SC. Studies on the metabolism of glycosaminoglycans under the influence of new herbal anti-inflammatory agents. Biochemical Pharmacology 1989;38:3527-3534

8.   Ammon HP, Mack T, Singh GB, Safayhi H. Inhibition of leukotriene B4 formation in rat peritoneal neutrophils by an ethanolic extract of the gum resin exudate of Boswellia serrata. Planta Medica 1991;57:203-207

9.   Kreck C, Saller R. Indischer Weihrauch und seine Zubereitungen einschliesslich H15 als traditionelle und moderne Therapeutika. Internistische Praxis 1998:857-872

10.   Büchele B, Simmet T. Analysis of 12 different pentacyclic triterpenic acids from frankincense in human plasma by high-performance liquid chromatography and photodiode array detection. Journal of Chromatography B, Analytical Technologies in the Biomedical and Life Sciences 2003;795:355-362

11.   Sterk V, Büchele B, Simmet T. Effect of food intake on the bioavailability of boswellic acids from a herbal preparation in healthy volunteers. Planta Medica 2004;70:1155-1160

12.   Mahajan B, Taneja SC, Sethi VK, Dhar KL. Two triterpenoids from Boswellia serrata gum resin. Phytochemistry 1995;39:453-455

13.   Schweizer S, von Brocke AF, Boden SE, Bayer E, Ammon HP, Safayhi H. Workup-dependent formation of 5-lipoxygenase inhibitory boswellic acid analogues. Journal of Natural Products 2000;63:1058-1061

14.   Shah BA, Qazi GN, Taneja SC. Boswellic acids: a group of medicinally important compounds. Natural Product Reports 2009;26:72-89

15.   Fattorusso E, Santacroce C, Xaasan CF. 4(23)-Dihydroroburic Acid from the resin (incense) of Boswellia carterii. Phytochemistry 1983;22:2868-2869

16.   Seitz S. Isolierung und Strukturaufklärung von entzündungshemmenden Inhaltsstoffen aus Weihrauchharz. In, Institut für Organische Chemie II. Saarbrücken: Universtät des Saarland; 2008

17.   Culioli G, Mathe C, Archier P, Vieillescazes C. A lupane triterpene from frankincense (Boswellia sp., Burseraceae). Phytochemistry 2003;62:537-541

18.   Belsner K, Buchele B, Werz U, Simmet T. Structural analysis of 3-alpha-acetyl-20(29)-lupene-24-oic acid, a novel pentacyclic triterpene isolated from the gum resin of Boswellia serrata, by NMR spectroscopy. Magnetic Resonance in Chemistry 2003;41:629-632

19.   Atta ur R, Naz H, Fadimatou, Makhmoor T, Yasin A, Fatima N, Ngounou FN, Kimbu SF, Sondengam BL, Choudhary MI. Bioactive Constituents from Boswellia papyrifera. Journal of Natural Products 2005;68:189-193

20.   Pardhy RS, Bhattacharyya SC. Tetracyclic triterpene acids from the resin of Boswellia serrata Roxb. Indian Journal of Chemistry 1978;16B:174-175

21.   Banno N, Akihisa T, Yasukawa K, Tokuda H, Tabata K, Nakamura Y, Nishimura R, Kimura Y, Suzuki T. Anti-inflammatory activities of the triterpene acids from the resin of Boswellia carteri. Journal of Ethnopharmacology 2006;107:249-253

22.   Werz O. 5-lipoxygenase: cellular biology and molecular pharmacology. Current Drug Targets Inflammation and Allergy 2002;1:23-44

23.   Safayhi H, Sailer ER, Ammon HP. Mechanism of 5-lipoxygenase inhibition by acetyl-11-keto-beta-boswellic acid. Molecular Pharmacology 1995;47:1212-1216

24.   Sailer ER, Subramanian LR, Rall B, Hoernlein RF, Ammon HP, Safayhi H. Acetyl-11-keto-beta-boswellic acid (AKBA): structure requirements for binding and 5-lipoxygenase inhibitory activity. British Journal of Pharmacology 1996;117:615-618

25.   Safayhi H, Mack T, Sabieraj J, Anazodo MI, Subramanian LR, Ammon HP. Boswellic acids: novel, specific, nonredox inhibitors of 5-lipoxygenase. The Journal of Pharmacology and Experimental Therapeutics 1992;261:1143-1146

26.   Wildfeuer A, Neu IS, Safayhi H, Metzger G, Wehrmann M, Vogel U, Ammon HP. Effects of boswellic acids extracted from a herbal medicine on the

biosynthesis of leukotrienes and the course of experimental autoimmune encephalomyelitis. Arzneimittel-Forschung 1998;48:668-674

27. Altmann A, Poeckel D, Fischer L, Schubert-Zsilavecz M, Steinhilber D, Werz O. Coupling of boswellic acid-induced Ca2+ mobilisation and MAPK activation to lipid metabolism and peroxide formation in human leucocytes. British Journal of Pharmacology 2004;141:223-232

28. Safayhi H, Boden SE, Schweizer S, Ammon HP. Concentration-dependent potentiating and inhibitory effects of Boswellia extracts on 5-lipoxygenase product formation in stimulated PMNL. Planta Medica 2000;66:110-113

29. Werz O, Szellas D, Henseler M, Steinhilber D. Nonredox 5-lipoxygenase inhibitors require glutathione peroxidase for efficient inhibition of 5-lipoxygenase activity. Molecular Pharmacology 1998;54:445-451

30. Werz O, Schneider N, Brungs M, Sailer ER, Safayhi H, Ammon HP, Steinhilber D. A test system for leukotriene synthesis inhibitors based on the in-vitro differentiation of the human leukemic cell lines HL-60 and Mono Mac 6. Naunyn-Schmiedeberg's Archives of Pharmacology 1997;356:441-445

31. Siemoneit U, Hofmann B, Kather N, Lamkemeyer T, Madlung J, Franke L, Schneider G, Jauch J, Poeckel D, Werz O. Identification and functional analysis of cyclooxygenase-1 as a molecular target of boswellic acids. Biochemical Pharmacology 2008;75:503-513

32. Poeckel D, Tausch L, Kather N, Jauch J, Werz O. Boswellic acids stimulate arachidonic acid release and 12-lipoxygenase activity in human platelets independent of Ca2+ and differentially interact with platelet-type 12-lipoxygenase. Molecular Pharmacology 2006;70:1071-1078

33. Safayhi H, Rall B, Sailer ER, Ammon HP. Inhibition by boswellic acids of human leukocyte elastase. The Journal of Pharmacology and Experimental Therapeutics 1997;281:460-463

34. Ying QL, Rinehart AR, Simon SR, Cheronis JC. Inhibition of human leucocyte elastase by ursolic acid. Evidence for a binding site for pentacyclic triterpenes. The Biochemical Journal 1991;277 (Pt 2):521-526

35. Bernstein PR, Edwards PD, Williams JC. Inhibitors of human leukocyte elastase. Progress in Medicinal Chemistry 1994;31:59-120

36. Altmann A, Fischer L, Schubert-Zsilavecz M, Steinhilber D, Werz O. Boswellic acids activate p42(MAPK) and p38 MAPK and stimulate Ca(2+) mobilization. Biochemical and Biophysical Research Communications 2002;290:185-190

37. Gijón MA, Leslie CC. Regulation of arachidonic acid release and cytosolic phospholipase A2 activation. Journal of Leukocyte Biology 1999;65:330-336

38. Poeckel D, Tausch L, Altmann A, Feisst C, Klinkhardt U, Graff J, Harder S, Werz O. Induction of central signalling pathways and select functional effects in human platelets by beta-boswellic acid. British Journal of Pharmacology 2005;146:514-524

39. Takada Y, Ichikawa H, Badmaev V, Aggarwal BB. Acetyl-11-keto-beta-boswellic acid potentiates apoptosis, inhibits invasion, and abolishes osteoclastogenesis by suppressing NF-kappa B and NF-kappa B-regulated gene expression. The Journal of Immunology 2006;176:3127-3140

40. Tausch L. Novel anti-inflammatory targets and mechanisms of boswellic acids and celecoxib. In, Institut für Pharmazeutische Chemie. Frankfurt: Goethe Universität Frankfurt; 2008

41. Kapil A, Moza N. Anticomplementary activity of boswellic acids--an inhibitor of C3-convertase of the classical complement pathway. International Journal of Immunopharmacology 1992;14:1139-1143

42. Sharma ML, Kaul A, Khajuria A, Singh S, Singh GB. Immunomodulatory activity of Boswellic acids (Pentacyclic triterpene acids) from Boswellia serrata. Phytotherapy Research 1996;10:107-112

43. Dahmen U, Gu YL, Dirsch O, Fan LM, Li J, Shen K, Broelsch CE. Boswellic acid, a potent antiinflammatory drug, inhibits rejection to the same extent as high dose steroids. Transplantation Proceedings 2001;33:539-541

44. Jing Y, Xia L, Han R. Growth inhibition and differentiation of promyelocytic cells (HL-60) induced by BC-4, an active principle from Boswellia carterii Birdw. Chinese Medical Sciences Journal 1992;7:12-15

45. Shao Y, Ho CT, Chin CK, Badmaev V, Ma W, Huang MT. Inhibitory activity of boswellic acids from Boswellia serrata against human leukemia HL-60 cells in culture. Planta Medica 1998;64:328-331

46. Hostanska K, Daum G, Saller R. Cytostatic and apoptosis-inducing activity of boswellic acids toward malignant cell lines in vitro. Anticancer Research 2002;22:2853-2862

47. Hoernlein RF, Orlikowsky T, Zehrer C, Niethammer D, Sailer ER, Simmet T, Dannecker GE, Ammon HP. Acetyl-11-keto-beta-boswellic acid induces apoptosis in HL-60 and CCRF-CEM cells and inhibits topoisomerase I. The Journal of Pharmacology and Experimental Therapeutics 1999;288:613-619

48. Xia L, Chen D, Han R, Fang Q, Waxman S, Jing Y. Boswellic acid acetate induces apoptosis through caspase-mediated pathways in myeloid leukemia cells. Molecular Cancer Therapeutics 2005;4:381-388

49. Liu J-J, Nilsson A, Oredsson S, Badmaev V, Duan R-D. Keto- and acetyl-keto-boswellic acids inhibit proliferation and induce apoptosis in Hep G2 cells via a caspase-8 dependent pathway. International Journal of Molecular Medicine 2002;10:501-505

50. Liu J-J, Nilsson A, Oredsson S, Badmaev V, Zhao W-Z, Duan R-D. Boswellic acids trigger apoptosis via a pathway dependent on caspase-8 activation but independent on Fas/Fas ligand interaction in colon cancer HT-29 cells. Carcinogenesis 2002;23:2087-2093

51. Liu J-J, Huang B, Hooi SC. Acetyl-keto-beta-boswellic acid inhibits cellular proliferation through a p21-dependent pathway in colon cancer cells. British Journal of Pharmacology 2006;148:1099-1107

52. Syrovets T, Gschwend JE, Büchele B, Laumonnier Y, Zugmaier W, Genze F, Simmet T. Inhibition of IkappaB kinase activity by acetyl-boswellic acids promotes apoptosis in androgen-independent PC-3 prostate cancer cells in vitro and in vivo. The Journal of Biological Chemistry 2005;280:6170-6180

53. Zhao W, Entschladen F, Liu H, Niggemann B, Fang Q, Zaenker KS, Han R. Boswellic acid acetate induces differentiation and apoptosis in highly metastatic melanoma and fibrosarcoma cells. Cancer Detection and Prevention 2003;27:67-75

54. Jing Y, Nakajo S, Xia L, Nakaya K, Fang Q, Waxman S, Han R. Boswellic acid acetate induces differentiation and apoptosis in leukemia cell lines. Leukemia Research 1999;23:43-50

55. Jakobsson PJ, Steinhilber D, Odlander B, Rådmark O, Claesson HE, Samuelsson B. On the expression and regulation of 5-lipoxygenase in human lymphocytes. Proceedings of the National Academy of Sciences of the United States of America 1992;89:3521-3525

56. Wang LG, Liu XM, Ji XJ. Determination of DNA topoisomerase II activity from L1210 cells-a target for screening antitumor agents. Zhongguo Yao Li Xue Bao 1991;12:108-114

57. Syrovets T, Büchele B, Gedig E, Slupsky JR, Simmet T. Acetyl-boswellic acids are novel catalytic inhibitors of human topoisomerases I and IIalpha. Molecular Pharmacology 2000;58:71-81

58. Lawen A. Apoptosis-an introduction. BioEssays: News and Reviews in Molecular, Cellular and Developmental Biology 2003;25:888-896

59. Chinnaiyan AM, O'Rourke K, Tewari M, Dixit VM. FADD, a novel death domain-containing protein, interacts with the death domain of Fas and initiates apoptosis. Cell 1995;81:505-512

60. Salvesen GS, Dixit VM. Caspases: intracellular signaling by proteolysis. Cell 1997;91:443-446

61. Stennicke HR, Salvesen GS. Properties of the caspases. Biochimica Et Biophysica Acta 1998;1387:17-31

62. Knudson CM, Brown NM. Mitochondria potential, bax "activation," and programmed cell death. Methods in Molecular Biology (Clifton, NJ) 2008;414:95-108

63. Saleh A, Srinivasula SM, Acharya S, Fishel R, Alnemri ES. Cytochrome c and dATP-mediated oligomerization of Apaf-1 is a prerequisite for procaspase-9 activation. The Journal of Biological Chemistry 1999;274:17941-17945

64.   Lu M, Xia L, Hua H, Jing Y. Acetyl-Keto-{beta}-Boswellic Acid Induces Apoptosis through a Death Receptor 5-Mediated Pathway in Prostate Cancer Cells. Cancer Research 2008;68:1180-1186

65.   Syrovets T, Büchele B, Krauss C, Laumonnier Y, Simmet T. Acetyl-boswellic acids inhibit lipopolysaccharide-mediated TNF-alpha induction in monocytes by direct interaction with IkappaB kinases. The Journal of Immunology 2005;174:498-506

66.   Tawab MA, Kaunzinger A, Bahr U, Karas M, Wurglics M, Schubert-Zsilavecz M. Development of a high-performance liquid chromatographic method for the determination of 11-keto-beta-boswellic acid in human plasma. Journal of Chromatography B, Biomedical Sciences and Applications 2001;761:221-227

67.   Sharma S, Thawani V, Hingorani L, Shrivastava M, Bhate VR, Khiyani R. Pharmacokinetic study of 11-Keto beta-Boswellic acid. Phytomedicine: International Journal of Phytotherapy and Phytopharmacology 2004;11:255-260

68.   Tausch L, Henkel A, Siemoneit U, Poeckel D, Kather N, Franke L, Hofmann B, Schneider G, Angioni C, Geisslinger G, Skarke C, Holtmeier W, Beckhaus T, Karas M, Jauch J, Werz O. Identification of Human Cathepsin G As a Functional Target of Boswellic Acids from the Anti-Inflammatory Remedy Frankincense. The Journal of Immunology 2009;183:3433-3442

69.   Krüger P, Kanzer J, Hummel J, Fricker G, Schubert-Zsilavecz M, Abdel-Tawab M. Permeation of Boswellia extract in the Caco-2 model and possible interactions of its constituents KBA and AKBA with OATP1B3 and MRP2. European Journal of Pharmaceutical Sciences 2009;36:275-284

70.   Krüger P, Daneshfar R, Eckert GP, Klein J, Volmer DA, Bahr U, Muller WE, Karas M, Schubert-Zsilavecz M, Abdel-Tawab M. Metabolism of Boswellic Acids in Vitro and in Vivo. Drug Metabolism and Disposition 2008;36:1135-1142

71.   Frank A, Unger M. Analysis of frankincense from various Boswellia species with inhibitory activity on human drug metabolising cytochrome P450 enzymes using liquid chromatography mass spectrometry after automated on-line extraction. Journal of Chromatography A 2006;1112:255-262

72.   Kar A, Menon MK. Analgesic effect of the gum resin of Boswellia serata Roxb. Life Sciences 1969;8:1023-1028

73.   Singh GB, Atal CK. Pharmacology of an extract of salai guggal ex-Boswellia serrata, a new non-steroidal anti-inflammatory agent. Agents and Actions 1986;18:407-412

74.   Fan AY, Lao L, Zhang RX, Zhou AN, Wang LB, Moudgil KD, Lee DYW, Ma ZZ, Zhang WY, Berman BM. Effects of an acetone extract of Boswellia carterii Birdw. (Burseraceae) gum resin on adjuvant-induced arthritis in lewis rats. Journal of Ethnopharmacology 2005;101:104-109

75.   Reichling J, Schmökel H, Fitzi J, Bucher S, Saller R. Dietary support with Boswellia resin in canine inflammatory joint and spinal disease. Schweizer Archiv Für Tierheilkunde 2004;146:71-79

76.   Kimmatkar N, Thawani V, Hingorani L, Khiyani R. Efficacy and tolerability of Boswellia serrata extract in treatment of osteoarthritis of knee-a randomized double blind placebo controlled trial. Phytomedicine: International Journal of Phytotherapy and Phytopharmacology 2003;10:3-7

77.   Kulkarni RR, Patki PS, Jog VP, Gandage SG, Patwardhan B. Treatment of osteoarthritis with a herbomineral formulation: a double-blind, placebo-controlled, cross-over study. Journal of Ethnopharmacology 1991;33:91-95

78.   Sengupta K, Alluri KV, Satish AR, Mishra S, Golakoti T, Sarma KV, Dey D, Raychaudhuri SP. A double blind, randomized, placebo controlled study of the efficacy and safety of 5-Loxin for treatment of osteoarthritis of the knee. Arthritis Research & Therapy 2008;10:R85-R85

79.   Sontakke S, Thawani V, Pimpalkhute S, Kabra P, Babhulkar S, Hingorani L. Open, randomized, controlled clinical trial of Boswellia serrata extract as compared to valdecoxib in osteoarthritis of knee. Indian Journal of Pharmacology 2007;39:27-29

80.   Sander O, Herborn G, Rau R. Is H15 (resin extract of Boswellia serrata, "incense") a useful supplement to established drug therapy of chronic polyarthritis? Results of a double-blind pilot study. Zeitschrift Für Rheumatologie 1998;57:11-16

81.   Krieglstein CF, Anthoni C, Rijcken EJ, Laukötter M, Spiegel HU, Boden SE, Schweizer S, Safayhi H, Senninger N, Schürmann G. Acetyl-11-keto-beta-boswellic acid, a constituent of a herbal medicine from Boswellia serrata resin, attenuates experimental ileitis. International Journal of Colorectal Disease 2001;16:88-95

82.   Anthoni C, Laukoetter MG, Rijcken E, Vowinkel T, Mennigen R, Müller S, Senninger N, Russell J, Jauch J, Bergmann J, Granger DN, Krieglstein CF. Mechanisms underlying the anti-inflammatory actions of boswellic acid derivatives in experimental colitis. American Journal of Physiology Gastrointestinal and Liver Physiology 2006;290:G1131-1137-G1131-1137

83.   Kiela PR, Midura AJ, Kuscuoglu N, Jolad SD, Sólyom AM, Besselsen DG, Timmermann BN, Ghishan FK. Effects of Boswellia serrata in mouse models of chemically induced colitis. American Journal of Physiology Gastrointestinal and Liver Physiology 2005;288:G798-808-G798-808

84.   Gupta I, Parihar A, Malhotra P, Singh GB, Lüdtke R, Safayhi H, Ammon HP. Effects of Boswellia serrata gum resin in patients with ulcerative colitis. European Journal of Medical Research 1997;2:37-43

85.   Gerhardt H, Seifert F, Buvari P, Vogelsang H, Repges R. Therapy of active Crohn's disease with Boswellia serrata extract H15. Zeitschrift Fuer Gastrienterologie 2001;39:11-17

86.   Gupta I, Parihar A, Malhotra P, Gupta S, Lüdtke R, Safayhi H, Ammon HP. Effects of gum resin of Boswellia serrata in patients with chronic colitis. Planta Medica 2001;67:391-395

87.   Huang MT, Badmaev V, Ding Y, Liu Y, Xie JG, Ho CT. Anti-tumor and anti-carcinogenic activities of triterpenoid, beta-boswellic acid. BioFactors (Oxford, England) 2000;13:225-230

88.   Winking M, Sarikaya S, Rahmanian A, Jödicke A, Böker DK. Boswellic acids inhibit glioma growth: a new treatment option? Journal of Neuro-Oncology 2000;46:97-103

89.   Janssen G, Bode U, Breu H, Dohrn B, Engelbrecht V, Göbel U. Boswellic acids in the palliative therapy of children with progressive or relapsed brain tumors. Klinische Pädiatrie 2000;212:189-195

90.   Streffer JR, Bitzer M, Schabet M, Dichgans J, Weller M. Response of radiochemotherapy-associated cerebral edema to a phytotherapeutic agent, H15. Neurology 2001;56:1219-1221

91.   Gupta I, Gupta V, Parihar A, Gupta S, Lüdtke R, Safayhi H, Ammon HP. Effects of Boswellia serrata gum resin in patients with bronchial asthma: results of a double-blind, placebo-controlled, 6-week clinical study. European Journal of Medical Research 1998;3:511-514

92.   Golec M. Cathelicidin LL-37: LPS-neutralizing, pleiotropic peptide. Annals of Agricultural and Environmental Medicine 2007;14:1-4

93.   Larrick JW, Lee J, Ma S, Li X, Francke U, Wright SC, Balint RF. Structural, functional analysis and localization of the human CAP18 gene. FEBS Letters 1996;398:74-80

94.   Ritonja A, Kopitar M, Jerala R, Turk V. Primary structure of a new cysteine proteinase inhibitor from pig leucocytes. FEBS Letters 1989;255:211-214

95.   Gennaro R, Zanetti M. Structural features and biological activities of the cathelicidin-derived antimicrobial peptides. Biopolymers 2000;55:31-49

96.   Zanetti M. Cathelicidins, multifunctional peptides of the innate immunity. Journal of Leukocyte Biology 2004;75:39-48

97.   Sørensen OE, Follin P, Johnsen AH, Calafat J, Tjabringa GS, Hiemstra PS, Borregaard N. Human cathelicidin, hCAP-18, is processed to the antimicrobial peptide LL-37 by extracellular cleavage with proteinase 3. Blood 2001;97:3951-3959

98.   Sørensen OE, Gram L, Johnsen AH, Andersson E, Bangsbøll S, Tjabringa GS, Hiemstra PS, Malm J, Egesten A, Borregaard N. Processing of seminal plasma hCAP-18 to ALL-38 by gastricsin: a novel mechanism of generating antimicrobial peptides in vagina. The Journal of Biological Chemistry 2003;278:28540-28546

99. Bulet P, Stöcklin R, Menin L. Anti-microbial peptides: from invertebrates to vertebrates. Immunological Reviews 2004;198:169-184

100. Murakami M, Lopez-Garcia B, Braff M, Dorschner RA, Gallo RL. Postsecretory processing generates multiple cathelicidins for enhanced topical antimicrobial defense. Journal of Immunology (Baltimore, Md: 1950) 2004;172:3070-3077

101. Gudmundsson GH, Agerberth B, Odeberg J, Bergman T, Olsson B, Salcedo R. The human gene FALL39 and processing of the cathelin precursor to the antibacterial peptide LL-37 in granulocytes. European Journal of Biochemistry / FEBS 1996;238:325-332

102. Cowland JB, Johnsen AH, Borregaard N. hCAP-18, a cathelin/pro-bactenecin-like protein of human neutrophil specific granules. FEBS Letters 1995;368:173-176

103. Dorschner RA, Lin KH, Murakami M, Gallo RL. Neonatal skin in mice and humans expresses increased levels of antimicrobial peptides: innate immunity during development of the adaptive response. Pediatric Research 2003;53:566-572

104. Marchini G, Lindow S, Brismar H, Ståbi B, Berggren V, Ulfgren AK, Lonne-Rahm S, Agerberth B, Gudmundsson GH. The newborn infant is protected by an innate antimicrobial barrier: peptide antibiotics are present in the skin and vernix caseosa. The British Journal of Dermatology 2002;147:1127-1134

105. Murakami M, Ohtake T, Dorschner RA, Schittek B, Garbe C, Gallo RL. Cathelicidin anti-microbial peptide expression in sweat, an innate defense system for the skin. The Journal of Investigative Dermatology 2002;119:1090-1095

106. Frohm M, Gunne H, Bergman AC, Agerberth B, Bergman T, Boman A, Lidén S, Jörnvall H, Boman HG. Biochemical and antibacterial analysis of human wound and blister fluid. European Journal of Biochemistry / FEBS 1996;237:86-92

107. Frohm Nilsson M, Sandstedt B, Sørensen O, Weber G, Borregaard N, Ståhle-Bäckdahl M. The human cationic antimicrobial protein (hCAP18), a peptide antibiotic, is widely expressed in human squamous epithelia and colocalizes with interleukin-6. Infection and Immunity 1999;67:2561-2566

108. Gordon YJ, Huang LC, Romanowski EG, Yates KA, Proske RJ, McDermott AM. Human cathelicidin (LL-37), a multifunctional peptide, is expressed by ocular surface epithelia and has potent antibacterial and antiviral activity. Current Eye Research 2005;30:385-394

109. Bals R, Wang X, Zasloff M, Wilson JM. The peptide antibiotic LL-37/hCAP-18 is expressed in epithelia of the human lung where it has broad antimicrobial activity at the airway surface. Proceedings of the National Academy of Sciences of the United States of America 1998;95:9541-9546

110. Agerberth B, Gunne H, Odeberg J, Kogner P, Boman HG, Gudmundsson GH. FALL-39, a putative human peptide antibiotic, is cysteine-free and expressed in

bone marrow and testis. Proceedings of the National Academy of Sciences of the United States of America 1995;92:195-199

111.   Tollin M, Bergman P, Svenberg T, Jörnvall H, Gudmundsson GH, Agerberth B. Antimicrobial peptides in the first line defence of human colon mucosa. Peptides 2003;24:523-530

112.   Sørensen O, Bratt T, Johnsen AH, Madsen MT, Borregaard N. The human antibacterial cathelicidin, hCAP-18, is bound to lipoproteins in plasma. The Journal of Biological Chemistry 1999;274:22445-22451

113.   Frohm M, Agerberth B, Ahangari G, Stâhle-Bäckdahl M, Lidén S, Wigzell H, Gudmundsson GH. The expression of the gene coding for the antibacterial peptide LL-37 is induced in human keratinocytes during inflammatory disorders. The Journal of Biological Chemistry 1997;272:15258-15263

114.   Li D, Li J, Duan Y, Zhou X. Expression of LL-37, human beta defensin-2, and CCR6 mRNA in patients with psoriasis vulgaris. Journal of Huazhong University of Science and Technology Medical Sciences 2004;24:404-406

115.   Kim JE, Kim BJ, Jeong MS, Seo SJ, Kim MN, Hong CK, Ro BI. Expression and modulation of LL-37 in normal human keratinocytes, HaCaT cells, and inflammatory skin diseases. Journal of Korean Medical Science 2005;20:649-654

116.   Hase K, Murakami M, Iimura M, Cole SP, Horibe Y, Ohtake T, Obonyo M, Gallo RL, Eckmann L, Kagnoff MF. Expression of LL-37 by human gastric epithelial cells as a potential host defense mechanism against Helicobacter pylori. Gastroenterology 2003;125:1613-1625

117.   Heilborn JD, Nilsson MF, Jimenez CIC, Sandstedt B, Borregaard N, Tham E, Sørensen OE, Weber G, Ståhle M. Antimicrobial protein hCAP18/LL-37 is highly expressed in breast cancer and is a putative growth factor for epithelial cells. International Journal of Cancer Journal International Du Cancer 2005;114:713-719

118.   Ong PY, Ohtake T, Brandt C, Strickland I, Boguniewicz M, Ganz T, Gallo RL, Leung DYM. Endogenous antimicrobial peptides and skin infections in atopic dermatitis. The New England Journal of Medicine 2002;347:1151-1160

119.   Heilborn JD, Nilsson MF, Kratz G, Weber G, Sørensen O, Borregaard N, Ståhle-Bäckdahl M. The cathelicidin anti-microbial peptide LL-37 is involved in re-epithelialization of human skin wounds and is lacking in chronic ulcer epithelium. The Journal of Investigative Dermatology 2003;120:379-389

120.   An L-L, Ma X-T, Yang Y-H, Lin Y-M, Song Y-H, Wu K-F. Marked reduction of LL-37/hCAP-18, an antimicrobial peptide, in patients with acute myeloid leukemia. International Journal of Hematology 2005;81:45-47

121.   Islam D, Bandholtz L, Nilsson J, Wigzell H, Christensson B, Agerberth B, Gudmundsson G. Downregulation of bactericidal peptides in enteric infections: a novel immune escape mechanism with bacterial DNA as a potential regulator. Nature Medicine 2001;7:180-185

122.   Larrick JW, Hirata M, Zhong J, Wright SC. Anti-microbial activity of human CAP18 peptides. Immunotechnology 1995;1:65-72

123.   den Hertog AL, van Marle J, van Veen HA, Van't Hof W, Bolscher JGM, Veerman ECI, Nieuw Amerongen AV. Candidacidal effects of two antimicrobial peptides: histatin 5 causes small membrane defects, but LL-37 causes massive disruption of the cell membrane. The Biochemical Journal 2005;388:689-695

124.   Bergman P, Walter-Jallow L, Broliden K, Agerberth B, Söderlund J. The antimicrobial peptide LL-37 inhibits HIV-1 replication. Current HIV Research 2007;5:410-415

125.   De Smet K, Contreras R. Human antimicrobial peptides: defensins, cathelicidins and histatins. Biotechnology Letters 2005;27:1337-1347

126.   Burton MF, Steel PG. The chemistry and biology of LL-37. Natural Product Reports 2009;26:1572-1584

127.   Johansson J, Gudmundsson GH, Rottenberg ME, Berndt KD, Agerberth B. Conformation-dependent antibacterial activity of the naturally occurring human peptide LL-37. The Journal of Biological Chemistry 1998;273:3718-3724

128.   Oren Z, Lerman JC, Gudmundsson GH, Agerberth B, Shai Y. Structure and organization of the human antimicrobial peptide LL-37 in phospholipid membranes: relevance to the molecular basis for its non-cell-selective activity. The Biochemical Journal 1999;341:501-513

129.   Dürr UHN, Sudheendra US, Ramamoorthy A. LL-37, the only human member of the cathelicidin family of antimicrobial peptides. Biochimica Et Biophysica Acta 2006;1758:1408-1425

130.   Koczulla R, von Degenfeld G, Kupatt C, Krötz F, Zahler S, Gloe T, Issbrücker K, Unterberger P, Zaiou M, Lebherz C, Karl A, Raake P, Pfosser A, Boekstegers P, Welsch U, Hiemstra PS, Vogelmeier C, Gallo RL, Clauss M, Bals R. An angiogenic role for the human peptide antibiotic LL-37/hCAP-18. The Journal of Clinical Investigation 2003;111:1665-1672

131.   Tjabringa GS, Ninaber DK, Drijfhout JW, Rabe KF, Hiemstra PS. Human cathelicidin LL-37 is a chemoattractant for eosinophils and neutrophils that acts via formyl-peptide receptors. International Archives of Allergy and Immunology 2006;140:103-112

132.   Niyonsaba F, Iwabuchi K, Someya A, Hirata M, Matsuda H, Ogawa H, Nagaoka I. A cathelicidin family of human antibacterial peptide LL-37 induces mast cell chemotaxis. Immunology 2002;106:20-26

133.   Niyonsaba F, Someya A, Hirata M, Ogawa H, Nagaoka I. Evaluation of the effects of peptide antibiotics human beta-defensins-1/-2 and LL-37 on histamine release and prostaglandin D(2) production from mast cells. European Journal of Immunology 2001;31:1066-1075

134. Yang D, Chen Q, Schmidt AP, Anderson GM, Wang JM, Wooters J, Oppenheim JJ, Chertov O. LL-37, the neutrophil granule- and epithelial cell-derived cathelicidin, utilizes formyl peptide receptor-like 1 (FPRL1) as a receptor to chemoattract human peripheral blood neutrophils, monocytes, and T cells. The Journal of Experimental Medicine 2000;192:1069-1074

135. Elssner A, Duncan M, Gavrilin M, Wewers MD. A novel P2X7 receptor activator, the human cathelicidin-derived peptide LL37, induces IL-1 beta processing and release. Journal of Immunology (Baltimore, Md: 1950) 2004;172:4987-4994

136. Tjabringa GS, Aarbiou J, Ninaber DK, Drijfhout JW, Sørensen OE, Borregaard N, Rabe KF, Hiemstra PS. The antimicrobial peptide LL-37 activates innate immunity at the airway epithelial surface by transactivation of the epidermal growth factor receptor. The Journal of Immunology 2003;171:6690-6696

137. Bowdish DME, Davidson DJ, Speert DP, Hancock REW. The human cationic peptide LL-37 induces activation of the extracellular signal-regulated kinase and p38 kinase pathways in primary human monocytes. Journal of Immunology (Baltimore, Md: 1950) 2004;172:3758-3765

138. Niyonsaba F, Ushio H, Nagaoka I, Okumura K, Ogawa H. The human beta-defensins (-1, -2, -3, -4) and cathelicidin LL-37 induce IL-18 secretion through p38 and ERK MAPK activation in primary human keratinocytes. The Journal of Immunology 2005;175:1776-1784

139. Larrick JW, Hirata M, Balint RF, Lee J, Zhong J, Wright SC. Human CAP18: a novel antimicrobial lipopolysaccharide-binding protein. Infection and Immunity 1995;63:1291-1297

140. Rosenfeld Y, Papo N, Shai Y. Endotoxin (lipopolysaccharide) neutralization by innate immunity host-defense peptides. Peptide properties and plausible modes of action. The Journal of Biological Chemistry 2006;281:1636-1643

141. Zughaier SM, Shafer WM, Stephens DS. Antimicrobial peptides and endotoxin inhibit cytokine and nitric oxide release but amplify respiratory burst response in human and murine macrophages. Cellular Microbiology 2005;7:1251-1262

142. Alexander C, Rietschel ET. Invited review: Bacterial lipopolysaccharides and innate immunity. Journal of Endotoxin Research 2001;7:167-202

143. Holst O, Ulmer AJ, Brade H, Flad HD, Rietschel ET. Biochemistry and cell biology of bacterial endotoxins. FEMS Immunology and Medical Microbiology 1996;16:83-104

144. Knirel YA. Polysaccharide antigens of Pseudomonas aeruginosa. Critical Reviews in Microbiology 1990;17:273-304

145. Knirel YA, Kochetkov NK. Structure of lipopolysaccharides from gram-negative bacteria. III. Structure of O-specific polysaccharides. Biokhimiia 1994;59:1784-1851

146. Rietschel ET, Brade H, Holst O, Brade L, Müller-Loennies S, Mamat U, Zähringer U, Beckmann F, Seydel U, Brandenburg K, Ulmer AJ, Mattern T, Heine H, Schletter J, Loppnow H, Schönbeck U, Flad HD, Hauschildt S, Schade UF, Di Padova F, Kusumoto S, Schumann RR. Bacterial endotoxin: Chemical constitution, biological recognition, host response, and immunological detoxification. Current Topics in Microbiology and Immunology 1996;216:39-81

147. Dröge W, Lehmann V, Lüderitz O, Westphal O. Structural investigations on the 2-keto-3-deoxyoctonate region of lipopolysaccharides. European Journal of Biochemistry / FEBS 1970;14:175-184

148. Galanos C. Physical state and biological activity of lipopolysaccharides. Toxicity and immunogenicity of the lipid A component. Zeitschrift Für Immunitätsforschung, Experimentelle Und Klinische Immunologie 1975;149:214-229

149. Kim YB, Watson DW. Biologically active endotoxins from Salmonella mutants deficient in O- and R-polysaccharides and heptose. Journal of Bacteriology 1967;94:1320-1326

150. Kasai N, Nowotny A. Endotoxic glycolipid from a heptoseless mutant of Salmonella minnesota. Journal of Bacteriology 1967;94:1824-1836

151. Haziot A, Chen S, Ferrero E, Low MG, Silber R, Goyert SM. The monocyte differentiation antigen, CD14, is anchored to the cell membrane by a phosphatidylinositol linkage. Journal of Immunology (Baltimore, Md: 1950) 1988;141:547-552

152. Kitchens RL. Role of CD14 in cellular recognition of bacterial lipopolysaccharides. Chemical Immunology 2000;74:61-82

153. Zhang FX, Kirschning CJ, Mancinelli R, Xu XP, Jin Y, Faure E, Mantovani A, Rothe M, Muzio M, Arditi M. Bacterial lipopolysaccharide activates nuclear factor-kappaB through interleukin-1 signaling mediators in cultured human dermal endothelial cells and mononuclear phagocytes. The Journal of Biological Chemistry 1999;274:7611-7614

154. Muzio M, Bosisio D, Polentarutti N, D'Amico G, Stoppacciaro A, Mancinelli R, van't Veer C, Penton-Rol G, Ruco LP, Allavena P, Mantovani A. Differential expression and regulation of toll-like receptors (TLR) in human leukocytes: selective expression of TLR3 in dendritic cells. Journal of Immunology (Baltimore, Md: 1950) 2000;164:5998-6004

155. Muzio M, Polentarutti N, Bosisio D, Prahladan MK, Mantovani A. Toll-like receptors: a growing family of immune receptors that are differentially expressed and regulated by different leukocytes. Journal of Leukocyte Biology 2000;67:450-456

156. Kleinert H, Schwarz PM, Forstermann U. Regulation of the expression of inducible nitric oxide synthase. Biological Chemistry 2003;384:1343-1364

157.   Aderem A, Ulevitch RJ. Toll-like receptors in the induction of the innate immune response. Nature 2000;406:782-787

158.   Tobias PS, Soldau K, Ulevitch RJ. Isolation of a lipopolysaccharide-binding acute phase reactant from rabbit serum. The Journal of Experimental Medicine 1986;164:777-793

159.   Wright SD, Tobias PS, Ulevitch RJ, Ramos RA. Lipopolysaccharide (LPS) binding protein opsonizes LPS-bearing particles for recognition by a novel receptor on macrophages. The Journal of Experimental Medicine 1989;170:1231-1241

160.   da Silva Correia J, Soldau K, Christen U, Tobias PS, Ulevitch RJ. Lipopolysaccharide is in close proximity to each of the proteins in its membrane receptor complex. transfer from CD14 to TLR4 and MD-2. The Journal of Biological Chemistry 2001;276:21129-21135

161.   Suzuki N, Suzuki S, Yeh W-C. IRAK-4 as the central TIR signaling mediator in innate immunity. Trends in Immunology 2002;23:503-506

162.   Irie T, Muta T, Takeshige K. TAK1 mediates an activation signal from toll-like receptor(s) to nuclear factor-kappaB in lipopolysaccharide-stimulated macrophages. FEBS Letters 2000;467:160-164

163.   Yoshida R, Takaesu G, Yoshida H, Okamoto F, Yoshioka T, Choi Y, Akira S, Kawai T, Yoshimura A, Kobayashi T. TRAF6 and MEKK1 play a pivotal role in the RIG-I-like helicase antiviral pathway. The Journal of Biological Chemistry 2008;283:36211-36220

164.   Xie QW, Kashiwabara Y, Nathan C. Role of transcription factor NF-kappa B/Rel in induction of nitric oxide synthase. The Journal of Biological Chemistry 1994;269:4705-4708

165.   Evans CH. Nitric oxide: what role does it play in inflammation and tissue destruction? Agents and Actions Supplements 1995;47:107-116

166.   Woltmann A, Hamann L, Ulmer AJ, Gerdes J, Bruch HP, Rietschel ET. Molecular mechanisms of sepsis. Langenbeck's Archives of Surgery 1998;383:2-10

167.   van Dissel JT, van Langevelde P, Westendorp RG, Kwappenberg K, Frölich M. Anti-inflammatory cytokine profile and mortality in febrile patients. Lancet 1998;351:950-953

168.   Volk HD, Reinke P, Döcke WD. Clinical aspects: from systemic inflammation to 'immunoparalysis'. Chemical Immunology 2000;74:162-177

169.   Brun-Buisson C, Doyon F, Carlet J. Bacteremia and severe sepsis in adults: a multicenter prospective survey in ICUs and wards of 24 hospitals. French Bacteremia-Sepsis Study Group. American Journal of Respiratory and Critical Care Medicine 1996;154:617-624

170.   Döcke WD, Randow F, Syrbe U, Krausch D, Asadullah K, Reinke P, Volk HD, Kox W. Monocyte deactivation in septic patients: restoration by IFN-gamma treatment. Nature Medicine 1997;3:678-681

171.   Brun-Buisson C. The epidemiology of the systemic inflammatory response. Intensive Care Medicine 2000;26 Suppl 1:S64-74-S64-74

172.   Bellingan G. Inflammatory cell activation in sepsis. British Medical Bulletin 1999;55:12-29

173.   Danner RL, Elin RJ, Hosseini JM, Wesley RA, Reilly JM, Parillo JE. Endotoxemia in human septic shock. Chest 1991;99:169-175

174.   Casey LC, Balk RA, Bone RC. Plasma cytokine and endotoxin levels correlate with survival in patients with the sepsis syndrome. Annals of Internal Medicine 1993;119:771-778

175.   Opal SM, Scannon PJ, Vincent JL, White M, Carroll SF, Palardy JE, Parejo NA, Pribble JP, Lemke JH. Relationship between plasma levels of lipopolysaccharide (LPS) and LPS-binding protein in patients with severe sepsis and septic shock. The Journal of Infectious Diseases 1999;180:1584-1589

176.   Burster T, Macmillan H, Hou T, Boehm BO, Mellins ED. Cathepsin G: Roles in antigen presentation and beyond. Molecular Immunology 2010;47:658-665

177.   Pham CTN. Neutrophil serine proteases: specific regulators of inflammation. Nature Reviews Immunology 2006;6:541-550

178.   Wiedow O, Meyer-Hoffert U. Neutrophil serine proteases: potential key regulators of cell signalling during inflammation. Journal of Internal Medicine 2005;257:319-328

179.   Shafer WM, Hubalek F, Huang M, Pohl J. Bactericidal activity of a synthetic peptide (CG 117-136) of human lysosomal cathepsin G is dependent on arginine content. Infection and Immunity 1996;64:4842-4845

180.   Shafer WM, Katzif S, Bowers S, Fallon M, Hubalek M, Reed MS, Veprek P, Pohl J. Tailoring an antibacterial peptide of human lysosomal cathepsin G to enhance its broad-spectrum action against antibiotic-resistant bacterial pathogens. Current Pharmaceutical Design 2002;8:695-702

181.   Owen CA, Campbell MA, Boukedes SS, Campbell EJ. Inducible binding of bioactive cathepsin G to the cell surface of neutrophils. A novel mechanism for mediating extracellular catalytic activity of cathepsin G. Journal of Immunology (Baltimore, Md: 1950) 1995;155:5803-5810

182.   Owen CA, Campbell EJ. Angiotensin II generation at the cell surface of activated neutrophils: novel cathepsin G-mediated catalytic activity that is resistant to inhibition. Journal of Immunology (Baltimore, Md: 1950) 1998;160:1436-1443

183.   Owen CA, Campbell EJ. The cell biology of leukocyte-mediated proteolysis. Journal of Leukocyte Biology 1999;65:137-150

184. Nufer O, Corbett M, Walz A. Amino-terminal processing of chemokine ENA-78 regulates biological activity. Biochemistry 1999;38:636-642

185. Berahovich RD, Miao Z, Wang Y, Premack B, Howard MC, Schall TJ. Proteolytic activation of alternative CCR1 ligands in inflammation. Journal of Immunology (Baltimore, Md: 1950) 2005;174:7341-7351

186. Wittamer V, Bondue B, Guillabert A, Vassart G, Parmentier M, Communi D. Neutrophil-mediated maturation of chemerin: a link between innate and adaptive immunity. Journal of Immunology (Baltimore, Md: 1950) 2005;175:487-493

187. Ryu OH, Choi SJ, Firatli E, Choi SW, Hart PS, Shen R-F, Wang G, Wu WW, Hart TC. Proteolysis of macrophage inflammatory protein-1alpha isoforms LD78beta and LD78alpha by neutrophil-derived serine proteases. The Journal of Biological Chemistry 2005;280:17415-17421

188. Sambrano GR, Huang W, Faruqi T, Mahrus S, Craik C, Coughlin SR. Cathepsin G activates protease-activated receptor-4 in human platelets. The Journal of Biological Chemistry 2000;275:6819-6823

189. Coughlin SR, Camerer E. PARticipation in inflammation. The Journal of Clinical Investigation 2003;111:25-27

190. Ossovskaya VS, Bunnett NW. Protease-activated receptors: contribution to physiology and disease. Physiological Reviews 2004;84:579-621

191. Lowy DR, Willumsen BM. Function and regulation of ras. Annual Review of Biochemistry 1993;62:851-891

192. Ehrhardt A, Ehrhardt GRA, Guo X, Schrader JW. Ras and relatives-job sharing and networking keep an old family together. Experimental Hematology 2002;30:1089-1106

193. Casey PJ. Protein lipidation in cell signaling. Science (New York, NY) 1995;268:221-225

194. Hancock JF, Magee AI, Childs JE, Marshall CJ. All ras proteins are polyisoprenylated but only some are palmitoylated. Cell 1989;57:1167-1177

195. Hancock JF, Paterson H, Marshall CJ. A polybasic domain or palmitoylation is required in addition to the CAAX motif to localize p21ras to the plasma membrane. Cell 1990;63:133-139

196. Roy S, Luetterforst R, Harding A, Apolloni A, Etheridge M, Stang E, Rolls B, Hancock JF, Parton RG. Dominant-negative caveolin inhibits H-Ras function by disrupting cholesterol-rich plasma membrane domains. Nature Cell Biology 1999;1:98-105

197. Prior IA, Harding A, Yan J, Sluimer J, Parton RG, Hancock JF. GTP-dependent segregation of H-ras from lipid rafts is required for biological activity. Nature Cell Biology 2001;3:368-375

198. Spaargaren M, Bischoff JR. Identification of the guanine nucleotide dissociation stimulator for Ral as a putative effector molecule of R-ras, H-ras, K-ras, and Rap. Proceedings of the National Academy of Sciences of the United States of America 1994;91:12609-12613

199. Kikuchi A, Demo SD, Ye ZH, Chen YW, Williams LT. ralGDS family members interact with the effector loop of ras p21. Molecular and Cellular Biology 1994;14:7483-7491

200. Wolthuis RM, Bauer B, van 't Veer LJ, de Vries-Smits AM, Cool RH, Spaargaren M, Wittinghofer A, Burgering BM, Bos JL. RalGDS-like factor (Rlf) is a novel Ras and Rap 1A-associating protein. Oncogene 1996;13:353-362

201. Shao H, Andres DA. A novel RalGEF-like protein, RGL3, as a candidate effector for rit and Ras. The Journal of Biological Chemistry 2000;275:26914-26924

202. Ehrhardt GR, Korherr C, Wieler JS, Knaus M, Schrader JW. A novel potential effector of M-Ras and p21 Ras negatively regulates p21 Ras-mediated gene induction and cell growth. Oncogene 2001;20:188-197

203. Vojtek AB, Hollenberg SM, Cooper JA. Mammalian Ras interacts directly with the serine/threonine kinase Raf. Cell 1993;74:205-214

204. Zhang XF, Settleman J, Kyriakis JM, Takeuchi-Suzuki E, Elledge SJ, Marshall MS, Bruder JT, Rapp UR, Avruch J. Normal and oncogenic p21ras proteins bind to the amino-terminal regulatory domain of c-Raf-1. Nature 1993;364:308-313

205. Russell M, Lange-Carter CA, Johnson GL. Direct interaction between Ras and the kinase domain of mitogen-activated protein kinase kinase kinase (MEKK1). The Journal of Biological Chemistry 1995;270:11757-11760

206. Lange-Carter CA, Pleiman CM, Gardner AM, Blumer KJ, Johnson GL. A divergence in the MAP kinase regulatory network defined by MEK kinase and Raf. Science (New York, NY) 1993;260:315-319

207. Xu S, Robbins DJ, Christerson LB, English JM, Vanderbilt CA, Cobb MH. Cloning of rat MEK kinase 1 cDNA reveals an endogenous membrane-associated 195-kDa protein with a large regulatory domain. Proceedings of the National Academy of Sciences of the United States of America 1996;93:5291-5295

208. Lee FS, Peters RT, Dang LC, Maniatis T. MEKK1 activates both IkappaB kinase alpha and IkappaB kinase beta. Proceedings of the National Academy of Sciences of the United States of America 1998;95:9319-9324

209. Nimnual AS, Yatsula BA, Bar-Sagi D. Coupling of Ras and Rac guanosine triphosphatases through the Ras exchanger Sos. Science (New York, NY) 1998;279:560-563

210. Han J, Luby-Phelps K, Das B, Shu X, Xia Y, Mosteller RD, Krishna UM, Falck JR, White MA, Broek D. Role of substrates and products of PI 3-kinase in

regulating activation of Rac-related guanosine triphosphatases by Vav. Science (New York, NY) 1998;279:558-560

211.   Filmus J, Robles AI, Shi W, Wong MJ, Colombo LL, Conti CJ. Induction of cyclin D1 overexpression by activated ras. Oncogene 1994;9:3627-3633

212.   Dobrowolski S, Harter M, Stacey DW. Cellular ras activity is required for passage through multiple points of the G0/G1 phase in BALB/c 3T3 cells. Molecular and Cellular Biology 1994;14:5441-5449

213.   Xu XS, Vanderziel C, Bennett CF, Monia BP. A role for c-Raf kinase and Ha-Ras in cytokine-mediated induction of cell adhesion molecules. The Journal of Biological Chemistry 1998;273:33230-33238

214.   Hughes PE, Renshaw MW, Pfaff M, Forsyth J, Keivens VM, Schwartz MA, Ginsberg MH. Suppression of integrin activation: a novel function of a Ras/Raf-initiated MAP kinase pathway. Cell 1997;88:521-530

215.   Shibayama H, Anzai N, Braun SE, Fukuda S, Mantel C, Broxmeyer HE. H-Ras is involved in the inside-out signaling pathway of interleukin-3-induced integrin activation. Blood 1999;93:1540-1548

216.   Caron E, Self AJ, Hall A. The GTPase Rap1 controls functional activation of macrophage integrin alphaMbeta2 by LPS and other inflammatory mediators. Current Biology 2000;10:974-978

217.   Katagiri K, Hattori M, Minato N, Irie Sk, Takatsu K, Kinashi T. Rap1 is a potent activation signal for leukocyte function-associated antigen 1 distinct from protein kinase C and phosphatidylinositol-3-OH kinase. Molecular and Cellular Biology 2000;20:1956-1969

218.   Reedquist KA, Ross E, Koop EA, Wolthuis RM, Zwartkruis FJ, van Kooyk Y, Salmon M, Buckley CD, Bos JL. The small GTPase, Rap1, mediates CD31-induced integrin adhesion. The Journal of Cell Biology 2000;148:1151-1158

219.   Enserink JM, Price LS, Methi T, Mahic M, Sonnenberg A, Bos JL, Taskén K. The cAMP-Epac-Rap1 pathway regulates cell spreading and cell adhesion to laminin-5 through the alpha3beta1 integrin but not the alpha6beta4 integrin. The Journal of Biological Chemistry 2004;279:44889-44896

220.   Crittenden JR, Bergmeier W, Zhang Y, Piffath CL, Liang Y, Wagner DD, Housman DE, Graybiel AM. CalDAG-GEFI integrates signaling for platelet aggregation and thrombus formation. Nature Medicine 2004;10:982-986

221.   Albelda SM, Buck CA. Integrins and other cell adhesion molecules. The FASEB Journal: Official Publication of the Federation of American Societies for Experimental Biology 1990;4:2868-2880

222.   Yajnik V, Paulding C, Sordella R, McClatchey AI, Saito M, Wahrer DCR, Reynolds P, Bell DW, Lake R, van den Heuvel S, Settleman J, Haber DA. DOCK4, a GTPase activator, is disrupted during tumorigenesis. Cell 2003;112:673-684

223. Price LS, Hajdo-Milasinovic A, Zhao J, Zwartkruis FJT, Collard JG, Bos JL. Rap1 regulates E-cadherin-mediated cell-cell adhesion. The Journal of Biological Chemistry 2004;279:35127-35132

224. Cullere X, Shaw SK, Andersson L, Hirahashi J, Luscinskas FW, Mayadas TN. Regulation of vascular endothelial barrier function by Epac, a cAMP-activated exchange factor for Rap GTPase. Blood 2005;105:1950-1955

225. Fukuhara S, Sakurai A, Sano H, Yamagishi A, Somekawa S, Takakura N, Saito Y, Kangawa K, Mochizuki N. Cyclic AMP potentiates vascular endothelial cadherin-mediated cell-cell contact to enhance endothelial barrier function through an Epac-Rap1 signaling pathway. Molecular and Cellular Biology 2005;25:136-146

226. Bos JL. Linking Rap to cell adhesion. Current Opinion in Cell Biology 2005;17:123-128

227. Asakura T, Nakanishi H, Sakisaka T, Takahashi K, Mandai K, Nishimura M, Sasaki T, Takai Y. Similar and differential behaviour between the nectin-afadin-ponsin and cadherin-catenin systems during the formation and disruption of the polarized junctional alignment in epithelial cells. Genes to Cells: Devoted to Molecular & Cellular Mechanisms 1999;4:573-581

228. Mandai K, Nakanishi H, Satoh A, Obaishi H, Wada M, Nishioka H, Itoh M, Mizoguchi A, Aoki T, Fujimoto T, Matsuda Y, Tsukita S, Takai Y. Afadin: A novel actin filament-binding protein with one PDZ domain localized at cadherin-based cell-to-cell adherens junction. The Journal of Cell Biology 1997;139:517-528

229. Boettner B, Van Aelst L. Control of cell adhesion dynamics by Rap1 signaling. Current Opinion in Cell Biology 2009;21:684-693

230. Katagiri K, Maeda A, Shimonaka M, Kinashi T. RAPL, a Rap1-binding molecule that mediates Rap1-induced adhesion through spatial regulation of LFA-1. Nature Immunology 2003;4:741-748

231. Lafuente EM, van Puijenbroek AAFL, Krause M, Carman CV, Freeman GJ, Berezovskaya A, Constantine E, Springer TA, Gertler FB, Boussiotis VA. RIAM, an Ena/VASP and Profilin ligand, interacts with Rap1-GTP and mediates Rap1-induced adhesion. Developmental Cell 2004;7:585-595

232. Krugmann S, Williams R, Stephens L, Hawkins PT. ARAP3 is a PI3K- and rap-regulated GAP for RhoA. Current Biology 2004;14:1380-1384

233. Arthur WT, Quilliam LA, Cooper JA. Rap1 promotes cell spreading by localizing Rac guanine nucleotide exchange factors. The Journal of Cell Biology 2004;167:111-122

234. Liao Y, Satoh T, Gao X, Jin TG, Hu CD, Kataoka T. RA-GEF-1, a guanine nucleotide exchange factor for Rap1, is activated by translocation induced by association with Rap1*GTP and enhances Rap1-dependent B-Raf activation. The Journal of Biological Chemistry 2001;276:28478-28483

235.   Poeckel D, Werz O. Boswellic acids: biological actions and molecular targets. Current Medicinal Chemistry 2006;13:3359-3369

236.   Jauch J, Bergmann J. An Efficient Method for the Large-Scale Preparation of 3-O-Acetyl-11-oxo-β-boswellic Acid and Other Boswellic Acids. European Journal of Organic Chemistry 2003;2003:4752-4756

237.   Kather N. Synthese und Struktur-Wirkungs-Beziehungen von Boswelliasäuren und deren Derivaten. In, Institut für Organische Chemie II. Saarbruecken: Universität des Saarlandes; 2007

238.   Raschke WC, Baird S, Ralph P, Nakoinz I. Functional macrophage cell lines transformed by Abelson leukemia virus. Cell 1978;15:261-267

239.   Schneider U, Schwenk HU, Bornkamm G. Characterization of EBV-genome negative "null" and "T" cell lines derived from children with acute lymphoblastic leukemia and leukemic transformed non-Hodgkin lymphoma. International Journal of Cancer 1977;19:621-626

240.   Collins SJ, Gallo RC, Gallagher RE. Continuous growth and differentiation of human myeloid leukaemic cells in suspension culture. Nature 1977;270:347-349

241.   Fontana JA, Colbert DA, Deisseroth AB. Identification of a population of bipotent stem cells in the HL60 human promyelocytic leukemia cell line. Proceedings of the National Academy of Sciences of the United States of America 1981;78:3863-3866

242.   Laemmli UK. Cleavage of structural proteins during the assembly of the head of bacteriophage T4. Nature 1970;227:680-685

243.   Schägger H, von Jagow G. Tricine-sodium dodecyl sulfate-polyacrylamide gel electrophoresis for the separation of proteins in the range from 1 to 100 kDa. Analytical Biochemistry 1987;166:368-379

244.   Griess P. Bemerkungen zu der Abhandlung der HH. Weselsky und Benedikt "Ueber einige Azoverbindungen". Berichte der deutschen chemischen Gesellschaft 1879;12:426-428

245.   Johansson A, Claesson R, Belibasakis G, Makoveichuk E, Hänström L, Olivecrona G, Sandström G, Kalfas S. Protease inhibitors, the responsible components for the serum-dependent enhancement of Actinobacillus actinomycetemcomitans leukotoxicity. European Journal of Oral Sciences 2001;109:335-341

246.   Grynkiewicz G, Poenie M, Tsien RY. A new generation of Ca2+ indicators with greatly improved fluorescence properties. The Journal of Biological Chemistry 1985;260:3440-3450

247.   Rubio I. Use of the Ras binding domain of c-Raf for biochemical and live-cell analysis of Ras activation. Biochemical Society Transactions 2005;33:662-663

248.   Nicoletti I, Migliorati G, Pagliacci MC, Grignani F, Riccardi C. A rapid and simple method for measuring thymocyte apoptosis by propidium iodide staining and flow cytometry. Journal of Immunological Methods 1991;139:271-279

249.   Aarbiou J, Tjabringa GS, Verhoosel RM, Ninaber DK, White SR, Peltenburg LTC, Rabe KF, Hiemstra PS. Mechanisms of cell death induced by the neutrophil antimicrobial peptides alpha-defensins and LL-37. Inflammation Research 2006;55:119-127

250.   De Y, Chen Q, Schmidt AP, Anderson GM, Wang JM, Wooters J, Oppenheim JJ, Chertov O. LL-37, the neutrophil granule- and epithelial cell-derived cathelicidin, utilizes formyl peptide receptor-like 1 (FPRL1) as a receptor to chemoattract human peripheral blood neutrophils, monocytes, and T cells. The Journal of Experimental Medicine 2000;192:1069-1074

251.   Zhang Z, Cherryholmes G, Chang F, Rose DM, Schraufstatter I, Shively JE. Evidence that cathelicidin peptide LL-37 may act as a functional ligand for CXCR2 on human neutrophils. European Journal of Immunology 2009;39:3181-3194

252.   Zheng Y, Niyonsaba F, Ushio H, Nagaoka I, Ikeda S, Okumura K, Ogawa H. Cathelicidin LL-37 induces the generation of reactive oxygen species and release of human alpha-defensins from neutrophils. The British Journal of Dermatology 2007;157:1124-1131

253.   Lee JC, Young PR. Role of CSB/p38/RK stress response kinase in LPS and cytokine signaling mechanisms. Journal of Leukocyte Biology 1996;59:152-157

254.   Tani K, Ogushi F, Shimizu T, Sone S. Protease-induced leukocyte chemotaxis and activation: roles in host defense and inflammation. Journal of Medical Investigation 2001;48:133-141

255.   Siemoneit U. Anti-inflammatory actions of boswellic acids: Identification and critical evaluation of molecular targets and signaling pathways. In, Institut für Pharmazie. Tübingen: Eberhard Karls Universität Tübingen; 2009

256.   Khanapure SP, Garvey DS, Janero DR, Letts LG. Eicosanoids in inflammation: biosynthesis, pharmacology, and therapeutic frontiers. Current Topics in Medicinal Chemistry 2007;7:311-340

257.   Ahmadian MR, Wittinghofer A, Herrmann C. Fluorescence methods in the study of small GTP-binding proteins. Methods in Molecular Biology (Clifton, NJ) 2002;189:45-63

258.   Liu X, Qi ZH. Experimental study on Jurkat cell apoptosis induced by Boswellia carterii Birdw extractive. Hunan Yi Ke Da Xue Xue Bao 2000;25:241-244

259.   Fuentes-Prior P, Salvesen GS. The protein structures that shape caspase activity, specificity, activation and inhibition. The Biochemical Journal 2004;384:201-232

260.   Smulson ME, Simbulan-Rosenthal CM, Boulares AH, Yakovlev A, Stoica B, Iyer S, Luo R, Haddad B, Wang ZQ, Pang T, Jung M, Dritschilo A, Rosenthal

DS. Roles of poly(ADP-ribosyl)ation and PARP in apoptosis, DNA repair, genomic stability and functions of p53 and E2F-1. Advances in Enzyme Regulation 2000;40:183-215

261. Jones DP, McConkey DJ, Nicotera P, Orrenius S. Calcium-activated DNA fragmentation in rat liver nuclei. The Journal of Biological Chemistry 1989;264:6398-6403

262. Siemoneit U, Pergola C, Jazzar B, Northoff H, Skarke C, Jauch J, Werz O. On the interference of boswellic acids with 5-lipoxygenase: mechanistic studies in vitro and pharmacological relevance. European Journal of Pharmacology 2009;606:246-254

263. Wang H, Peters T, Kess D, Sindrilaru A, Oreshkova T, Van Rooijen N, Stratis A, Renkl AC, Sunderkötter C, Wlaschek M, Haase I, Scharffetter-Kochanek K. Activated macrophages are essential in a murine model for T cell-mediated chronic psoriasiform skin inflammation. The Journal of Clinical Investigation 2006;116:2105-2114

264. Wang H, Syrovets T, Kess D, Büchele B, Hainzl H, Lunov O, Weiss JM, Scharffetter-Kochanek K, Simmet T. Targeting NF-{kappa}B with a Natural Triterpenoid Alleviates Skin Inflammation in a Mouse Model of Psoriasis. The Journal of Immunology 2009

265. Pestonjamasp VK, Huttner KH, Gallo RL. Processing site and gene structure for the murine antimicrobial peptide CRAMP. Peptides 2001;22:1643-1650

266. Mpofu CM, Campbell BJ, Subramanian S, Marshall-Clarke S, Hart CA, Cross A, Roberts CL, McGoldrick A, Edwards SW, Rhodes JM. Microbial mannan inhibits bacterial killing by macrophages: a possible pathogenic mechanism for Crohn's disease. Gastroenterology 2007;133:1487-1498

267. Hofseth LJ. Nitric oxide as a target of complementary and alternative medicines to prevent and treat inflammation and cancer. Cancer Letters 2008;268:10-30

268. Kolios G, Petoumenos C, Nakos A. Mediators of inflammation: production and implication in inflammatory bowel disease. Hepato-Gastroenterology 1998;45:1601-1609

269. Nathan C. Inducible nitric oxide synthase: what difference does it make? The Journal of Clinical Investigation 1997;100:2417-2423

270. Granfors K, Jalkanen S, Mäki-Ikola O, Lahesmaa-Rantala R, Saario R, Toivanen A, Lindberg AA, von Essen R, Isomaki H, Arnold WJ. Salmonella lipopolysaccharide in synovial cells from patients with reactive arthritis. Lancet 1990;335:685-688

271. Rylander R, Bake B, Fischer JJ, Helander IM. Pulmonary function and symptoms after inhalation of endotoxin. The American Review of Respiratory Disease 1989;140:981-986

272.   Michel O, Duchateau J, Sergysels R. Effect of inhaled endotoxin on bronchial reactivity in asthmatic and normal subjects. Journal of Applied Physiology (Bethesda, Md: 1985) 1989;66:1059-1064

273.   Michel O, Nagy AM, Schroeven M, Duchateau J, Nève J, Fondu P, Sergysels R. Dose-response relationship to inhaled endotoxin in normal subjects. American Journal of Respiratory and Critical Care Medicine 1997;156:1157-1164

274.   Michel O, Ginanni R, Le Bon B, Content J, Duchateau J, Sergysels R. Inflammatory response to acute inhalation of endotoxin in asthmatic patients. The American Review of Respiratory Disease 1992;146:352-357

275.   Herbert A, Carvalheiro M, Rubenowitz E, Bake B, Rylander R. Reduction of alveolar-capillary diffusion after inhalation of endotoxin in normal subjects. Chest 1992;102:1095-1098

276.   Michel O. Role of lipopolysaccharide (LPS) in asthma and other pulmonary conditions. Journal of Endotoxin Research 2003;9:293-300

277.   Hotchkiss RS, Karl IE. The pathophysiology and treatment of sepsis. The New England Journal of Medicine 2003;348:138-150

278.   Greco MN, Hawkins MJ, Powell ET, Almond HR, Corcoran TW, de Garavilla L, Kauffman JA, Recacha R, Chattopadhyay D, Andrade-Gordon P, Maryanoff BE. Nonpeptide inhibitors of cathepsin G: optimization of a novel beta-ketophosphonic acid lead by structure-based drug design. Journal of the American Chemical Society 2002;124:3810-3811

279.   Capodici C, Berg RA. Cathepsin G degrades denatured collagen. Inflammation 1989;13:137-145

280.   Heck LW, Blackburn WD, Irwin MH, Abrahamson DR. Degradation of basement membrane laminin by human neutrophil elastase and cathepsin G. American Journal of Pathology 1990;136:1267-1274

281.   Büchele B, Zugmaier W, Estrada A, Genze F, Syrovets T, Paetz C, Schneider B, Simmet T. Characterization of 3alpha-acetyl-11-keto-alpha-boswellic acid, a pentacyclic triterpenoid inducing apoptosis in vitro and in vivo. Planta Medica 2006;72:1285-1289

282.   Campanelli D, Detmers PA, Nathan CF, Gabay JE. Azurocidin and a homologous serine protease from neutrophils. Differential antimicrobial and proteolytic properties. The Journal of Clinical Investigation 1990;85:904-915

283.   Maryanoff BE. Inhibitors of serine proteases as potential therapeutic agents: the road from thrombin to tryptase to cathepsin G. Journal of Medicinal Chemistry 2004;47:769-787

284.   Roughley PJ, Barrett AJ. The degradation of cartilage proteoglycans by tissue proteinases. Proteoglycan structure and its susceptibility to proteolysis. The Biochemical Journal 1977;167:629-637

285.   de Garavilla L, Greco MN, Sukumar N, Chen Z-W, Pineda AO, Mathews FS, Di Cera E, Giardino EC, Wells GI, Haertlein BJ, Kauffman JA, Corcoran TW, Derian CK, Eckardt AJ, Damiano BP, Andrade-Gordon P, Maryanoff BE. A Novel, Potent Dual Inhibitor of the Leukocyte Proteases Cathepsin G and Chymase: Molecular mechanisms and anti-inlfammatory activity in vivo. The Journal of Biological Chemistry 2005;280:18001-18007

286.   Navarro P, Valverde AM, Benito M, Lorenzo M. Activated Ha-ras induces apoptosis by association with phosphorylated Bcl-2 in a mitogen-activated protein kinase-independent manner. The Journal of Biological Chemistry 1999;274:18857-18863

287.   Bos JL. ras oncogenes in human cancer: a review. Cancer Research 1989;49:4682-4689

288.   Crespo P, León J. Ras proteins in the control of the cell cycle and cell differentiation. Cellular and Molecular Life Sciences 2000;57:1613-1636

289.   Frische EW, Zwartkruis FJT. Rap1, a mercenary among the Ras-like GTPases. Developmental Biology 2010;340:1-9

290.   Glaser T, Winter S, Groscurth P, Safayhi H, Sailer ER, Ammon HP, Schabet M, Weller M. Boswellic acids and malignant glioma: induction of apoptosis but no modulation of drug sensitivity. British Journal of Cancer 1999;80:756-765

291.   Novotný L, Vachálková A, Biggs D. Ursolic acid: an anti-tumorigenic and chemopreventive activity. Minireview. Neoplasma 2001;48:241-246

292.   Laszczyk MN. Pentacyclic triterpenes of the lupane, oleanane and ursane group as tools in cancer therapy. Planta Medica 2009;75:1549-1560

293.   Wu B, Wang X, Wang H-H, Wang H-T, Yang W, Chi Z-F, Liu Z-G. Apoptosis of jurkat cells induced by ursolic Acid and its mechanison. Zhongguo Shi Yan Xue Ye Xue Za Zhi 2010;18:61-66

294.   Pang X, Yi Z, Zhang X, Sung B, Qu W, Lian X, Aggarwal BB, Liu M. Acetyl-11-keto-beta-boswellic acid inhibits prostate tumor growth by suppressing vascular endothelial growth factor receptor 2-mediated angiogenesis. Cancer Research 2009;69:5893-5900

7.   Summary

Lipophilic extracts from the gum resin of *Boswellia* spec. (BEs) have been traditionally used for the treatment of several inflammatory diseases. A growing public interest in drugs based on natural compounds led the focus to intense investigations of the mechanisms by which BEs mediate their beneficial effects. The extracts contain large amount of triterpenes, among them the prominent group of boswellic acids (BAs), as well as roburic acids (RAs) and lupanic acids (LAs). In search of the molecular mechanism of BEs, several targets of BAs were identified, among them 5-lipoxygenase, cyclooxygenase-1, human leukocyte elastase, IκB kinases and Akt. In many studies by others, 3-*O*-acetyl-11-keto-β-boswellic acid (AKBA) was identified as most active principle among the BAs. However, rather high concentrations were needed for efficient inhibition of these targets, while AKBA has a rather poor bioavailability. Therefore, it seems likely that there are either additional high-affinity targets for AKBA, or that other BAs or other ingredients (e.g. RAs or LAs) participate in the beneficial outcome observed in several diseases treated with BEs.

One important aim of the present study was the identification of new targets of BAs. By utilizing a pull-down strategy with immobilized BAs, several new targets were identified, among them LL-37, lipopolysaccharides (LPS), cathepsin G (catG), p21 Ras and Rap1B. The binding mode was analyzed, as well as the functional consequences of the molecular interactions between BAs and their respective targets. Structure-activity relationship (SAR) studies were performed with synthetically modified BAs in order to identify essential structural moieties and to obtain more potent (semi-synthetic) derivatives.

The pull-down strategy led to the discovery of LL-37 as a molecular target of BAs. LL-37 is an LPS-neutralizing antimicrobial peptide, which modulates the immune response and is upregulated in diseases as psoriasis. The direct interaction between BAs and LL-37 had a functional consequence, as BAs inhibited the ability of LL-37 to neutralize LPS. This effect was most prominent for 3-*O*-acetyl-β-boswellic acid (ABA, $EC_{50} = 0.2\ \mu M$) and AKBA ($EC_{50} = 0.8\ \mu M$). A SAR study revealed the importance of the C-3 and the C-11 position. Thus, a 3-acetoxy or a 3-hydroxy group was necessary for potent interference, while the 11-keto group was less important. Besides BAs, LAs and RAs were identified as LL-37-inhibiting compounds from frankincense. Moreover,

the inhibitory effect was also relevant in a more physiological environment. Thus, the LPS-neutralizing properties of the supernatant of degranulated neutrophils (containing LL-37) was inhibited by ABA (EC_{50} = 1.3 µM), as well as the LPS-neutralizing properties of plasma from cytochalasin B/fMLP-stimulated blood (EC_{50} = 3.5 µM). At higher concentrations (≥10 µM), BAs also stimulated LL-37 release from cytochalasin B/fMLP-stimulated neutrophils. Since inhibition of LL-37 activity occurs at much lower BA concentrations, the inhibitory effects seemingly dominates and might be of higher pharmacological relevance. BAs, RAs and LAs are virtually the first identified inhibitors of LL-37 and might open a new field for the development of novel drugs applicable for LL-37-mediated diseases such as psoriasis.

A second target identified by pull-down experiments was LPS, a prominent inflammatory compound from Gram-negative bacteria that plays a major role in severe diseases as sepsis and septic shock. BAs without 11-keto group bound to LPS in a direct manner, and this binding led to a potent inhibition of LPS activity (IC_{50} ~2 µM). Notably, 11-keto BAs were completely inactive, suggesting a detrimental function of the 11-keto moiety for LPS-binding, hence explaining the specific binding of 11-keto-free BAs. Those BAs also influenced LPS signaling in cell-based assays, as both LPS-induced iNOS expression and nitric oxide generation were inhibited by 11-keto-free BAs. Detailed *in vivo* studies about the effects of BAs on LPS-mediated diseases like sepsis or septic shock are still missing, but the obtained *in vitro* data suggests that BAs may become potentially valuable compounds for the treatment of these severe diseases and call for more detailed analysis.

CatG was identified as a third functional target of BAs, which was bound by BAs through a direct interaction. It is a serine protease from leukocytes that modulates the immune system. The direct interference of BAs with catG led to an inhibition of the proteolytic activity of catG, as well as suppression of several catG-mediated cellular functions. Therefore, catG-stimulated Ca^{2+} influx in platelets was inhibited by AKBA, and cell migration into an extracellular matrix was inhibited by BAs, a process in which catG might participate. CatG activity of the plasma of stimulated blood from BE-treated patients (3 × 800 mg/day, 4 weeks) was reduced, compared to the placebo-treated control group. Conclusively, catG inhibition by BAs might contribute to the anti-inflammatory effects of frankincense extracts.

Besides LL-37, LPS and catG, two novel targets of BAs, small G-proteins belonging to the protein family Ras, were identified: p21 Ras and Rap1B. BAs bound to p21 Ras in a direct manner, but this binding had only minor functional consequences in the present investigation. The activity of p21 Ras in neutrophils was not influenced by BAs alone, but when neutrophils were co-stimulated with 5-HETE, p21 Ras was activated by AKBA (but not by β-BA) in relative high concentrations ($\geq$ 30 µM). This implicates that AKBA might act *via* some kind of priming effect on neutrophils. Since relative high concentrations were necessary for p21 Ras activation and plasma levels of AKBA are significantly lower (~0.1 µM), the pharmacological relevance of this interaction is questionable.

Similar to p21 Ras, Rap1B is a small G-protein that was identified as a direct binding partner of BAs. However, the binding of AKBA to Rap1B did not influence the nucleotide exchange activity. Further experiments are necessary to completely rule out an inhibition of cellular Rap1B functions, but an activation mode *via* nucleotide exchange was at least excluded.

An additional aim of the present study was the analysis of apoptosis induction by ingredients of BEs. BAs without an 11-keto moiety showed cytotoxic effects on Jurkat T-lymphocytes with EC_{50} values between 2.8 µM and 9.8 µM, while the related 11-keto BAs displayed less cytotoxicity. In PBMCs, BAs in general had less cytotoxic effects, but most compounds that were cytotoxic for Jurkat cells were also cytotoxic for PBMCs. A prominent exception to this rule was ABA, which was cytotoxic for Jurkat cells but not for PBMCs. Such selectivity for cancer cells versus non-transformed cells might be of interest for the development of novel anti-cancer agents. Besides BAs, RAs and LAs were identified as apoptosis-inducing compounds from frankincense, which might also contribute to the beneficial effects of BEs. In Jurkat cells, the induction of apoptosis by BAs and LAs was mediated by caspase-8 and caspase-3, which finally led to PARP-cleavage and DNA fragmentation.

Taken together, LL-37, LPS and catG, all involved in inflammatory processes, were identified as novel targets of BAs. The BA concentrations needed for an efficient inhibition of LL-37, LPS and catG are in the range of BA plasma levels reached after treatment with BEs. The physiological relevance still has to be validated in more detailed *in vivo* studies, but the obtained data suggest that these molecular mechanisms might have physiological relevance and may eventually lead to the development of

novel anti-inflammatory drugs. Moreover, novel triterpenes derived from frankincense were identified as potent apoptosis-inducing agents encouraging for future studies of BE-derived compounds for their potential in the treatment of cancer and cancer-related diseases.

8.   Zusammenfassung

Lipophile Extrakte des Harzes von Weihrauchbäumen (*Boswellia* spec., BEs) werden in der Volksmedizin eingesetzt, um diverse Entzündungs- und Krebskrankheiten zu behandeln. Ein wachsendes öffentliches Interesse an Naturstoffen und ihrer Anwendung in der modernen Medizin führte zu verstärkten Bemühungen, die molekulare Grundlage für die Wirkung von Weihrauchextrakten aufzuklären. Die Extrakte enthalten einen großen Anteil an verschiedenen Triterpenen, unter anderem die in großen Mengen vorkommenden Boswelliasäuren (BAs), sowie Robursäuren (RAs) und Lupansäuren (LAs). Die Suche nach den molekularen Wirkmechanismen der BEs führte zu einer Identifizierung verschiedener Targets, u.a. 5-Lipoxygenase, Cyclooxygenase-1, Humane Leukocyten Elastase, IκB-Kinasen und Akt. Für die meisten Targets wurde 3-*O*-acetyl-11-keto-β-boswellic acid (AKBA) als die BA mit der stärksten biologischen Aktivität identifiziert, welche sich allerdings erst in relativ hohen Konzentrationen zeigte. Demgegenüber steht eine niedrige Bioverfügbarkeit von AKBA. Höchstwahrscheinlich gibt es entweder weitere bisher unbekannte hochaffine Targets für AKBA, oder andere Inhaltsstoffe der Extrakte wie weitere BAs, RAs oder LAs spielen eine Rolle bei der entzündungshemmenden Wirkung von Weihrauchextrakten.

Ein wichtiges Ziel der vorliegenden Arbeit war die Identifikation neuer molekularer Targets von BAs. Durch eine sogenannte „pull-down"-Strategie konnten verschiedene neue Targets identifiziert werden, zu diesen gehörten LL-37, Lipopolysaccharide (LPS), Cathepsin G (catG), p21 Ras und Rap1B. Die Bindung dieser Targets an BAs wurde charakterisiert und schließlich wurde nach funktionelle Konsequenzen der Bindung gesucht. Um die für die Wechselwirkung relevanten strukturellen Merkmale zu identifizieren und um stärker wirkende (semi-synthetische) Derivate zu finden, wurden Struktur-Wirkungsbeziehungen mit Hilfe von synthetisch modifizierten BAs erstellt.

Die „pull-down"-Strategie führte zunächst zu einer Identifizierung von LL-37 als molekulares Target von BAs. LL-37 ist ein LPS-neutralisierendes Peptid, welches die Immunantwort moduliert und in verschiedenen Krankheiten wie Psoriasis hochreguliert wird. Die direkte Wechselwirkung zwischen BAs und LL-37 hatte eine funktionelle Konsequenz: die Fähigkeit von LL-37, LPS zu neutralisieren, wurde durch BAs gehemmt. Dieser Effekt war am stärksten bei 3-*O*-acetyl-β-boswellic acid (ABA, $EC_{50} = 0{,}2$ µM) und AKBA ($EC_{50} = 0{,}8$ µM) ausgeprägt. Die Analyse der Struktur-

Wirkungsbeziehung zeigte die Bedeutung der C-3- und der C-11-Gruppe auf. Eine 3-acetoxy- oder eine 3-hydroxy-Gruppe waren notwendig für eine effiziente LPS-Neutralisation, während eine 11-keto-Gruppe keinen großen Einfluss auf die Aktivität der BAs hatte. Neben BAs wurden mit RAs und LAs weitere Inhaltsstoffe des Weihrauchs als aktive, LL-37-hemmende Komponenten identifiziert. Darüber hinaus konnte der hemmende Effekt auch in einer physiologischeren Umgebung beobachtet werden. So wurde sowohl die LPS-neutralisierende Eigenschaft des LL-37-reichen Überstandes von degranulierten Neutrophilen durch ABA gehemmt (EC_{50} = 1,3 µM), als auch die LPS-neutralisierenden Eigenschaften des Plasmas von Cytochalasin B/fMLP-stimuliertem Blut (EC_{50} = 3,5 µM). In höheren Konzentrationen ($\geq$ 10 µM) stimulierten BAs die Freisetzung von LL-37 aus Cytochalasin B/fMLP-stimulierten Neutrophilen. Da allerdings geringere Konzentrationen für eine Hemmung der Aktivität ausreichen, als für eine verstärkte Freisetzung nötig sind, könnten die Hemmeffekte im Endeffekt eine größere pharmakologische Bedeutung besitzen. BAs, RAs und LAs gehören zu den ersten identifizierten LL-37-Inhibitoren und könnten eine Basis für die Entwicklung neuer Wirkstoffe gegen LL-37-bedingter Krankheiten wie Psoriasis darstellen.

LPS war ein zweites durch „pull-down"-Experimente identifiziertes Target. Das bakterielle LPS stellt einen starken entzündungsinduzierenden Stoff dar, welches eine Hauptrolle bei schwerwiegenden Krankheiten wie Sepsis oder Septischer Schock spielt. BAs, die keine 11-keto-Gruppe besaßen, banden direkt an LPS und führten zu einer starken Hemmung der LPS-Aktivität (IC_{50} ~2 µM). Bemerkenswerterweise waren die entsprechenden 11-keto-BAs komplett inaktiv, daher scheint die LPS-Hemmung spezifisch für BAs ohne 11-keto-Gruppe zu sein. Diese BAs beeinflussten ebenfalls die LPS-induzierte Signaltransduktion. Sowohl die iNOS-Expression als auch die Stickstoffmonoxid-Freisetzung wurde durch BAs ohne 11-keto-Gruppe gehemmt. Weiterführende *in vivo*-Studien, die sich mit den Effekten von BAs in LPS-vermittelten Krankheiten, wie Sepsis oder Septischer Schock, beschäftigen, fehlen zwar noch, die entsprechenden *in vitro*-Daten deuten allerdings an, dass BAs eventuell das Potential dazu hätten, eine Grundlage für die Behandlung dieser schwerwiegenden Krankheiten zu bieten.

CatG konnte als drittes funktionelles Target von BAs identifiziert werden, welches direkt von BAs gebunden wurde. Es handelt sich um eine Serinprotease aus

Leukozyten, welche eine Rolle bei der Modulation des Immunsystems spielt. Die direkte Bindung an BAs führte zum einen zu einer Hemmung der proteolytischen Aktivität von catG, zum anderen wurden ebenfalls catG-beeinflusste zelluläre Mechanismen gehemmt. So wurde der catG-stimulierte Ca^{2+}-Einstrom in Thrombozyten durch BAs verringert, und die Zellmigration in eine extrazelluläre Matrix wurde ebenfalls gehemmt, ein Prozess, an dem catG vermutlich beteiligt ist. Im Vergleich zu einer Placebo-behandelten Kontrollgruppe war die catG-Aktivität des Plasmas von stimulierten Blut von BE-behandelten Patienten (3×800 mg/Tag, 4 Wochen) reduziert. Alles in allem scheint die catG-Hemmung durch BAs an den entzündungshemmenden Effekten von Weihrauchextrakten beteiligt zu sein.

Es konnten neben LL-37, LPS und catG auch zwei neue Targets von BAs identifiziert werden, die zu den kleinen G-Proteinen der Proteinfamilie Ras gehören: p21 Ras und Rap1B. BAs banden direkt an p21 Ras, allerdings hatte diese Bindung nur kleinere funktionelle Konsequenzen in den durchgeführten Experimenten. Die p21 Ras-Aktivität von Neutrophilen wurde durch BAs alleine nicht beeinflusst, dieses änderte sich allerdings, wenn Neutrophile zusätzlich mit 5-HETE behandelt wurden. Hier führte AKBA, aber nicht β-BA, zu einer Aktivitätssteigerung, diese allerdings nur bei vergleichsweise hohen Konzentrationen (≥ 30 µM). Da die Plasmaspiegel von AKBA deutlich niedriger liegen (~0,1 µM) ist es fraglich, ob die Aktivierung von p21 Ras zu den heilsamen Effekten von Weihrauchextrakten beiträgt.

In einer ähnlichen Weise konnte gezeigt werden, dass neben p21 Ras auch Rap1B direkt an BAs gebunden hat. Die Bindung von AKBA an Rap1B beeinflusste allerdings nicht die Nukleotidaustauschkinetik. Um Rap1B als relevantes Target komplett auszuschließen, sind weitere Studien notwendig, eine Beeinflussung der Aktivierung über einen Nukleotidaustausch konnte zumindest nicht beobachtet werden.

Ein weiteres Ziel der vorliegenden Arbeit war die Analyse der Apoptoseinduktion durch Inhaltsstoffe von BEs. BAs ohne 11-keto-Gruppe zeigten cytotoxische Effekte in Jurkat T-Lymphozyten mit EC_{50} Werten zwischen 2,8 µM und 9,8 µM. Die entsprechenden 11-keto-BAs waren grundsätzlich weniger cytotoxisch. Die cytotoxischen Effekte waren in PBMCs prinzipiell weniger stark ausgeprägt, allerdings waren hier auch nahezu alle BAs aktiv, die auch auf Jurkat Zellen cytotoxisch wirkten. Eine bemerkenswerte Ausnahme stellte ABA da, welches cytotoxisch auf Jurkatzellen, nicht aber auf PBMCs wirkte. Diese Selektivität (Krebszellen gegen nicht-transformierte

Zellen) könnte wichtig für die Entwicklung von Krebsmedikamenten werden. Zusätzlich zu BAs wurden RAs und LAs als Apoptoseinduktoren aus Weihrauch identifiziert, die zu den heilsamen Effekten von BEs beitragen könnten. Die Apoptoseinduktion durch BAs und LAs wurde durch Caspase-8 und Caspase-3 vermittelt und resultierte letztendlich in der PARP-Spaltung und in der Fragmentierung der zellulären DNA.

Zusammengefasst wurden in der vorliegenden Arbeit LL-37, LPS und catG als neue Targets von BAs identifiziert, die an Entzündungsvorgängen beteiligt sind. Die BA-Konzentrationen, die für eine effiziente Hemmung erforderlich waren, lagen auf oder unter dem Level der BA-Plasmaspiegel, die nach einer BE-Behandlung erreicht wurden. Die Frage nach einer physiologischen Relevanz kann letzten Endes nur durch weiterführenden *in vivo*-Studien geklärt werden, die vorliegende Arbeit liefert dazu allerdings eine rationale Grundlage, die zukünftig eventuell zu einer Entwicklung von neuartigen entzündungshemmenden Medikamenten auf Weihrauchbasis führen könnte. Darüber hinaus wurden bisher unbekannte Triterpene aus Weihrauch als wirksame Apoptoseinduktoren identifiziert, welche weitergehende Studien über einzelne BE-Bestandteile und ihrer Wirkung auf Krebs und krebsassoziierte Krankheiten interessant werden lassen.

9.   Publications

9.1 Original publications

Tausch L, **Henkel A**, Siemoneit U, Poeckel D, Kather N, Franke L, Hofmann B, Schneider G, Angioni C, Geisslinger G, Skarke C, Holtmeier W, Beckhaus T, Karas M, Jauch J, Werz O (2009). Identification of human cathepsin G as a functional target of boswellic acids from the anti-inflammatory remedy frankincense. *The Journal of Immunology* 183(5):3433-3442

Poeckel D, Greiner C, Pergola C, **Henkel A**, Popescu L, Rau O, Schubert-Zsilavecz M, Werz O (2009). Interference of alpha-alkyl-substituted pirinixic acid derivatives with neutrophil functions and signalling pathways. *European Journal of Pharmacology* 619(1-3):1-7.

Wolf M, Nunes F, **Henkel A**, Heinick A, Paul RJ (2008). The MAP kinase JNK-1 of the *Caenorhabditis elegans* nervous system modulates insulin-like signaling and stress responses in peripheral cells. *Journal of Cellular Physiology* 214:721-729.

9.2 Poster presentations

Henkel A, Seitz S, Jauch J, Werz O (2009). Triterpenic acids derived from frankincense inhibit LL-37 activity. *Jahrestagung 2009 der Deutschen Pharmazeutischen Gesellschaft e.V.*

Henkel A, Tausch L, Werz O (2009). Identification of LL-37 as a molecular target for boswellic acids. *ÖPhG annual meeting, Vienna.*

Nunes F, Voss M, **Henkel A**, Wolf M, Paul RJ (2006). Evaluating the role of the neuronal MAP Kinase JNK-1 in orientation behavior and thermotaxis. *European Worm Meeting, Hersonissos.*

9.3 Oral presentations

Janowitz T, Wolf M, Nunes F, **Henkel A**, Heinick A, Paul RJ (2009). The role of insulin-like signalling in the response to stress of the nematode *Caenorhabditis elegans*. *26th Congress of the new European Society of Comparative Biochemistry and Physiology, Innsbruck.*

Wolf M, **Henkel A**, Heinick A, Nunes F, Paul RJ (2006). The MAP kinase JNK-1 of the Caenorhabditis elegans nervous system modulates insulin-like signaling and stress responses in peripheral cells. *DZG annual meeting, Münster.*

9.4 Book contributions

Ammon H, Hunnius C. Hunnius Pharmazeutisches Wörterbuch (10th edition).

9.5 Manuscripts

Henkel A, Seitz S, Jauch J, Werz O (2010) Boswellic acids as novel LPS inhibiting compounds. Manuscript.

Henkel A, Seitz S, Jauch J, Werz O (2010) Identification of LL-37 as a functional target of boswellic acids. Manuscript.

Henkel A, Seitz S, Jauch J, Werz O (2010) Apoptotic mode of action of new synthetic boswellic acids and new isolated natural triterpenes derived from frankincense. Manuscript.

Kather N, **Henkel A**, Werz O, Jauch J (2010) Identification of new triterpenes derived from frankincense and synthetic modifications. Manuscript.

9.6 Patents

Henkel A, Siemoneit U, Jauch J, Werz O (2008). Synthetische Boswelliasäurederivate zur Hemmung der mikrosomalen Prostaglandin E2 Synthase und des Cathepsin G zur Behandlung Prostaglandin E2- und Cathepsin G-vermittelter krankhafter Zustände (priority date: 26.03.2008).

Henkel A, Verhoff M, Jauch J, Werz O (2008). Verwendung von Robursäure, Lupansäure oder Tirucallensäure als Arzneimittel (priority date: 15.10.2008).

10. Acknowledgements

Ich danke Herrn Prof. Dr. Oliver Werz für die Überlassung des spannenden Themas, die hervorragende Betreuung und die vielen hilfreichen Ratschläge, die eine sehr große Hilfe für mich waren und die meine Tübinger Zeit zu einer produktiven Zeit haben werden lassen.

Bei Frau Dr. Düfer möchte ich mich für die Übernahme des Zweitgutachtens bedanken.

Vielen Dank an Herrn Prof. Dr. Laufer für die Unterstützung der finalen Phase meiner Arbeit und die großartige Möglichkeit, meine Arbeit in Tübingen fertigstellen zu können.

Für die hervorragende Hilfsbereitschaft bedanke ich mich sehr herzlich bei Herrn Prof. Dr. Jauch (Universität des Saarlandes), sowie bei seinen engagierten Mitarbeitern Stefanie Seitz und Nicole Kather.

Danke an Frau Prof. Dr. Lidia Sautebin und Dr. Antonietta Rossi der Universität von Neapel, für die kompetente Hilfe und die großartige neapolitanische Gastfreundschaft.

Lars Tausch danke ich für die hervorragenden Vorarbeiten der Weihrauchforschung, sowie Daniel Pöckel, für das Bilden eines soliden Forschungsfundamentes.

Vielen Dank an die Kollegen aus der Transfusionsmedizin des Universitätsklinikums Tübingen für die Organisation von Blutspenden.

Ein besonderes Dankeschön geht an alle Mitarbeiter des Arbeitskreises Werz, die mich auf meinem Weg begleitet haben und für ein hervorragendes Arbeitsklima gesorgt haben: meinen Biochemie-Mitkämpfern Bianca Jazzar, Christine Greiner, Dagmar Bläsius, Julia Bauer und Andreas Köberle, den Weihrauchexperten Moritz Verhoff und Ulf Siemoneit, meiner Laborkollegin Katja Wiechmann, und nicht zuletzt bei meinen KollegInnen Carlo Pergola, Felix Behnke, Ulrike Bühring, Friederike Dehm, Anja Rogge, Susann Luderer, Daniela Müller und Hannelore Braun. Ihr wart ein großartiges Team, in dem ich mich immer wohlgefühlt habe, sowohl bei der Arbeit im Labor als auch außerhalb der Uni!

Bei meinen Eltern Christiane und Gerald Henkel möchte ich mich für ihre bedingungslose Unterstützung bedanken, ebenso gilt mein Dank meinen beiden Brüdern Malte und Björn Henkel, die immer für großartige Gespräche zur Verfügung gestanden haben.

11. Akademische Lehrer

Meine akademischen Lehrer waren:

Prof. Dr. M. Bähler	Zellbiologie
Prof. Dr. G. Clemen	Evolutionsbiologie
Prof. Dr. F. Daniels	Botanik
Prof. Dr. H. Galla	Biochemie
Prof. Dr. F. Hahn	Anorganische Chemie
Prof. Dr. C. Klämbt	Neurobiologie
Prof. Dr. K. Klempnauer	Biochemie
Prof. Dr. H. Kohl	Physik
Prof. Dr. H. Kuhlmann	Allgemeine Zoologie und Genetik
Prof. Dr. A. Meinhardt	Mikrobiologie
Prof. Dr. N. Michiels	Evolutionsbiologie
Prof. Dr. B. Moerschbacher	Biochemie
Prof. Dr. R.J. Paul	Tierphysiologie
Prof. Dr. N. Sacher	Verhaltensbiologie
Prof. Dr. H. Schäfer	Anorganische Chemie
Prof. Dr. W. Scharlau	Mathematik
Prof. Dr. A. Steinbüchel	Mikrobiologie
Prof. Dr. W. Stöcker	Tierphysiologie
Prof. Dr. A. von Schaewen	Pflanzenphysiologie
Prof. Dr. W. Storkebaum	Organische Chemie
Prof. Dr. P. Tudzynski	Botanik
Prof. Dr. W. Weber	Tierphysiologie
Prof. Dr. E. Weiß	Pflanzenphysiologie
Prof. Dr. O. Werz	Pharmazeutische Chemie